

IMPACTS OF NATURAL AND MAN-MADE INFLUENCES ON SEDIMENT
SOURCES AND SUSPENDED SOLIDS CONCENTRATIONS
IN THE LOWER COLORADO RIVER, TEXAS

Karen Katherine Peters Harris

B.S. Geology

THESIS

Presented to the Faculty of the Graduate School of
The University of Texas at Austin
in Partial Fulfillment
of the Requirements

for the Degree

MASTER OF SCIENCE IN
Supervisor:

APPROVED:

Neal E. Armstrong

Howard M. Liljestrand

John M. Sharp, Jr.

THIS IS AN ORIGINAL MANUSCRIPT
IT MAY NOT BE COPIED WITHOUT
THE AUTHOR'S PERMISSION

IMPACTS OF NATURAL AND MAN-MADE INFLUENCES ON SEDIMENT
SOURCES AND SUSPENDED SOLIDS CONCENTRATIONS
IN THE LOWER COLORADO RIVER, TEXAS

by

Karen Katherine Peters Harris

B.S. Geology

THESIS

Presented to the Faculty of the Graduate School of
The University of Texas at Austin
in Partial Fulfillment
of the Requirements
for the Degree of
MASTER OF SCIENCE IN ENGINEERING

THE UNIVERSITY OF TEXAS AT AUSTIN

December, 1989

TABLE OF CONTENTS

1.0	Introduction.....	1
1.1	Need For Study.....	1
1.2	Objectives.....	3
1.3	Scope.....	4
1.4	Acknowledgments.....	7
2.0	Literature Review.....	8
2.1	Introduction.....	8
2.2	The Fluvial System.....	8
2.3	Sediment in Flowing Waters.....	15
2.3.1	Sources of Sediment.....	15
2.3.2	Sediment Transport.....	17
2.3.2.1	Fluvial Dynamics.....	17
2.3.2.2	Particle Motion.....	21
2.3.2.2.1	Particle Size Classification.....	21
2.3.2.2.2	Mechanics of Motion.....	23
2.3.2.3	Modes of Transport.....	29
2.3.3	Sediment Sinks.....	31
2.3.4	Sediment Loading Estimation.....	35
2.3.4.1	Sediment Load in Channel.....	35
2.3.4.1.1	Direct Measurement.....	35
2.3.4.1.2	Sediment Transport Models.....	38
2.3.4.2	Watershed Sediment Yield.....	45
2.4	Colorado River Study Area.....	52
2.4.1	General Description.....	52
2.4.1.1	Location.....	52
2.4.1.2	Climate.....	54
2.4.1.3	Physiographic Setting.....	57
2.4.1.4	Soils.....	59
2.4.1.5	Vegetation.....	62
2.4.1.6	Highland Lakes System.....	64
2.4.2	Geology.....	68
2.4.2.1	General.....	68
2.4.2.2	Colorado River Sediment.....	75
2.4.3	Groundwater Hydrology.....	93
2.4.4	Sediment Sources.....	98
2.4.4.1	Natural Sources.....	98
2.4.4.2	Influence of Man.....	105
2.4.4.2.1	Stream Regulation.....	105
2.4.4.2.2	Land Use and Management.....	113
2.4.4.2.3	Sand and Gravel Mining.....	118
2.5	Discussion.....	135

3.0	Quantitative Analysis.....	140
3.1	Introduction.....	140
3.2	Upstream Contribution.....	141
3.2.1	Simple Average.....	141
3.2.2	Unbiased Stratified Ratio Estimator....	143
3.2.3	Results.....	144
3.3	Study Area and Downstream Loading	
	Estimation.....	145
3.3.1	Tributary Contribution.....	145
3.3.1.1	SSLOAD Model.....	146
3.3.1.2	Sediment Rating Curve.....	152
3.3.2	River Channel Erosion.....	159
3.3.2.1	Solids Balance.....	160
3.3.2.2	Results.....	166
3.4	Sediment Budget.....	167
3.5	Results.....	170
3.5.1	Drainage Basin Sediment.....	171
3.5.2	Channel Sediment.....	190
4.0	Discussion.....	194
5.0	Conclusions and Recommendations.....	203
Appendices		
A	USTRAT Program.....	208
B	Model SSLOAD.....	211
C	Model SSLOAD Results.....	216
Bibliography.....		223

LIST OF TABLES

Table 2.1:	Classification of Alluvial Channels.....	14
Table 2.2:	Particle Size Classification Scales.....	24
Table 2.3:	Velocity Relationships For Typical Bedload Formulas.....	40
Table 2.4:	Applicability of Sediment Transport Relations.....	44
Table 2.5:	Highland Lakes Data.....	67
Table 2.6:	Ten Highest Floods in Order of Occurrence (Up To 1976).....	103
Table 3.1:	Annual Suspended Sediment Loading of the Colorado River Upstream of the Study Area.....	142
Table 3.2:	Description of the Subbasins of the Lower Colorado River Drainage Basin By Tributary/Outfall and County.....	148
Table 3.3:	A Comparison of HILOADSS Calculated Flow vs. Actual Flow at the USGS Bastrop Gage (No. 08159200).....	153
Table 3.4:	The Short Term and Long Term Sediment Budgets for the Lower Colorado River Drainage Basin.....	168

LIST OF FIGURES

Figure 1.1:	Generalized map locating area of interest between Austin and Bastrop.....	5
Figure 2.1:	Idealized fluvial system.....	10
Figure 2.2:	Straight, braided, and meandering channel patterns.....	13
Figure 2.3:	Distribution of velocity and turbulence within a meandering river.....	18
Figure 2.4:	Velocity distribution curve within a river.....	22
Figure 2.5:	Shield's relation for the beginning of motion.....	26
Figure 2.6:	Basic Hjulstrom's diagram showing relationship between erosion, transportation, and deposition of sedimentary particles.....	28
Figure 2.7:	Illustration of various fluvial deposits.....	33
Figure 2.8:	Three methods of abandoning river channels: (A) chute cut-off (B) neck cut-off (C) avulsion.....	33
Figure 2.9:	Graphical representation of the suspended sediment concentration relationship for a range of W/u ratios.....	42
Figure 2.10:	Colorado River drainage basin, including major streams and tributaries.....	53
Figure 2.11:	Colorado River between Austin and Bastrop.....	55
Figure 2.12:	Mean annual precipitation for Texas based on records for 1931-60.....	56

Figure 2.13: Colorado River basin in relation to physiographic regions.....	58
Figure 2.14: General soil map of the soil associations between Austin and Bastrop.....	61
Figure 2.15: Highland Lakes system of the Colorado River.....	65
Figure 2.16: Geologic map of Texas, including an outline of the Colorado River drainage basin and the area of interest.....	69
Figure 2.17: Geologic time scale.....	70
Figure 2.18: Geologic map of Travis and Bastrop counties between Austin and Bastrop...	74
Figure 2.19: Generalized sequence of terrace formation.....	76
Figure 2.20: Geomorphic map of the alluvial valley of the Colorado River between east Austin and Webberville.....	79
Figure 2.21: Cumulative frequency curve for grain size in the modern Colorado River channel bed (1) and the various older channel phases (2-7).....	82
Figure 2.22: Graph of sand size quartz, granitic feldspar, and rock fragment percentages vs. distance from mouth of the modern Colorado River.....	84
Figure 2.23: Colorado River pre-dam profile from the Burnet-Llano area to Wharton, Texas.....	86
Figure 2.24: Graph of gravel size limestone, chert, quartz, granite, and miscellaneous (sandstone and metamorphic) rock percentages vs. location along the modern Colorado River.....	88
Figure 2.25: Major aquifers of Texas.....	94

Figure 2.26: Coarse-grained point bar plan view and cross-sections illustrating principle physiographic features.....	100
Figure 2.27: Map of streams draining north Austin...	115
Figure 2.28(a): Sand and gravel operations on the Colorado River, 1951.....	120
Figure 2.28(b): Sand and gravel operations on the Colorado River, 1966.....	121
Figure 2.28(c): Sand and gravel operations on the Colorado River, 1973.....	122
Figure 2.28(d): Sand and gravel operations on the Colorado River, 1984.....	123
Figure 2.28(e): Sand and gravel operations on the Colorado River, 1987.....	124
Figure 2.29: Locations of active sand and gravel producers as indicated by the Bureau of Economic Geology March 1988 listing.....	129
Figure 2.30: Relative time for (A) filling of in- stream gravel pit for a low flow event, (B) filling of in-stream gravel pit for a high flow event, and, (C) critical time for erosion of a floodplain gravel pit.....	133
Figure 3.1: The twenty subbasins of the lower Colorado River drainage basin between Austin and the Gulf of Mexico.....	147
Figure 3.2(a): Sediment rating curve for Walnut Creek.....	155
Figure 3.2(b): Sediment rating curve for Onion Creek.....	156
Figure 3.2(c): Sediment rating curve for Big Sandy Creek near Elgin.....	157

Figure 3.2(d): Composite graph of the Walnut Creek, Onion Creek, and Big Sandy Creek sediment rating curves.....	158
Figure 3.3: Cross-section of a stream, illustrating key parameters of the solids balance equation.....	161
Figure 3.4: Average annual suspended sediment concentration as a function of distance downstream.....	164
Figure 3.5: Distribution of drainage area for each subbasin between Austin and Wharton.....	173
Figure 3.6: Relationship between sediment yield and subbasin distance from mouth.....	174
Figure 3.7: Relationship between sediment flux and drainage area.....	175
Figure 3.8: Relationship between sediment flux and subbasin distance from mouth.....	177
Figure 3.9: Distribution of land use based on subbasin distance from mouth.....	179
Figure 3.10: Sediment yield vs. percent cropland between Austin and Wharton.....	180
Figure 3.11: Sediment yield vs. percent rangeland between Austin and Wharton.....	181
Figure 3.12: Sediment yield vs. percent forest between Austin and Wharton.....	183
Figure 3.13: Distribution of soil type based on subbasin distance from mouth.....	185
Figure 3.14: Sediment yield vs. percent D soil between Austin and Wharton.....	187
Figure 3.15: Sediment yield vs. percent B soil between Austin and Wharton.....	188

CHAPTER 1

INTRODUCTION

1.1 NEED FOR STUDY

In recent years, an abundance of plant life, particularly rooted plant life, in the Colorado River below Austin has been a cause of concern for many residents in the area. The impression was that the excessive plant life was a result of the City of Austin's wastewater discharges into the river, and that these discharges may be adversely affecting water quality in the area.

A Select Committee on Water Quality Standards was appointed in 1984 by then Governor Mark White to address the problem. The Committee recommended that the City of Austin, the Texas Water Commission (TWC), and the Lower Colorado River Authority conduct a joint study concerning the effects of nutrients in wastewater discharges. The main portion of the study was conducted by The University of Texas at Austin for the City of Austin. The central question to be answered by the study was "Will removing

nutrients from point sources reduce the amount of submerged rooted aquatic vegetation (SRAV) in the Colorado River below Austin?" The study was completed in 1988 and recommendations were reported to the City of Austin. The basic conclusion was that nutrient removal should not be required of wastewater dischargers in the study area. This conclusion was based on (Armstrong et al., 1987):

- o . . . strong evidence that large populations of SRAV's live in streams with lower concentrations of nutrients than can be achieved with nutrient removal from point sources . . .
- o strong evidence that SRAV requires small quantities of nutrients for maximum growth rate and that most if not all of the nutrients are obtained from the sediment (which has sources of nutrients other than by diffusion from the water above) . . .
- o how the Colorado River flow and water clarity have been modified by the impoundments upstream and how sand and gravel operations have changed channel morphology below Austin . . .
- o evidence of how SRAV responds to changes in flow, turbidity, and nutrients in other rivers . . .
- o good evidence of how the historical populations of SRAV in the Colorado River have changed in the last 40 years and what changed them . . .
- o the forecasts of the nutrient levels and estimated SRAV populations that will

result with and without nutrient removal from point sources.

It was also concluded that adopting a stream standard for nutrients could not be supported by the study (Armstrong et al., 1987).

The study has thus provided strong evidence that the nutrients required to support the growth of SRAV would be present in the Colorado River even if all point sources of nutrients were removed. This would indicate that the SRAV derive their necessary nutrients from another source. The study suggested that most if not all of the nutrients were obtained from the river sediment, which has nutrient sources other than from diffusion from the water column. The sources of nutrients to the sediment must then be determined in order to understand and predict SRAV activity in the river system. In order to determine the nutrient sources to the river sediment, the origin and nature of the sediment itself must be examined.

1.2 OBJECTIVES

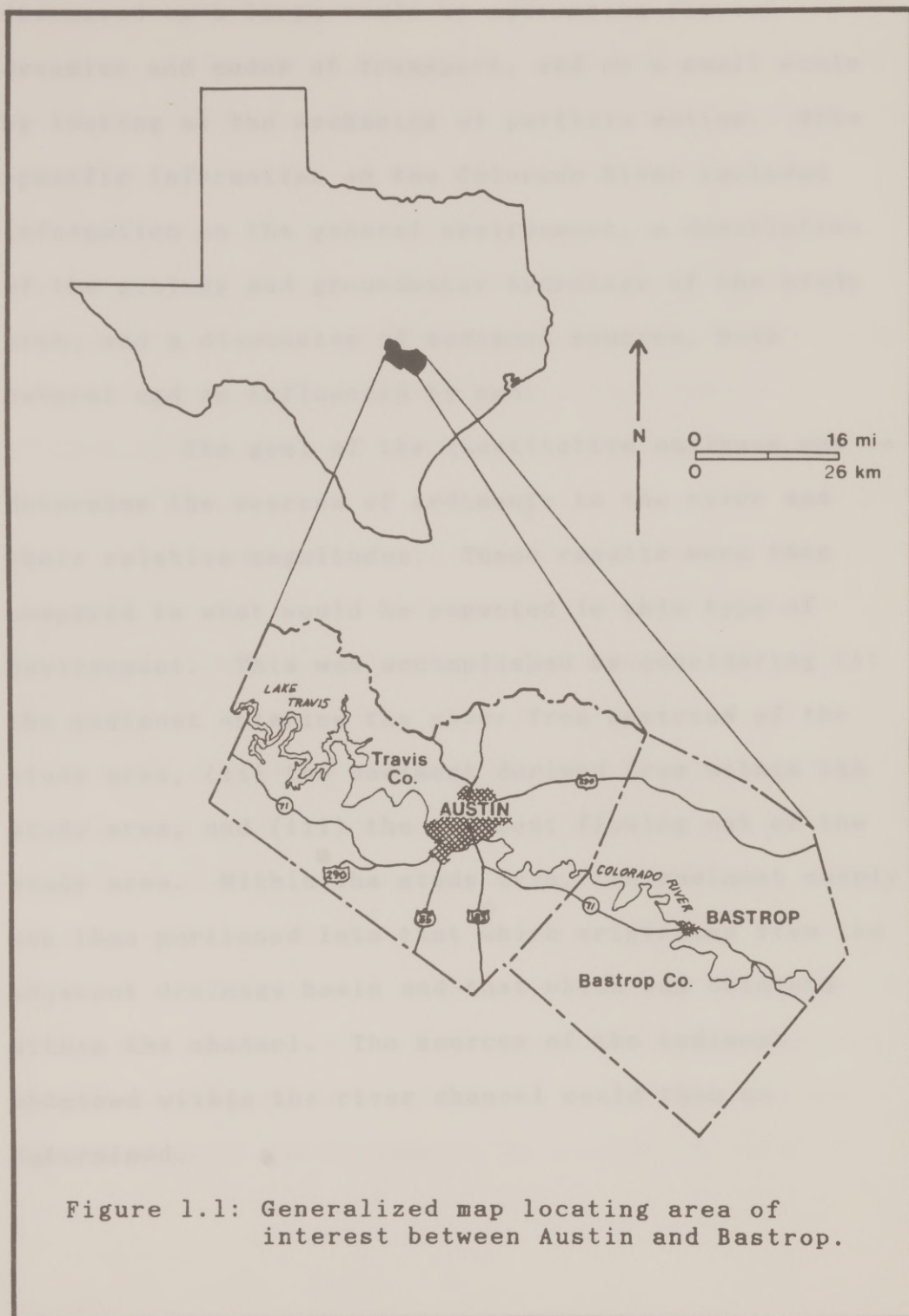
The overall objective of the study was to determine the origin and nature of the Colorado River sediments. The reach of interest extended from Austin

to Bastrop, approximately 89 km (55 mi) downstream (Figure 1.1). The overall objective was accomplished through the following subobjectives:

- (i) investigate the fluvial dynamics of this particular reach of the river, including sedimentation and scour patterns;
- (ii) investigate the geology of the study area and its role in influencing the nature and behavior of channel sediment;
- (iii) study the groundwater hydrology of the study area and the possible effects on the sediment supply to the river
- (iv) examine how man's interference has affected the sediment supply to the Colorado river; and
- (v) develop an investigative framework as a basis for possible future experimental work.

1.3 SCOPE

To meet these subobjectives, this study combined and compared the information from an extensive literature survey with the results of quantitative analyses. The literature review covered the information available on topics pertinent to the understanding of a river system and sediment transport and disposition within the system on the theoretical as well as site specific levels. The typical or expected behavior of sediment within flowing waters was



discussed on a large scale by addressing fluvial dynamics and modes of transport, and on a small scale by looking at the mechanics of particle motion. Site specific information on the Colorado River included information on the general environment, a description of the geology and groundwater hydrology of the study area, and a discussion of sediment sources, both natural and as influenced by man.

The goal of the quantitative analyses was to determine the sources of sediments to the river and their relative magnitudes. These results were then compared to what would be expected in this type of environment. This was accomplished by considering (i) the sediment entering the river from upstream of the study area, (ii) the sediment derived from within the study area, and (iii) the sediment flowing out of the study area. Within the study area, the sediment supply was then portioned into that which originated from the adjacent drainage basin and that which was obtained within the channel. The sources of the sediment obtained within the river channel could then be determined.

1.4 ACKNOWLEDGMENTS

I would first and foremost like to thank my thesis advisor, Dr. Neal E. Armstrong, who provided the idea for this study. I am very grateful for his instruction, patience, and encouragement throughout this learning process. His confidence in this novice engineering student is truly appreciated. I would also like to thank my committee members, Drs. Howard M. Liljestrang and John M. Sharp, Jr. for their valuable time and talents.

I am indebted to the City of Austin (C.I.P. no. 237435) and to the Center for Research in Water Resources (CRWR) for providing the funding for this study.

I wish to thank Dr. Wagner for his help in researching weather data, Randy Larkin, for helping with the literature search, and Karen Harrington, for running numerous errands on campus.

Last but not least, my special thanks go to David Harris who provided encouragement and support and helped me keep my perspective while working on this thesis project and throughout my graduate studies.

CHAPTER 2

LITERATURE REVIEW

2.1 INTRODUCTION

The purpose of this literature review was to research and gather available data pertinent to the understanding of the behavior and responses of the Lower Colorado River system to its environment. To accomplish this, general information was gathered on fluvial systems and the behavior of sediment in flowing waters, along with information on the geology, groundwater hydrology, and general environment of the Colorado River. Theoretical behavior and expectations were then considered along with the observed behavior of the Colorado River in later sections for purposes of discussion, comparison, and conclusion.

2.2 THE FLUVIAL SYSTEM

An understanding of the general nature of a fluvial, or river system is necessary before discussing any component of the system. For convenience, Schumm (1977) has divided the fluvial system into three parts,

as shown in Figure 2.1. Zone 1 represents the drainage basin, watershed, or sediment source area, and is the zone in which water and sediment are derived. For the most part, it is the zone of sediment production, although some sediment storage does occur in this area. Zone 2 is the transfer zone or zone of predominant transport, where sediment input can equal sediment output for a stable channel. Zone 3 represents the zone of deposition or the sediment sink. Although some degree of sediment production, transfer, and deposition takes place in all three zones, one process is usually dominant within each zone.

Simons, Li, and Associates (1982) list the variables that are significant to the morphology and mechanics of Zone 1 in order of increasing degree of dependence:

1. Time
2. Initial relief
3. Geology (lithology, structure)
4. Climate
5. Vegetation (type and density)
6. Relief or volume of system above base level
7. Hydrology (runoff and sediment yield per unit area within Zone 1)
8. Drainage network morphology (drainage density, channel shape, gradient, pattern)
9. Hillslope morphology (angle of inclination, length, profile form)
10. Hydrology (discharge of water and sediment to Zones 2 and 3)
11. Channel and valley morphology and sediment characteristics (Zone 2)

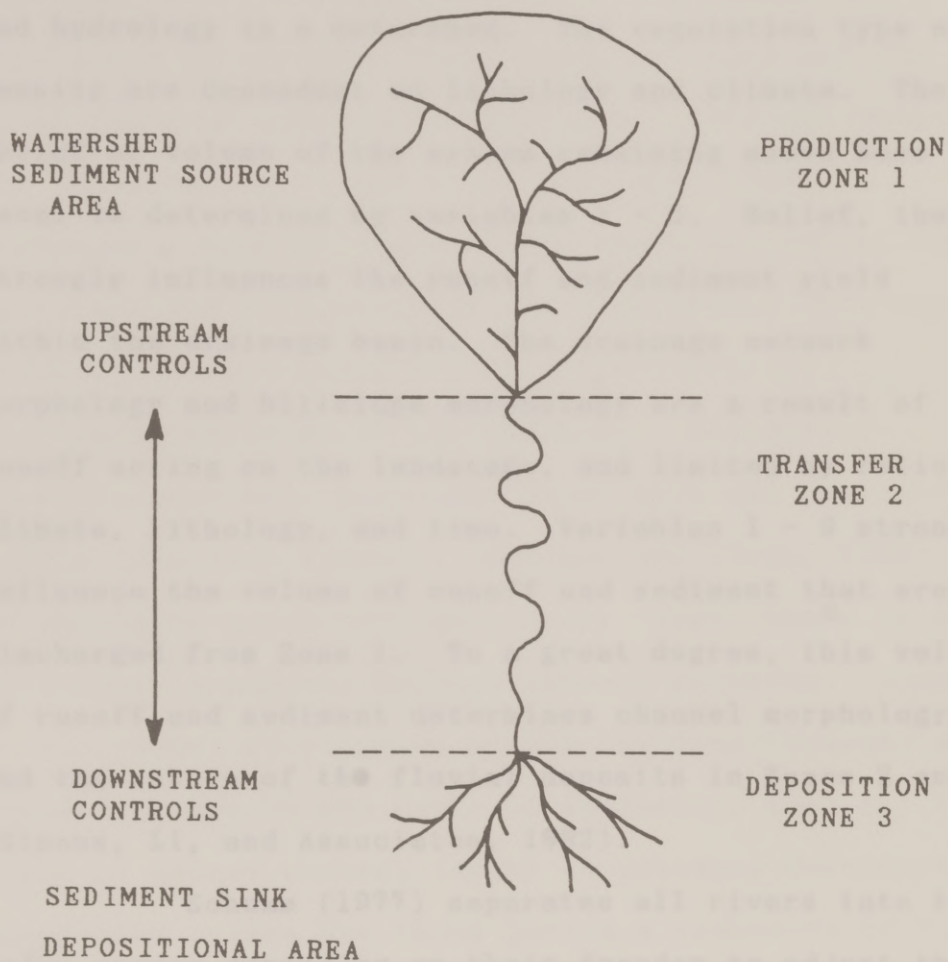


Figure 2.1: Idealized fluvial system. (After Schumm, 1977 and Simons, Li, and Associates, 1982)

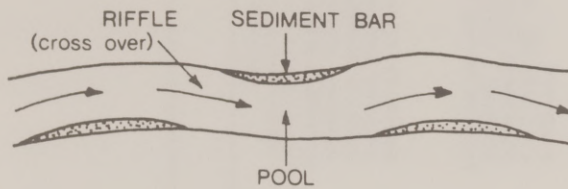
12. Depositional system morphology and sediment characteristics (Zone 3)

Time, initial relief, geology, and climate are the dominant independent variables that influence erosion and hydrology in a watershed. The vegetation type and density are dependant on lithology and climate. The relief or volume of the system remaining above base level is determined by variables 1 - 5. Relief, then, strongly influences the runoff and sediment yield within the drainage basin. The drainage network morphology and hillslope morphology are a result of runoff acting on the landscape, and limited by relief, climate, lithology, and time. Variables 1 - 9 strongly influence the volume of runoff and sediment that are discharged from Zone 1. To a great degree, this volume of runoff and sediment determines channel morphology and the nature of the fluvial deposits in Zones 2 and 3 (Simons, Li, and Associates, 1982).

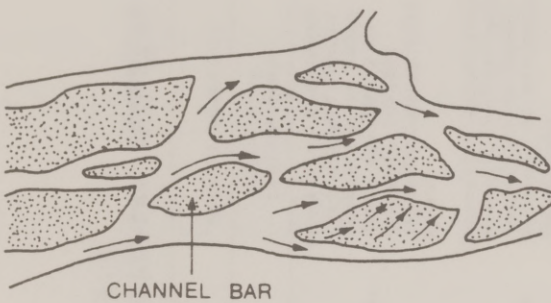
Schumm (1977) separates all rivers into two major groups depending on their freedom to adjust their shape and gradient. Bedrock-controlled channels are those in which the confining rocks are resistant to erosion such that the morphology of the channel is dictated by the confining rock material. In contrast, alluvial channels are able to adjust dimensions, shape,

pattern, and gradient in response to the environment, and are made up of the materials that they transport. Most workers recognize three types of alluvial channel patterns, i.e., straight, braided, and meandering. Figure 2.2 illustrates these three patterns and the major features associated with each. Straight channels are relatively rare and exist only over short distances. Braided channels are characterized by the divisions and rejoinings of the flow around alluvial islands, and are usually wide, with rapid and continuous shifting of the sediment. Meandering channels have well developed point bars and pool and riffle (shallow) sequence (Reineck and Singh, 1980). It should be noted that with every river, there is a continuous gradation between channel patterns. Leopold et al. (1964) distinguish meandering from straight and braided rivers on the basis of sinuosity, that is, the ratio of actual channel length to distance downslope. Meandering rivers are those having a sinuosity of 1.5 or greater, while those < 1.5 are straight and braided.

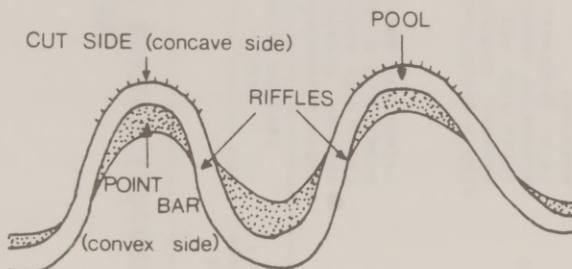
Perhaps the most significant parameter used for classifying alluvial channels is that of sediment load. The Schumm (1977) classification of alluvial channels (Table 2.1) is frequently referenced by other



STRAIGHT



BRAIDED



MEANDERING

Figure 2.2: Straight, braided, and meandering channel patterns. (After Reineck and Singh, 1980)

TABLE 2.1
CLASSIFICATION OF ALLUVIAL CHANNELS

Mode of sediment transport and type of channel	Channel sediment (M) (percent)	Bedload (percent of total load)	Channel stability		
			Stable (graded stream)	Depositing (excess load)	Eroding (deficiency of load)
Suspended load	>20	<3	Stable suspended-load channel. Width/depth ratio <10; sinuosity usually >2.0; gradient, relatively gentle	Depositing suspended-load channel. Major deposition on banks cause narrowing of channel; initial streambed deposition minor	Eroding suspended-load channel. Streambed erosion predominant; initial channel widening minor
Mixed load	5-20	3-11	Stable mixed-load channel. Width/depth ratio >10, <40; sinuosity usually <2.0, >1.3; gradient, moderate	Depositing mixed-load channel. Initial major deposition on banks followed by streambed deposition	Eroding mixed-load channel. Initial streambed erosion followed by channel widening
Bed load	<5	>11	Stable bed-load channel. Width/depth ratio >40; sinuosity usually <1.3; gradient, relatively steep	Depositing bed-load channel. Streambed deposition and island formation	Eroding bed-load channel. Little streambed erosion; channel widening predominant

(After Schumm, 1977)

workers (Simons, Li, and Associates, 1982, Reineck and Singh, 1980, Galloway and Hobday, 1983) and distinguishes nine subclasses of channels based on channel stability and the predominant mode of sediment transport. The mode of sediment transport is defined by the relation between percent channel bed sediment M (silt and clay) and the percentage of transported bedload. The different modes of sediment transport are explained in greater detail in a later section.

2.3 SEDIMENT IN FLOWING WATERS

Rivers are the major transporters of sediment from the continents to the oceans. The sediments found in these flowing waters are the products of erosion. To understand the behavior of a river system, one must understand the nature of the sediment it transports and deposits, and the origin of that sediment.

2.3.1 SOURCES OF SEDIMENT

The amount of sediment derived from the watershed of a river system is controlled by many factors. This 'sediment yield' is influenced by the land use (e.g., urban, cultivated land, meadow, forest

land, or range land), the climate (including the intensity, duration, and distribution of rainfall), the geology and types of soils present, the vegetative cover, and the topography.

Sediment may also be derived from the river channel itself. The amount of sediment eroded from the channel is dependent on several physical variables including depth of flow, slope of energy gradient, density of sediment-water mixture, size of bed material, gradation of bed material, particle fall velocity, shape factor for the reach and cross-section, bed and bank material (i.e., cohesive, non-cohesive, or stratified), subsurface flow through bank material, and piping of river banks (erosion of bank material that can occur as changes in river stage induce flow in and out of the more permeable layers) (Simons, Li, and Associates, 1982). Simons, Li, and Associates also list the principle forces and factors causing bank erosion, including hydraulic factors, shape geometry, velocity, tractive force (drag force exerted by the flowing water and sediment on the banks), drag and lift forces on individual particles, momentum of objects carried in the water, wind, and boat waves, and climatic factors.

The quality of the sediment entering the river or stream is influenced by its size, settling velocity, specific gravity, shape, resistance to wear, state of dispersion, and cohesion (Simons, Li, and Associates, 1982).

2.3.2 SEDIMENT TRANSPORT

Sediment transport within flowing waters is not only influenced by the nature of the sediment, but is a function of the flow regime within the channel. To fully explain sediment transport, the following discussion begins with the general fluvial dynamics of a river system, followed by an examination of individual particle motion, and lastly, a look at the different modes of transportation.

2.3.2.1 Fluvial Dynamics

Most workers agree that the flow in a channel and its effect on the sediment is determined by the distributions of velocity and turbulence. Erosion is most likely to occur in areas of maximum velocity and turbulence. Where velocity and turbulence are relatively low, areas of bed stability or deposition are common (Galloway and Hobday, 1983). Figure 2.3

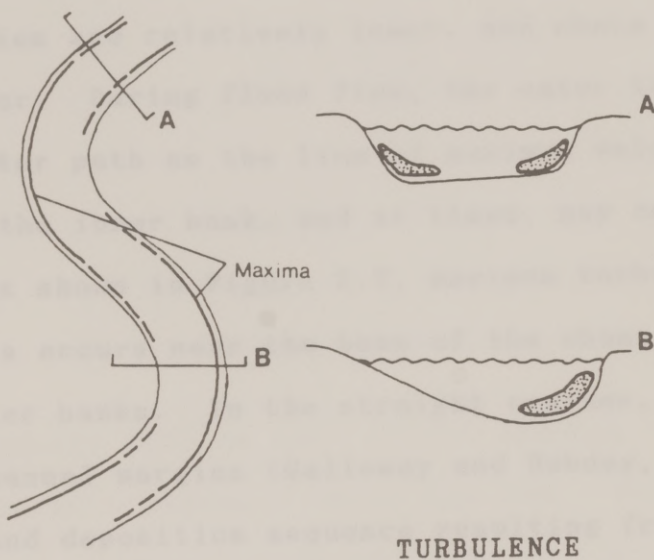
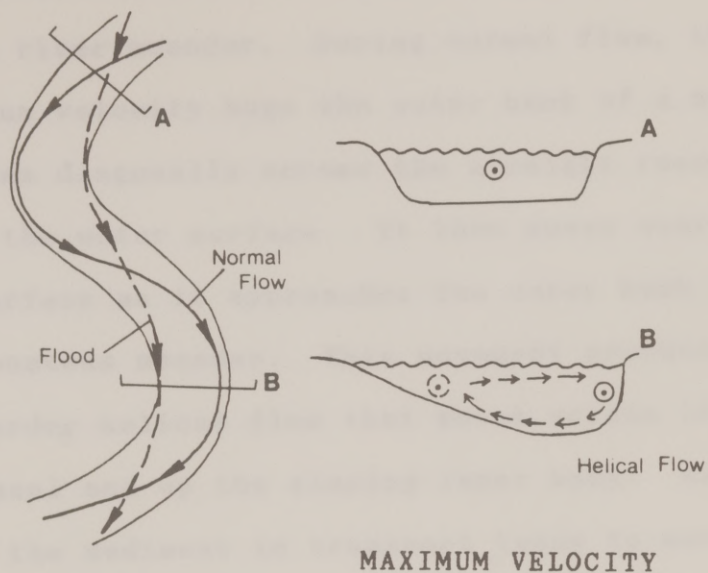


Figure 2.3: Distribution of velocity and turbulence within a meandering river. (After Galloway and Hobday, 1983)

shows the distribution of velocity and turbulence within a river meander. During normal flow, the line of maximum velocity hugs the outer bank of a meander, then moves diagonally across the straight reach, nearing the water surface. It then moves away from the water surface as it approaches the outer bank of the next downstream meander. This movement produces a second-order helical flow that moves across the base of the channel and up the sloping inner bank. As a result, the sediment in transport tends to move across the channel and up the inner bank into an area where velocities are relatively lower, and where deposition may occur. During flood flow, the water takes a straighter path as the line of maximum velocity moves toward the inner bank, and at times, may cut across the bar. As shown in Figure 2.3, maximum turbulence in the meanders occurs near the base of the channel against the outer banks. In the straight reaches, it occurs on both channel margins (Galloway and Hobday, 1983). This scour and deposition sequence resulting from the velocity and turbulence distributions can cause significant lateral changes in the river meanders. The degree of change can be qualitatively analyzed by comparing the channel form and geometry over a number

of years. Furbish (1988) presents a quantitative analysis relating average curvature of a river bend to its average migration rate by integrating the effects of curvature and associated bed forms over bend length.

Leopold et al. (1964) explain that the two principal external forces acting on water flowing in an open channel are gravity and friction between the water and the channel boundaries. This frictional, or resisting force on the water by the channel is a shearing stress. Shear stress, τ , in a river channel can be expressed theoretically as

$$\tau = K \frac{dv}{dy}$$

where v = velocity
 y = depth
 K = eddy viscosity

The velocity will be zero at the channel bed and will increase with distance above the bed. The rate of increase, dv/dy , depends upon the mixing between the slower-moving elements near the bottom and the faster-moving elements above. In turbulent flow, turbulent eddies provide the mixing. In cross-section, the velocity profile decreases toward the channel bed in a

logarithmic curve, as shown in Figure 2.4. The shape of the curve will depend on the roughness of the bed. The mean velocity equals the local velocity at a point approximately 0.6 the depth of the river. The mean velocity can also be calculated by taking the average of the velocities at 0.2 and 0.8 of the total river depth from the surface (Figure 2.4). These relationships are used in stream gaging to estimate mean velocity (Leopold et al., 1964).

2.3.2.2 Particle Motion

The size of the particles or sediments in a river channel can vary from clays to gravels to boulders. Particle size is a major factor controlling particle motion. Standard particle size scales have been developed and are used to avoid confusion in communication in reference to specific sizes of particles. For this reason, examples of these scales are included before the discussion of the mechanics of particle motion.

2.3.2.2.1 Particle Size Classification

Toward standardization of particle sizes, particle size classification scales have been developed

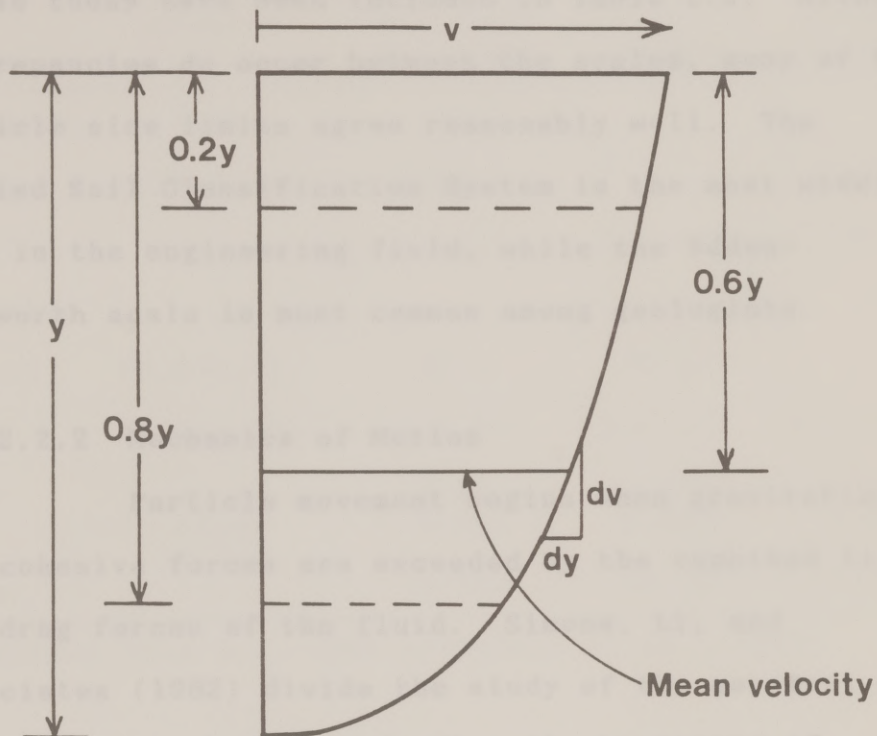


Figure 2.4: Velocity distribution curve within a river. (Modified from Leopold et al., 1964)

in both the engineering field and in the geological sciences. Some of the more common particle size scales in use today have been included in Table 2.2. Although discrepancies do occur between the scales, many of the particle size limits agree reasonably well. The Unified Soil Classification System is the most widely used in the engineering field, while the Udden-Wentworth scale is most common among geologists.

2.3.2.2.2 Mechanics of Motion

Particle movement begins when gravitational and cohesive forces are exceeded by the combined lift and drag forces of the fluid. Simons, Li, and Associates (1982) divide the study of the movement of particles into before and after the beginning of motion. Prior to motion, the problem of resistance to flow is one of rigid boundary hydraulics. After motion begins, the problem involves defining the bed configuration and resistance.

At the critical or threshold condition, the hydrodynamic forces acting on a particle or grain have reached a stage where if increased only slightly, will cause movement of the particle. The beginning of particle motion has been shown to be a function of

TABLE 2.2
PARTICLE SIZE CLASSIFICATION SCALES

(mm)	Unified Soil Classif. System	USDA and Soil Sci. Soc. Amer.	AASHTO	Udden- Wentworth
Boulders	>254			
Cobbles	254-76.2	>80		>64
Pebbles				64-4
Granules				4-2
Gravel	76.2-4.76	80-2	76.2-2	
Sand	4.76-0.074	2-0.05	2-0.075	2-0.0625
Silt		0.05-	0.075-	0.0625-
	Fines <0.074	0.002	0.002	0.0039
Clay		<0.002	<0.002	<0.0039

(Modified from Das, 1985 and Blatt et al., 1972)

$$F = \tau_c / (\gamma_s - \gamma) D$$

where τ_c = critical boundary shear stress
 γ_s = specific weight of sediment
 γ = specific weight of water
 D = characteristic diameter of sediment particle
 F = Shields parameter (dimensionless)

A standard critical condition curve, Figure 2.5, was empirically developed by Shields (in 1936), whereby the Shields parameter was graphed as a function of the shear velocity Reynolds number, R_* , in which U_* and ν represent the shear velocity and kinematic viscosity, respectively. The Shields curve has been used extensively in predicting the largest grain size a given flow can carry, or the velocity required for initial movement of a particular grain size.

Komar (1988) submits that although the Shields diagram is difficult to use, it offers advantages over more simple critical relationships. It has universal application in that it may be used with any combination of grain and liquid (not gases) and with different gravity fields. Other workers have done detailed analyses of the Shields relationship, some modifying the curve to apply to specific conditions.

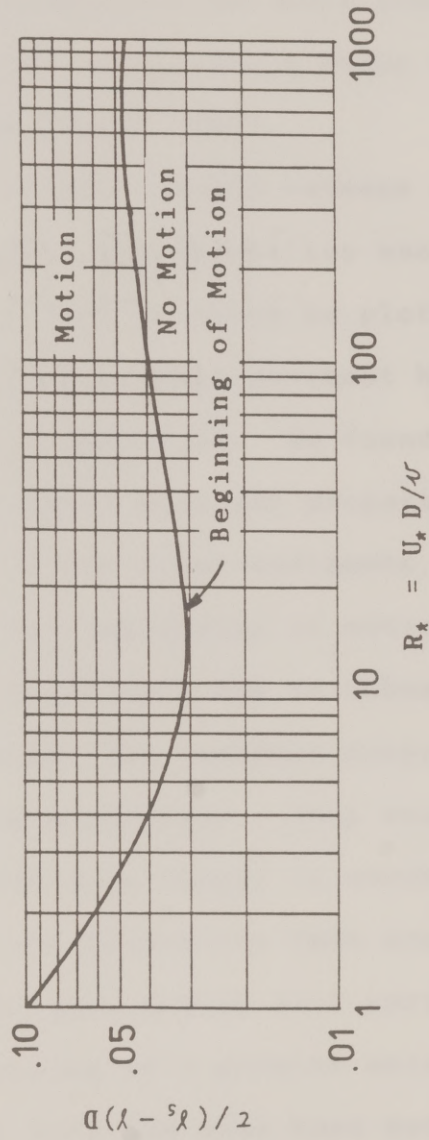


Figure 2.5: Shield's relation for the beginning of motion. (After Simons, Li, and Associates, 1982)

Criticism of the Shields relationship includes the fact that the experimental data for the curve was obtained from sediments with a normal, random arrangement. In nature, the sediments are more commonly overloose or closely-packed, producing a wider scatter of data (Reineck and Singh, 1980).

A relationship between erosion, transportation, and deposition was developed by Hjulstrom in 1939 in which he plotted the critical velocity at which grain movement begins against the grain size (Figure 2.6). He found that for coarser grains, the grain size was proportional to the velocity. In the finer sediments, however, the energy needed for setting grains in motion increased with decreasing grain size due to cohesive forces. Once in motion, though, the sediment response was a function of the settling velocities. This would imply, for example, that more energy is needed to set clay particles into suspension than sand particles. However, the sand grains will settle more rapidly than the clay because of a greater settling velocity. Hjulstrom's work has also been modified by later workers (Reineck and Singh, 1980).

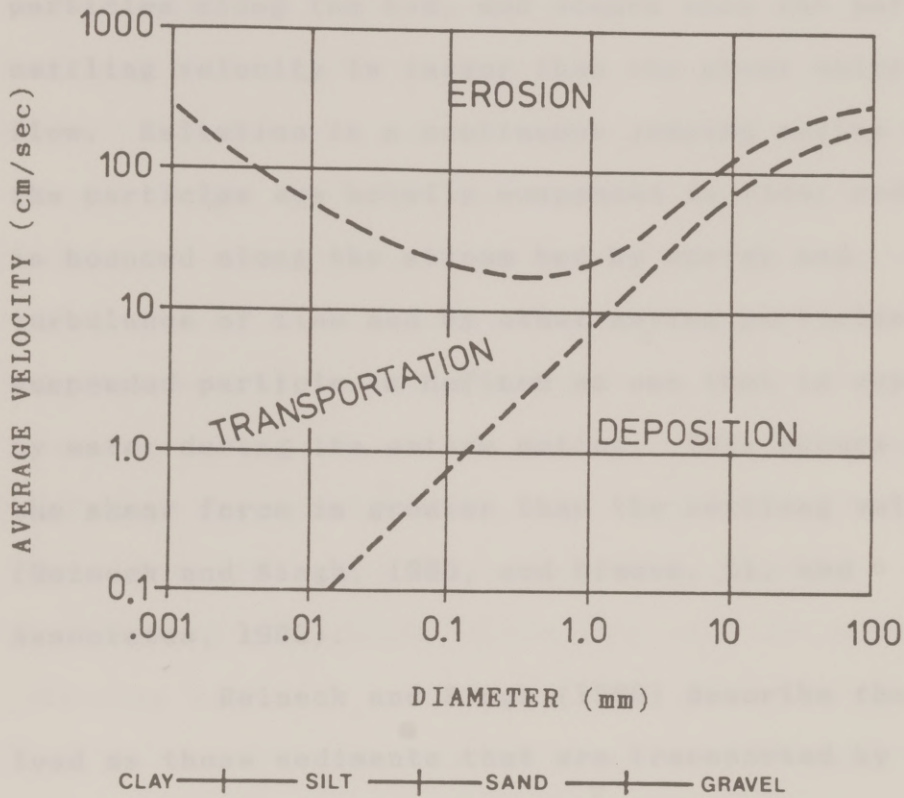


Figure 2.6: Basic Hjulstrom's diagram showing relationship between erosion, transportation, and deposition of sedimentary particles. (Modified from Reineck and Singh, 1980)

2.3.2.3 Modes of Transport

Sediments are transported in moving waters by surface creep, saltation, and suspension. Surface creep, or traction, is the rolling or sliding of particles along the bed, and occurs when the particle settling velocity is larger than the shear velocity of flow. Saltation is a continuous jumping motion where the particles are briefly suspended in flow; sediment is bounced along the stream bed by energy and turbulence of flow and by other moving particles. A suspended particle is defined as one that is supported by water during its entire motion. This occurs when the shear force is greater than the settling velocity (Reineck and Singh, 1980, and Simons, Li, and Associates, 1982).

Reineck and Singh (1980) describe the bed load as those sediments that are transported by sliding and rolling along the bed, and is usually about a two-grain-thick layer. They include as suspended load those sediments transported by saltation and the coarser suspension particles. The wash load is described as the very fine-grained particles that, once taken into suspension, remain in suspension until deposited by decelerating flows. Simons, Li, and

Associates (1982) designate the bed load to include those particles moving by sliding, rolling, and saltation. The suspended load is described as sediment that stays in suspension for an appreciable length of time. They further define the bed-material load to be the sum of the bed load and suspended bed-material load. Simons, Li, and Associates (1982) and Einstein et al. (1940) have divided the total sediment load with regard to ease in engineering analysis and agree that the bed load is that part of the total sediment discharge which is composed of grain sizes found in the bed, regardless if, at the time, they are moving on the bed or in suspension. The wash load, then, refers to those particle sizes finer than those found in significant quantities in the bed, and are usually silt and clay size.

Although this labeling and classification of sediment and modes of transport by different authors appears to be arbitrary and somewhat confusing, it is generally agreed for discussion purposes that the suspended load refers to those sediments that stay in suspension for an appreciable length of time, and the bed load includes those particles that move along the

channel bed. The total sediment load would then be the sum of the bed load and the suspended load.

As shown in Table 2.1, Schumm (1977) classified the mode of sediment transport and type of channel based on the percent of silt and clay, M , in the channel perimeter and on the percentage of bedload to total load. A suspended load channel carries $>20\%$ silts and clays and $<3\%$ bed load. A bed load channel transports $>11\%$ bed load, with $<5\%$ silts and clays. The mixed-load channel falls between the suspended and bed load channel percentages.

2.3.3 SEDIMENT SINKS

A sediment sink is referred to here as the loss of any of the active portion of the channel sediment. Sediment losses to a particular reach of a river include the sediment which exits the downstream boundary of the reach by passing through in suspension or moving as bedload. A sediment sink can also occur if material is deposited within the reach of the river or adjacent lands, although this may be only a temporary sink, as given certain conditions, the sediment may be retransported. Reineck and Singh (1980) provide an extensive discussion on fluvial

deposits. In brief, they separate fluvial deposits into three major groups:

1. Channel deposits. They are sediment deposits formed mainly from the activity of river channels. They include channel lag deposits, point bar deposits, and channel fill deposits.

2. Bank deposits. They are sediment deposits formed on the river banks and are produced during flood periods. They include levee deposits and crevasse splay deposits.

3. Flood basin deposits. They are essentially fine-grained sediment deposits formed during heavy floods when river water flows over the levees into the flood basin. They include flood basin deposits and marsh deposits.

Figure 2.7 is a block diagram illustrating various fluvial deposits. A point bar deposit is that sediment deposited on the inside sloping bank of a meandering channel where velocities are low. Natural levee deposits are wedge-shaped ridges of sediment bordering stream channels that are deposited when flood waters of a river spill over its banks, resulting in a reduction in velocity. Crevasse splay deposits result when the main river channel is breached during high floods, allowing excess water and the sediment it carries to leave the main channel. Flood basin deposits are essentially fine-grained sediment deposits formed

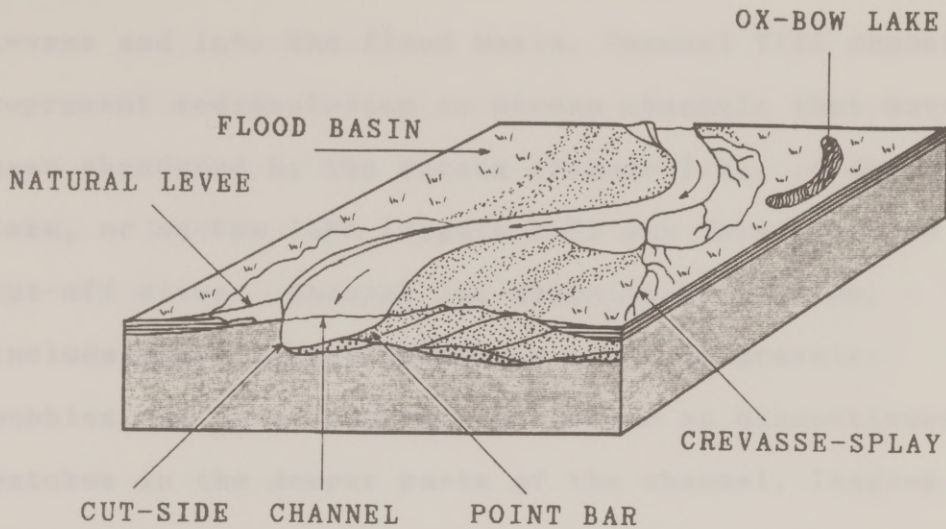


Figure 2.7: Illustration of various fluvial deposits. (After Reineck and Singh, 1980)

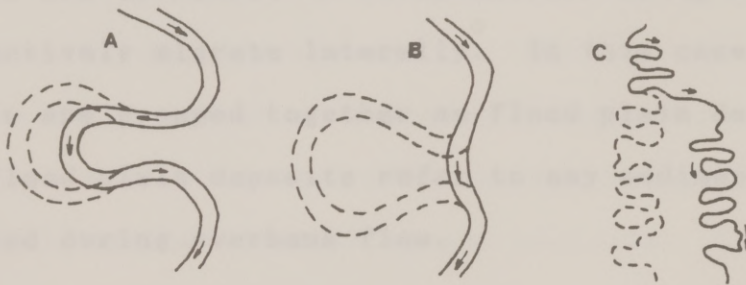


Figure 2.8: Three methods of abandoning river channels: (A) chute cut-off (B) neck cut-off (C) avulsion. (After Reineck and Singh, 1980)

during heavy floods when the river spills over its levees and into the flood basin. Channel fill deposits represent sedimentation in stream channels that have been abandoned by the stream (Figure 2.8). A cut-off lake, or ox-bow lake (Figure 2.7) may form at these cut-off sites. Channel lag deposits, not shown, include those larger sediments (such as gravels, pebbles, or river debris) that occur as discontinuous patches in the deeper parts of the channel, lagging behind the sand which moves as bedload and the finer silts and clays that move much faster in suspension. Other fluvial deposits not shown include channel bars, or channel islands, which are characteristic features of braided rivers and are composed of the coarser-grained lag deposits not carried by the river. Reineck and Singh (1980) point out that bank and flood basin deposits are difficult to differentiate along rivers which actively migrate laterally. In this case, the deposits are grouped together as flood plain deposits. These flood plain deposits refer to any sediment deposited during overbank flow.

2.3.4 SEDIMENT LOADING ESTIMATION

The prediction of the quantity and rate of sediment transport together with sediment disposition within a river system has been the subject of much study. Many methods have been developed to estimate the amount of mobile sediment in a river system at a particular time, the amount of sediment the river is capable of carrying given specific conditions, and the amount of sediment available to a river from adjacent watersheds.

2.3.4.1 Sediment Load in Channel

The sediment load of a river can be determined by methods of direct measurement and sampling and by analysis of sediment movement by means of various transport models.

2.3.4.1.1 Direct Measurement

The amount of sediment in motion in a river at a particular place and time can be physically measured by means of sampling and analysis. The U.S. Geological Survey (USGS) has set up a nationwide network of gaging and sampling stations along various rivers and streams. From these stations, stream

discharge data is usually reported daily. A variety of water quality parameters, including suspended sediment concentration, are monitored at certain stations at various times of the year. To estimate the average suspended sediment concentration, water samples are usually taken at several intervals in the cross section or at one fixed point, with a coefficient applied to the results to obtain a mean concentration. The discharge and water quality data is published annually by the USGS by water year (October to September).

The suspended sediment load of the river can be determined from data on the suspended sediment concentration and the concurrent stream discharge by simply multiplying the two and making the appropriate unit conversions. Thomann and Mueller (1987) present the "unbiased stratified ratio estimator" method of calculating mass loading rates which takes into account estimation errors which may arise when using continuously monitored data, e.g., streamflow, together with periodically monitored data, e.g., suspended sediment concentration.

A standard guide for the sampling of fluvial sediment in motion is published by the American Society For Testing and Materials (ASTM, 1984). This document

presents guidelines for the sampling apparatus and sampling techniques for suspended sediment and bed load measurement. Several different types of bed load monitoring apparatus have been developed; however, the information provided in the document is merely descriptive because no specific sampling equipment or procedures are presently accepted as representative of the state-of-the-art. Hubbell (1987) discusses bed load sampling and analysis and the problems with the calibration and use of portable direct-measuring bed load samplers due to the extreme temporal variations in transport rates. Bedload discharge can be determined by measuring the rate of (i) migration of bedforms, (ii) movement of tracer particles, (iii) deposition or erosion in a given area, and (iv) change with distance in the concentration of some non-conservative property associated with the bed load, such as radioactivity. The ASTM (1984) standards also include guidelines for the calculation of suspended sediment discharge. A companion ASTM document (ASTM, 1980) provides standards for the determination of suspended sediment concentration in water samples.

As mentioned earlier, the suspended sediment load can be calculated from the suspended sediment

concentration and the stream discharge at the time of sampling. This information can be used to develop a sediment rating curve, i.e., a plot of suspended sediment load vs. corresponding stream discharge. Using a log-log scale, the data will often approximate a straight line through most of the range of discharge. This curve can be used to predict the suspended sediment load at the sampling location for any given discharge (Soil Conservation Service, 1971).

2.3.4.1.2 Sediment Transport Models

Many sediment transport equations have been developed over the years to describe sediment transport capacity. In choosing a transport formula for a particular problem, Simons, Li, and Associates (1982) suggest that consideration should first be given to deciding on what portion of the transported sediment needs to be estimated, e.g., bed load, suspended load. The formula selected should also be one that was developed under conditions similar to the given problem.

The earliest bed load transport model was developed by Dubois in 1879 and is based on the assumption that sediment moves along the stream bed in

layers of progressively decreasing velocity with depth within the bed layer (Komar, 1988). The Dubois relationship is of the form

$$q_s = \xi \tau (\tau - \tau_t)$$

where

- q_s = volume transport rate of sediment per unit channel width
- τ = actual flow stress
- τ_t = threshold stress required for initiating sediment movement
- ξ = proportionality coefficient (based on actual measurements of sediment transport)

The sediment transport rate calculated by this equation is based on the amount of excess shear stress (Komar, 1988 and Simons, Li, and Associates, 1982). Although Dubois' model has been criticized over the years for its basic assumptions, many bed load formulas used today are similar in form to the above relationship (Komar, 1988).

Komar (1988) notes the strong dependence of the Dubois equation on mean flow velocity, \bar{u} . He notes that because $\tau \propto \bar{u}^2$, then $q \propto \bar{u}^4$. He further states that the dependency of q_s on τ and \bar{u} are typical for bed load transport formulas and has summarized these relationships in Table 2.3. From the various equations

TABLE 2.3
VELOCITY RELATIONSHIPS FOR TYPICAL BEDLOAD FORMULAS

Source and Date	Transport Dependence	Velocity Proportionality
DuBoys, 1879	$\tau (\tau - \tau_t)$	\bar{u}^4
Donat, 1929	$\bar{u}^2 (\bar{u}^2 - \bar{u}_t^2)$	\bar{u}^4
Schoklitsch, 1930	$S^{1.4} q^{0.6} (q^{0.6} - q_t^{0.6})$	\bar{u}^4
Schoklitsch, 1934	$S^{3/2} (q - q_t)$	\bar{u}^3
O'Brien, 1934	$(\tau - \tau_t)^m$ with $1.5 < m < 1.8$	\bar{u}^3 to $\bar{u}^{3.6}$
Straub, 1935	$\frac{1}{D^{3/4}} \tau (\tau - \tau_t)$	\bar{u}^4
Shields, 1936	$\frac{qS}{D} (\tau - \tau_t)$	\bar{u}^5
Meyer-Peter, 1948	$\tau^{3/2}$	\bar{u}^3
Einstein, 1950	-----	\bar{u}^3
Bagnold, 1966	$\tau \bar{u}$	\bar{u}^3

(Modified from Komar, 1988)

where τ = actual flow stress
 τ_t = threshold stress required for
initiating sediment movement
 \bar{u} = mean flow velocity
 \bar{u}_t = threshold mean flow velocity
 S = channel slope
 q = flow rate
 q_t = threshold flow rate
 D = grain diameter

it can be seen that the transport rate of bed load is proportional to the flow velocity with an exponent ranging from 3 to 5.

The quantities of suspended sediment in transport depend upon the availability of grains that are capable of being lifted above the bed by the flow. The sediment concentration C at an elevation Z above the bed can be approximated by

$$\frac{C}{C_a} = \left(\frac{h-Z}{Z} \frac{Z_a}{h-Z_a} \right)^{W_s / ku_*}$$

where

C_a	=	reference concentration at Z_a
Z_a	=	reference elevation
h	=	water depth
W_s	=	grain settling velocity
k	=	von Karman's constant (= 0.4)
u_*	=	shear velocity

A graphical representation of this equation for a range of W_s/u_* ratios is shown in Figure 2.9. As expected, the suspended sediment concentration decreases upward from the bottom for each particular W_s/u_* ratio curve. The higher the W_s/u_* ratio, the lower the concentration of grains at a given level, so that for a given u_* ,

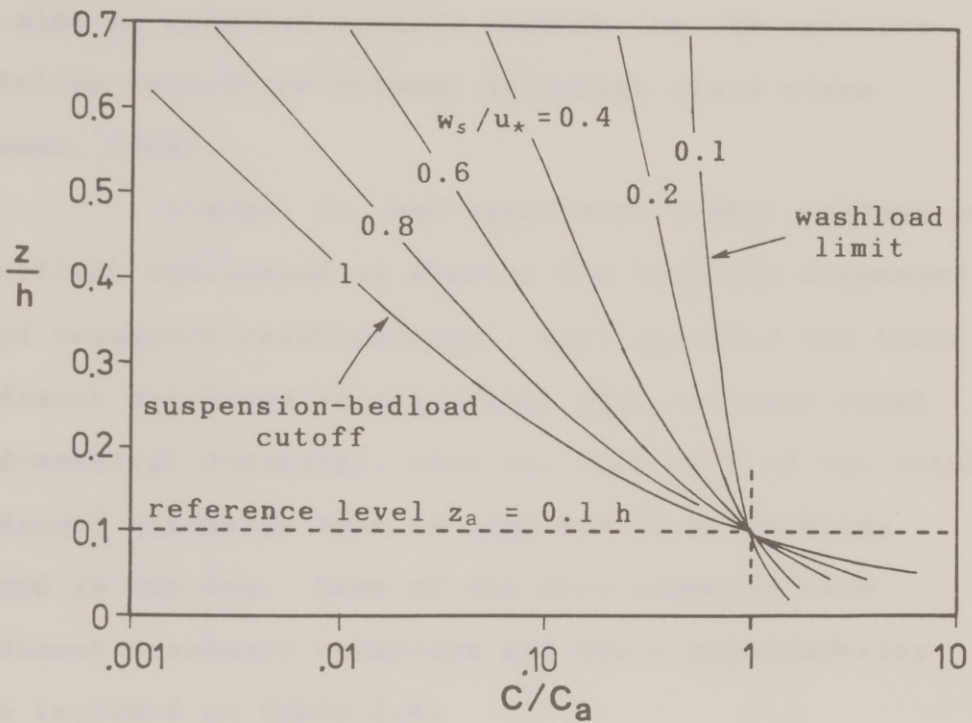


Figure 2.9: Graphical representation of the suspended sediment concentration relationship for a range of w_s/u_* ratios. (After Komar, 1988)

most of the coarser grains would be found near the bottom, while the finer grains would occur in higher concentrations throughout the depth of the river. This is also an expected result, considering the relative settling velocities between different grain sizes (Komar, 1988).

Simons, Li, and Associates (1982) include an excellent discussion on similar bed load and suspended load transport relationships. Also included are three sediment discharge relationships that estimate total bed-material discharge, that is, that part of the total sediment discharge that is composed of grain sizes found in the bed. Some of the more commonly used sediment transport relations and their applicability are included in Table 2.4.

Thomann and Mueller (1987) present a model for calculating the suspended sediment concentration which takes into account the settling and resuspension of particles within a river system. The model is based on the mass balance between the water column and the bed sediment. A detailed examination of this model is presented in a later section.

As a result of investigations concerning sediment transport and flooding, Komar (1988) concluded

TABLE 2.4
APPLICABILITY OF SEDIMENT TRANSPORT RELATIONS

Material	Method	Bed Material Load			Total Load	Design	Analysis
		Wash Load	Suspended	Bed Load			
Wash Load	Direct	X	X				X
	Measurement Estimated from watershed and channel response	X	X				X
Sand	Einstein Modified Einstein	X	X	X	X	X	X
	Colby	Measured or Estimated	X	X	X	X	X
	Statistical Relations	X	X	X	X	X	X
	Meyer-Peter, Muller Composite Relation (SLA)			X		X	X
Gravel & Cobble Beds			X	X	X	X	X

(After Simons, Li, and Associates, 1982)

that any estimates of sediment transport rates for flood events can only lead to questionable results. However, he notes that trends are clear and evident. Floods can result in dramatic increases in bed load transport due to the relationship between the transport rate, q_s , and the order of magnitude of the flow velocity, \bar{u} . In addition, increases of 1000-fold in the suspended sediment load have been directly measured during flood events.

It should be remembered that with all models predicting sediment transport rates, the capacity, or maximum amount of sediment capable of being carried, is the calculated value. In nature, the sediment must be available in order to be transported.

2.3.4.2 Watershed Sediment Yield

Many approaches can be used to determine watershed sediment yield, that is, the amount of sediment from a particular drainage area that enters a river or stream. The quality and quantity of available data together with the desired results will determine which method of estimation is most appropriate for a specific problem.

The most widely used model for predicting soil loss is the Universal Soil Loss Equation (USLE). It was designed to predict soil loss from sheet and rill erosion (Wischmeier, 1976). The model was developed empirically from extensive research using numerous and varied experimental plots of land. The basic equation is

$$A = R K L S C P$$

where

- A = soil loss
- R = measure of the erosive forces of rainfall and runoff
- K = soil erodibility (usually tons/acre)
- L, S = account for length, steepness, and shape of the field slope, commonly grouped as the topographic factor (dimensionless)
- C = cropping management factor
- P = adjustment for erosion-control practices (such as contouring or terracing)

The cropping-management factor is the ratio of soil loss for a given set of conditions to soil loss from cultivated continuous fallow land. The soil loss, A, reflects the time period of factor R and is expressed in the dimensions of soil erodibility K (Mills et al.,

1985, Simons, Li, and Associates, 1982, Schwab et al., 1981, and Wischmeier, 1976).

Wischmeier (1976) presents a detailed discussion of the intended use of the USLE and how the model and results may be misused or misinterpreted. Simons, Li, and Associates (1982) point out several limitations to the USLE: (i) the data base used to develop the USLE was collected east of the Rocky Mountains and can therefore introduce significant error when used in the more arid western regions, (ii) the model requires large amounts of data for development, (iii) the data are restricted to a certain collection period and may not represent long-term conditions, (iv) because the model was developed from data taken from small plots, the results become questionable when applied to larger areas, and (v) the model was developed for sediment ≤ 1 mm, and does not predict sediment load for larger sizes.

Wischmeier (1976) makes the distinction between soil loss and sediment yield. He defines soil loss as soil moved from its original position, and sediment yield as soil loss minus the sediment deposited within the watershed. Mills et al. (1985), Simons, Li, and Associates (1982), Schwab et al.

(1981), and the SCS (1971) all suggest the use of the sediment delivery ratio together with gross erosion estimates (such as the USLE) to obtain the net sediment loss

$$Y = E (DR) / W_s$$

where Y = sediment yield per unit area
 E = gross erosion ('A' from the USLE)
 DR = delivery ratio
 W_s = watershed area

The SCS (1971) presents some general guidelines for determining the delivery ratio.

Simons, Li, and Associates (1982) stated that the Modified Universal Soil Loss Equation (MUSLE) was developed by Williams and Berndt to compute watershed sediment yields based on single storm events. The rainfall energy of the USLE was replaced with a runoff factor to estimate soil loss. The MUSLE is then

$$Y_s = a (Q_v \cdot q_p)^\beta K L S C P$$

where Y_s = sediment yield for the storm event
 Q_v = runoff volume
 q_p = peak flow rate
 a, β = coefficients

All other terms are as defined in the USLE. The MUSLE is more applicable to the arid regions as it can more accurately represent the short-duration, high-intensity events. If desired, the MUSCLE can also be used to predict the sediment yield on an annual basis (Simons, Li, and Associates, 1982).

Another model for estimating watershed sediment yield involves the use of the SCS (1972) method for estimating storm runoff. The direct runoff, or excess precipitation, is calculated given the depth of precipitation and the potential maximum land retention. The land retention is determined from the land use, the soil type, and the antecedent moisture condition of the watershed. The volume of runoff can be computed from the excess precipitation and watershed area. The sediment yield for a given period is then a product of the concentration of the sediment in transport and the volume of flow. This method can also be adapted to estimate the loading of other parameters, such as nutrients. Miertschin and Armstrong (1986) developed the model HILOADS from this method in order to estimate the phosphorus loading from various tributaries entering a lake system. The HILOADS model is discussed in further detail in a later section.

The SCS (1971) suggests that watershed sediment yield can also be estimated from the measured sediment accumulation in reservoirs of known age and history. However, it is pointed out that sediment yield and reservoir deposition are not synonymous, as the amount of sediment passing through the reservoir's trap, or trap efficiency, should be accounted for. The sediment yield measured in this manner for a particular watershed can be used to estimate the sediment yield for an unmeasured watershed, given similar topography, soils, and land use. The equation used is

$$S_e = S_m \left(\frac{A_e}{A_m} \right)^{0.8}$$

where

S_e	=	sediment yield of the unmeasured watershed (tons/yr)
S_m	=	sediment yield of the measured watershed (tons/yr)
A_e	=	drainage area of the unmeasured watershed
A_m	=	drainage area of the measured watershed

The size of the drainage area of the measured reservoir should not be less than one-half or more than twice that of the unmeasured watershed in order to directly transpose the data. Use of this method is generally

confined to the humid areas east of the Rocky Mountains.

If a more general or approximate sediment yield estimate is needed, the Pacific Southwest Interagency Committee (PSIAC) has developed a method which consists of a numerical rating of nine factors affecting sediment production in a watershed. These nine factors include surficial geology, soil, climate, runoff, topography, ground cover, land use, upland erosion, and channel erosion and transport. The numerical rating correlates to one of five sediment yield classifications which, in turn, corresponds to specific ranges of sediment yields:

<u>Rating</u>	<u>Classification</u>	<u>Annual Sediment Yield ac-ft/sq.mi.</u>
> 100	1	> 3.0
75 to 100	2	1.0 to 3.0
50 to 75	3	0.5 to 1.0
25 to 50	4	0.2 to 0.5
0 to 25	5	< 0.2

Again, this method was designed to aid in broad planning purposes only (Simons, Li, and Associates, 1982).

Simons, Li, and Associates (1982) present a very thorough discussion on the methods for calculating

sediment yield. In addition to those already discussed, models which include estimations for sediment larger than 1 mm, other physical process simulation models, and complex watershed and on-site erosion models are also examined.

2.4 COLORADO RIVER STUDY AREA

The Colorado River basin of Texas extends from about 129 km (80 mi) west of the Texas-New Mexico state border southeastward to Matagorda Bay on the Gulf of Mexico (Figure 2.10). The head waters are near the rim of the High Plains Escarpment, and the river flows about 966 km (600 mi) to the gulf (Tovar and Maldonado, 1981, and A. H. Belo Corp., 1987). Colorado is a Spanish word meaning "reddish". It has been conjectured that this name was originally given to the muddier Brazos River by Spanish explorers, and the two names were later transposed by Spanish mapmakers (A. H. Belo Corp., 1987).

2.4.1 GENERAL DESCRIPTION

2.4.1.1 Location

The study area includes the reach of the Colorado River that extends from Longhorn Dam in Austin

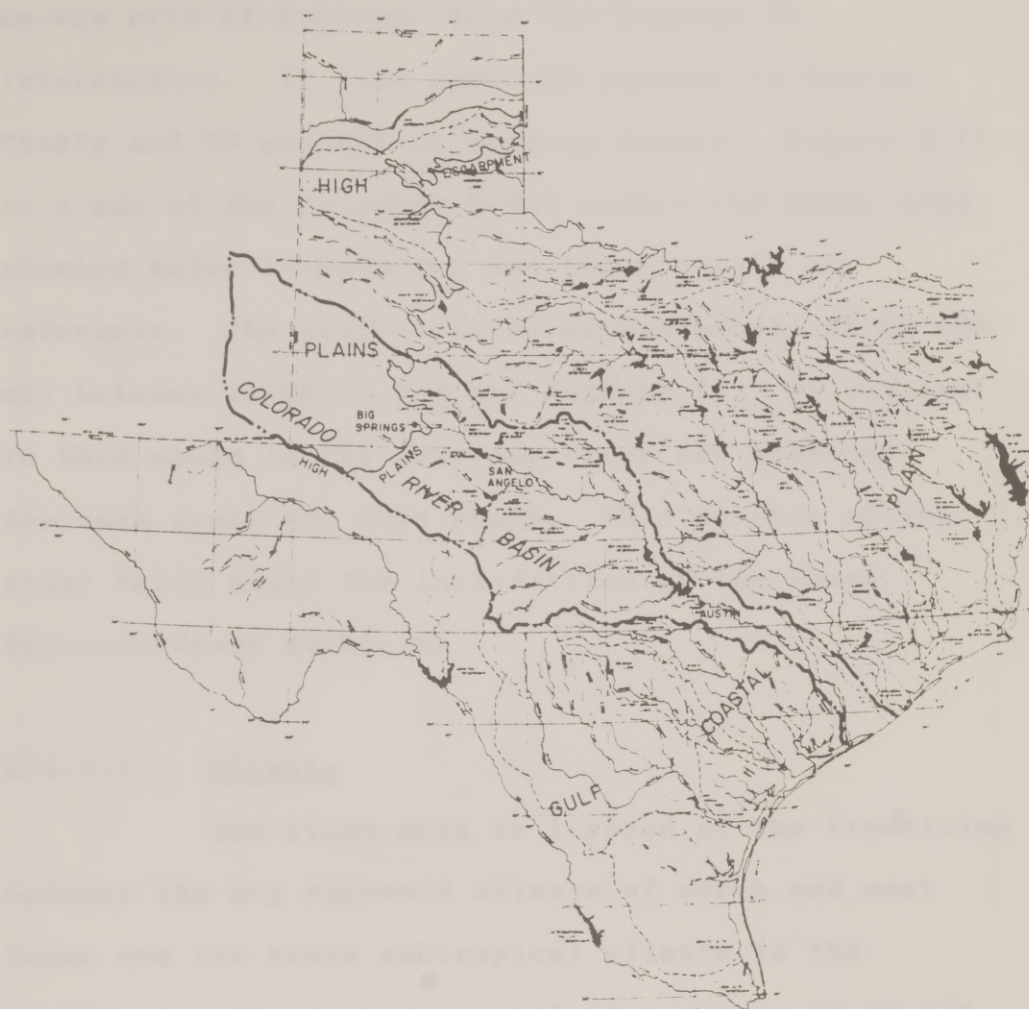


Figure 2.10: Colorado River drainage basin, including major streams and tributaries. (after Tovar and Maldonado, 1981)

to the city of Bastrop, near the Highway 71 intersection. It lies about 50 percent in Travis County and 50 percent in Bastrop County. Figure 2.11 is a map of the Colorado River within the study area, showing major tributaries and other points of reference. The river travels approximately 89 km (55 mi) between Longhorn Dam and Highway 71. Of interest in this study is the Colorado river and adjacent drainage areas for this reach. This portion of the river falls under the jurisdiction of the Lower Colorado River Authority.

2.4.1.2 Climate

The study area is located at the transition between the dry subhumid climate of north and west Texas and the humid subtropical climate to the southeast. The average annual temperature is 20.3°C (68.5°F). Winters are mild, with an average minimum temperature for January of about 5°C (41°F). Summers are hot, with a mean maximum temperature of 35°C (95°F) for July (Brune and Duffin, 1983, and Follett, 1970).

The mean annual precipitation varies greatly geographically across the state as shown in Figure 2.12. Precipitation in the study area is fairly evenly

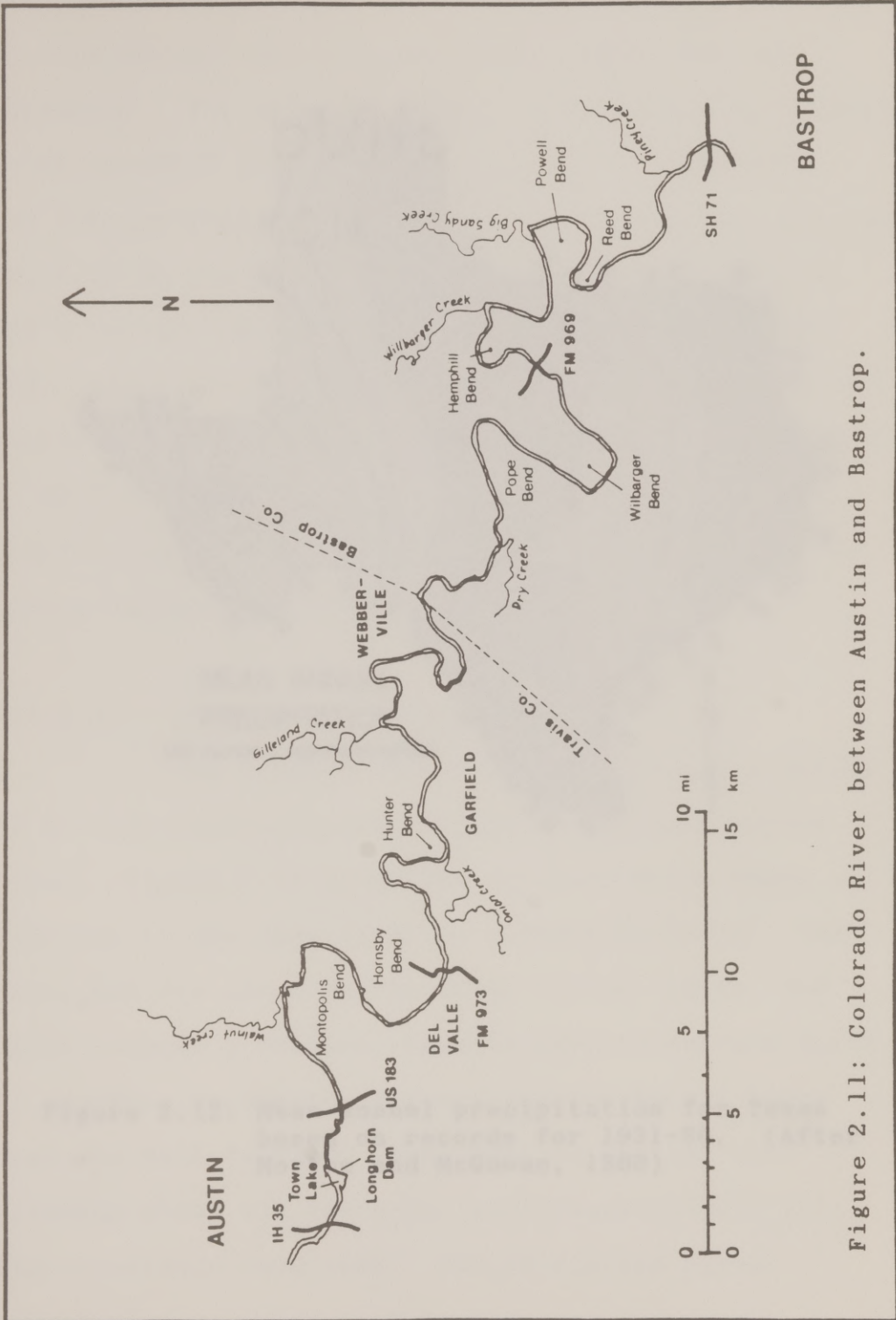


Figure 2.11: Colorado River between Austin and Bastrop.

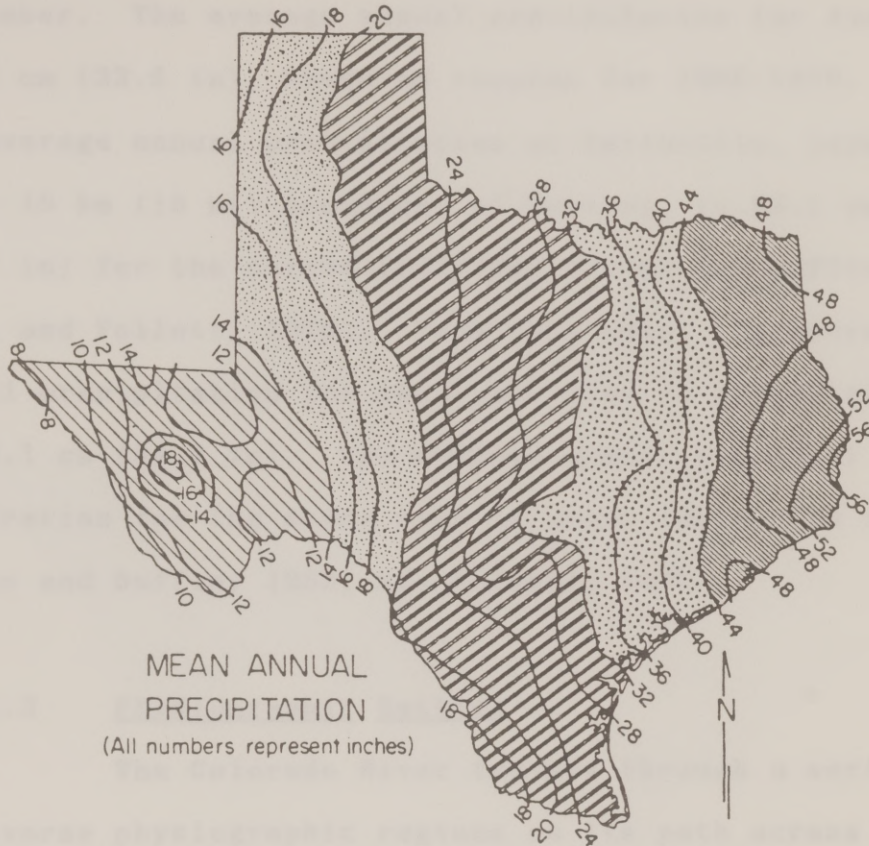


Figure 2.12: Mean annual precipitation for Texas based on records for 1931-60. (After Morton and McGowen, 1980)

distributed temporally, the heaviest amounts occurring in late Spring, and a secondary rainfall peak in September. The average annual precipitation for Austin is 85 cm (33.5 in), based on records for 1900-1976.

The average annual precipitation at Smithville, located about 16 km (10 mi) southeast of Bastrop, is 93.1 cm (36.7 in) for the period 1917-1966 (Brune and Duffin, 1983, and Follett, 1970). From this data, the average annual precipitation for the study area is estimated to be 88.1 cm (34.7 in). The average annual potential evaporation for the study area is about 152 cm (60 in) (Brune and Duffin, 1983, and Follett, 1970).

2.4.1.3 Physiographic Setting

The Colorado River travels through a series of diverse physiographic regions on its path across Texas. Figure 2.13 shows the Colorado River basin in relation to the physiographic regions in Texas. The river has its start in the Great Plains region, and flows through a rolling, usually prairie terrain until it reaches the Edwards Plateau and the Burnet-Llano Area and Hill Country. Just west of Austin, the Colorado River has cut high, picturesque cliffs into the relatively hard rock. The cliffs end rather

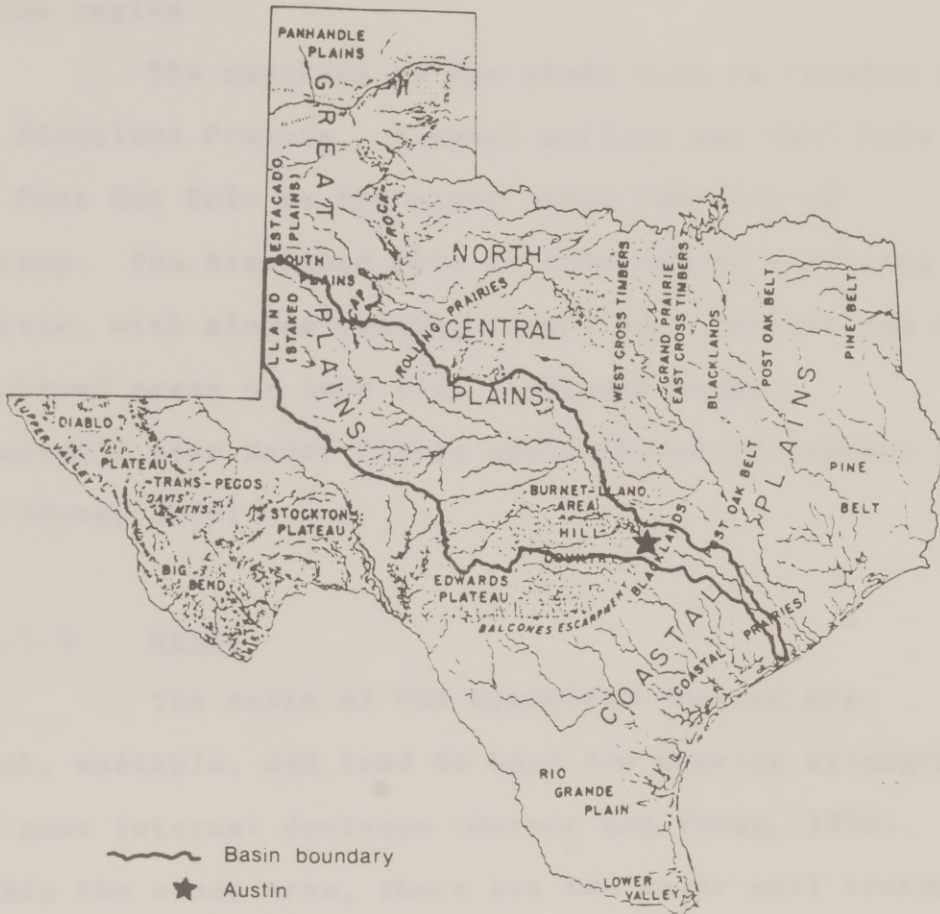


Figure 2.13: Colorado River basin in relation to physiographic regions. (Modified from U. S. Army Corps of Engineers, 1973)

abruptly as the river crosses the Balcones Escarpment. Here the river enters the Blackland Prairie, the Post Oak Belt, and the Coastal Prairies of the Coastal Plains region.

The majority of the study area is located in the Blackland Prairie. A small portion may fall into the Post Oak Belt as the river nears the city of Bastrop. The Blackland belt is typified by a rolling prairie, with slopes ranging from 2 to 5 percent and a few broad areas of less than 2 percent slope, especially near major rivers and tributaries (Garner and Young, 1976).



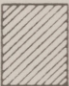


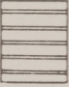



2.4.1.4 Soils

The soils of the Blackland Prairie are thick, unstable, and tend to have low bearing strength and poor internal drainage (Garner and Young, 1976). Within the study area, there are two major soil trends. One trend follows the Colorado river and its tributaries and is developed on the various alluvial deposits. The other trend is related to bedrock and is aligned parallel to the regional northeast-southwest strike. These trends can be seen in Figure 2.14, a general soil map of the soil associations found between

LEGEND: SOIL ASSOCIATIONSSCS SOIL
GROUP

TRAVIS CO.

BASTROP CO.

C	Undifferentiated: mainly shallow, rolling, and steep soils of the Edwards Plateau		
C	Austin-Eddy: Moderately deep and shallow, calcareous, clayey and loamy soils overlying chalk		
D	Houston Black-Heiden: Deep nearly level and gently sloping, calcareous, clayey soils overlying marl		Behring-Crocket-Heiden: Gently sloping to strongly sloping soils with loamy to clayey surface layer and slowly to very slowly permeable layers;
D	Ferris-Heiden: Deep, rolling and moderately steep, calcareous, clayey soils overlying marl		
D	Burleson-Wilson: Deep, clayey and loamy soils overlying marl		Crockett-Wilson: Nearly level to strongly sloping soils with a loamy surface layer and very slowly permeable lower layers
B, C	Lewisville-Patrick: Deep, and moderately deep, calcareous, clayey soils overlying old gravelly alluvium		
B	Bergstrom-Norwood: Deep, calcareous, loamy soils overlying recent and old alluvium		Bosque-Smithville-Norwood: Nearly level soils with a loamy surface layer and moderately permeable lower layers
C, D	Travis-Chaney: Deep, acid, loamy soils overlying old alluvium		Axtell-Tabor: Nearly level to strongly sloping soils with a loamy surface layer and very slowly permeable lower layers
B, D			Patilo-Demons-Silstid: Gently sloping to strongly sloping soils with a sandy surface layer and moderately slowly to moderately permeable lower layers

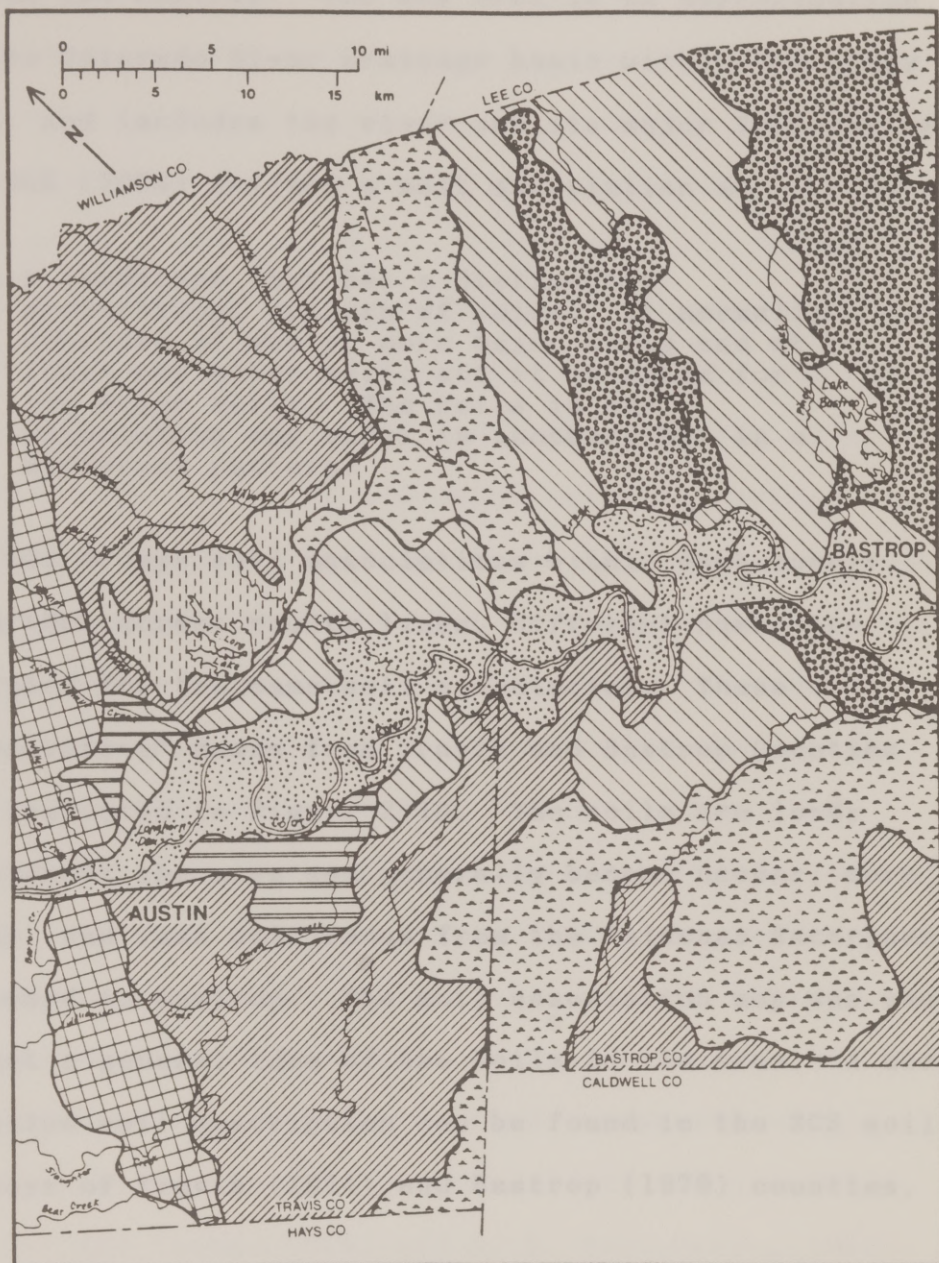


Figure 2.14: General soil map of the soil associations between Austin and Bastrop. (Adapted from SCS soil surveys of Travis (1974) and Bastrop (1979) counties)

Austin and Bastrop. The map area is an approximation of the Colorado River drainage basin within the study area, and includes the river and its major tributaries. The SCS (1974) defines a soil association as

a landscape that has a distinctive proportional pattern of soils. It normally consists of one or more major soils and at least one minor soil, and it is named for the major soils. The soils in one association may occur in another, but in a different pattern.

The SCS groups soil associations within each county, such that across county lines, different names are assigned for the same soil association. These "correlative" names from Travis and Bastrop Counties are indicated in Figure 2.14. The soils are loamy throughout the area and generally become deeper, more sandy, and less calcareous from the Balcones Escarpment eastward to Bastrop. The soil association map was used to get a general idea of the soils in the area. A more detailed soil description can be found in the SCS soil surveys of Travis (1974) and Bastrop (1979) counties.

2.4.1.5 Vegetation

The vegetation assemblages of the study area are generally associated with the underlying soils and

bedrock. The grassland-mesquite assemblage of the Blackland Prairie is primarily grassland prairie with scattered mesquites. Most of the area has been farmed and only small acreages of original vegetation remain. In heavily grazed pastures, "buffalograss", "Texas grama", and other less productive grasses have replaced "tall bunchgrass". The elm-oak-mesquite and post oak-blackjack assemblages are associated with the alluvial terrace deposits. The elm-oak-mesquite assemblage is characterized by a thick growth of shrub vegetation and occurs on remnants of the high Colorado River terraces overlying the clayey bedrock east of Austin, and on the limestone terraces developed along Onion Creek. The post oak-blackjack assemblage has heavy shrub undergrowth and is found on the unconsolidated sand and gravel terraces along the Colorado River. The bottomland assemblage is located along the Colorado River and some of its tributaries and consists of a wide variety of trees (cottonwood, sycamore, willow, pecan, ash, hackberry, and bois d'arc) and grasses (Garner and Young, 1976, and A. H. Belo Corp., 1987). Various species of rooted aquatic plant life can be found growing in the river bed itself, including

species of the genera Myriophyllum, Potomageton, and Heteranthera (Koenig, 1987).

2.4.1.6 Highland Lakes System

The Highland Lakes System of the Colorado River is a unique series of man-made lakes that extend from the Texas Hill Country near Burnet southeast into Austin. Figure 2.15 shows the location of the seven lakes and various points of reference. The lakes were built mainly for the purpose of hydroelectric power generation and water supply. Lake Travis is the only reservoir which has allocated storage for flood control (U.S. Army Corps of Engineers, 1976). Lake Austin, a constant level lake, is now largely filled with silt but serves to maintain a head for power production (A. H. Belo Corp., 1987). Town Lake is also a constant level lake, a majority of its inflow coming from Lake Austin. Commercial suction dredging of Town Lake for sand and gravel was conducted from 1960-1975, resulting in discrepancies in estimates of the present day lake volume. The release schedule for the lake system is determined by the LCRA and based on the need for conservation purposes, upstream flood protection, and downstream water supply, primarily for rice farming

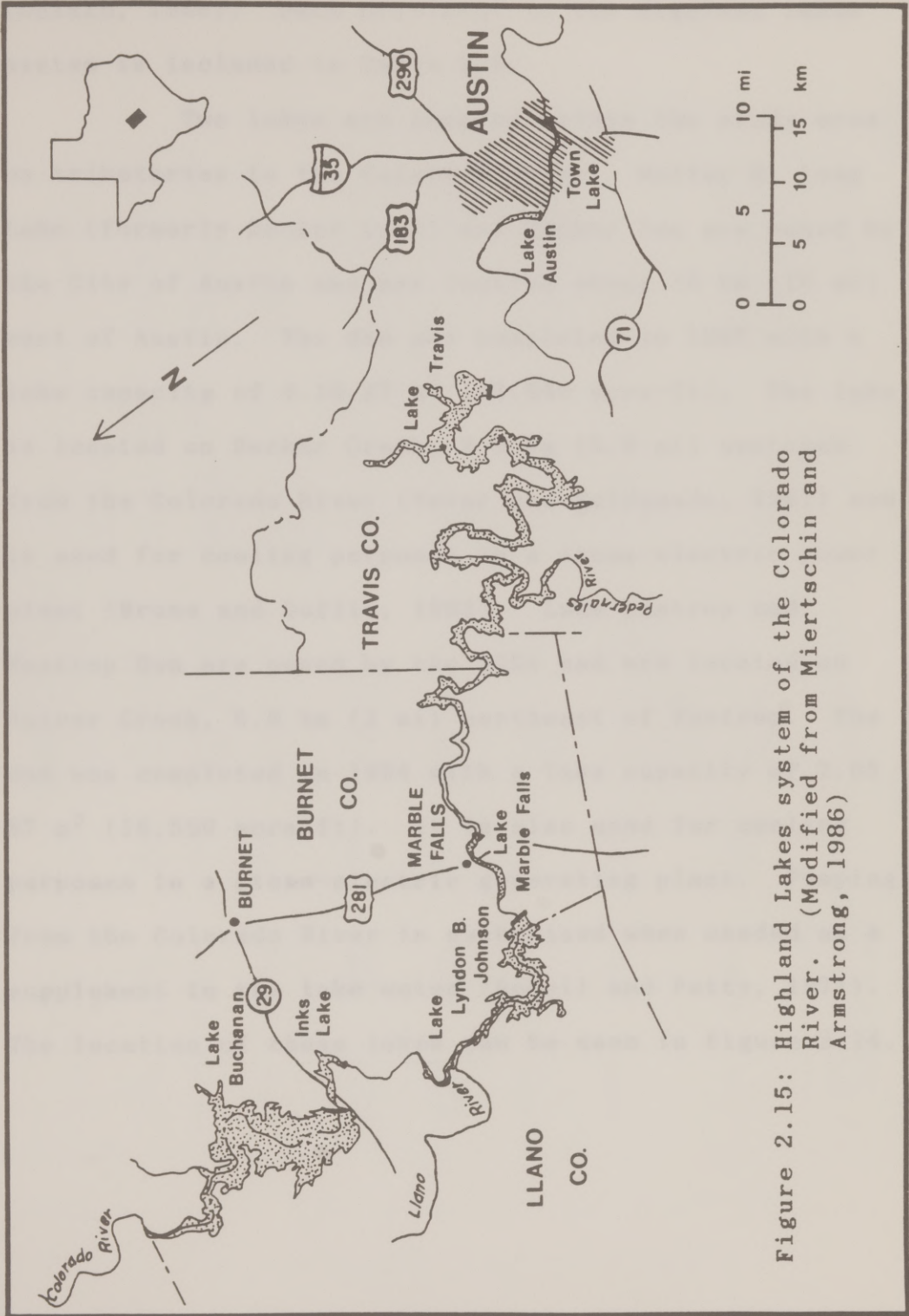


Figure 2.15: Highland Lakes system of the Colorado River. (Modified from Miertschin and Armstrong, 1986)

(Culkin, 1986). Data pertinent to the Highland Lakes system is included in Table 2.5.

Two lakes are located within the study area on tributaries to the Colorado River. Walter E. Long Lake (formerly Decker Lake) and Decker Dam are owned by the City of Austin and are located about 16 km (10 mi) east of Austin. The dam was completed in 1967 with a lake capacity of 4.19 E7 m^3 (33,940 acre-ft). The lake is located on Decker Creek, 9.5 km (5.9 mi) upstream from the Colorado River (Tovar and Maldonado, 1981) and is used for cooling purposes in a steam-electric power plant (Brune and Duffin, 1983). Lake Bastrop and Bastrop Dam are owned by the LCRA and are located on Spicer Creek, 4.8 km (3 mi) northeast of Bastrop. The dam was completed in 1964 with a lake capacity of 2.05 E7 m^3 (16,590 acre-ft). It is also used for cooling purposes in a steam-electric generating plant. Pumping from the Colorado River is authorized when needed as a supplement to the lake water (Dowell and Petty, 1971). The location of these lakes can be seen in Figure 2.14.

TABLE 2.5
HIGHLAND LAKES DATA

Lake	Dam	Owner	Dam Type	Orig. Capac. m ³ (ac-ft)	Com- pleted	Original Purpose
Buchanan	Buchanan	LCRA	Multiple concrete arch, gated and gravity sections	1.18 E9 (955,200) (usable)	1938	Hydroelectric power production
Inks	Roy Inks	LCRA	Concrete gravity	2.16 E7 (17,540) (spillway elev.)	1938	Hydroelectric power production
Lyndon B. Johnson	Alvin Wirtz	LCRA	Concrete and earthfill	1.17 E8 (138,500) (oper. elev.)	1951	Conservation, irrigation, hydroelectric power prod.
Marble Falls	Max Starcke	LCRA	Concrete with roof-weir gates	1.08 E7 (8,760) (oper. elev.)	1951	Conservation, irrigation, hydroelectric power prod.
Travis	Mansfield	LCRA	Concrete gravity, earth and rock fill	2.41 E9 (1,954,000)* (spillway elev.)	1942	Municipal, irrigation, mining, recreation, hydroelectric power
Austin	Tom Miller	City of Austin	Concrete gravity overflow, piers and slab with gated spillway, and rockfill sections	2.59 E7 (21,000) (oper. elev.)	1939#	Hydroelectric power production
Town	Longhorn	City of Austin	Concrete with earthen approaches	7.40 E6 (6,000) (top of gates)	1960	Provide cooling water for two electric generating plants on lake

* Maximum design flood capacity is 3,223,000 acre-feet.

Original dam completed in 1893 (Lake McDonald) and destroyed by 1900 flood. Second dam completed in 1915.

(Dowell and Petty, 1971, City of Austin, 1988, and Culkin, 1986)

2.4.2 GEOLOGY

2.4.2.1 General

The rocks within the Colorado River drainage basin vary in age from the Precambrian (570+ million years) rocks of the Burnet-Llano region to the Holocene (Recent) deposits along the Gulf Coast. Figure 2.16 shows the river basin and study area superimposed on a geologic map of Texas. Figure 2.17 is included to orient the reader to the geologic time scale referred to in Figure 2.16.

The river and terrace sediment in the study area was partially derived from the drainage basin upstream of the Austin area, therefore a brief description of the rocks in Figure 2.16 follows. The western extreme of the drainage basin is underlain by the Tertiary age (Pliocene, Miocene, Oligocene) gravels, sands, silts, and clays of fluvial deposits. Between the Great Plains region and the Burnet-Llano area lie rocks of early Cretaceous (Comanche series), Triassic, and Permian age. The early Cretaceous rocks, mostly limestone, were deposited by the shallow seas which covered most of Texas at this time. The Triassic rocks are mostly made up of sandy and clayey lake deposits. The Permian age rocks are remnants of

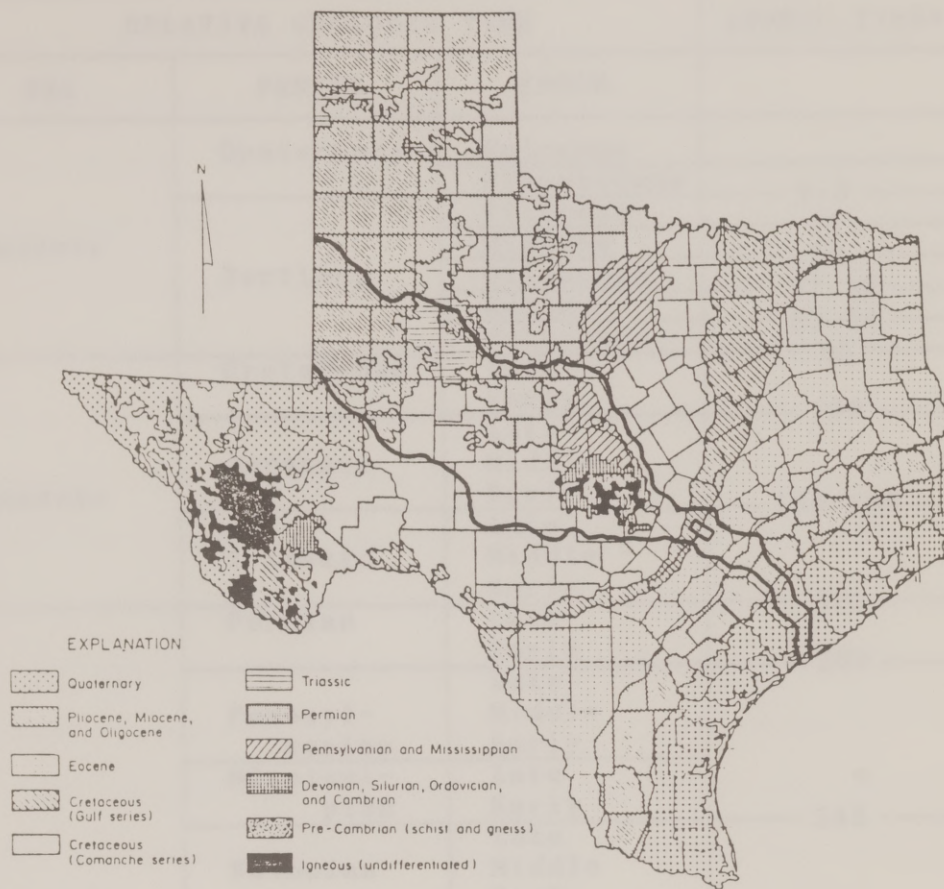


Figure 2.16: Geologic map of Texas, including an outline of the Colorado River drainage basin and the area of interest. (Modified from A. H. Belo Corp., 1987)

RELATIVE GEOLOGIC TIME			ATOMIC TIME*
ERA	PERIOD	EPOCH	
Cenozoic	Quaternary	Holocene	
		Pleistocene	2-3
	Tertiary	Pliocene	12
		Miocene	26
		Oligocene	37-38
		Eocene	53-54
		Paleocene	65
Mesozoic	Cretaceous	Late	
		Early	136
	Jurassic	Late	
		Middle	
		Early	190-195
	Triassic	Late	
Middle			
Early			
Paleozoic	Permian	Late	225
		Early	280
	Pennsylvanian	Late	
		Middle	
	Mississippian	Early	
		Late	345
	Devonian	Early	
		Late	395
	Silurian	Middle	
Early		430-440	
Ordovician	Late		
	Middle	430-440	
Cambrian	Early	500	
	Late		
Precambrian		Early	570
			3,600+







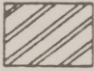

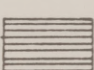
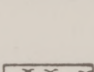
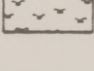
*Estimated ages of time boundaries (millions of years)

Figure 2.17: Geologic time scale. (Modified after Putnam and Bassett, 1971)

limestone shelf deposits and deeper limestone reefs along with the salt, gypsum, and red mud deposits in the shallow basins and wide tidal flats. The Pennsylvanian and Mississippian rocks (sands, shales, limestones) resulted from fluvial, deltaic, and shallow marine near-shore deposits. The Burnet-Llano area is characterized by Precambrian igneous and metamorphic rocks (granites, schists, gneisses) that form a central lowland. The Precambrian rocks are encircled by early Paleozoic (Cambrian, Ordovician, Silurian, Devonian) sandstones, limestones, shales, and dolomites that form a highlands. Just west of Austin, the river flows through relatively flat-lying Cretaceous (Comanche series) limestones and marls (calcareous clay) that the river has deeply incised, forming high cliffs. At Austin, the Balcones Escarpment separates the relatively resistant limestones to the west from the softer rocks to the east. The rocks of late Cretaceous age (Gulf series) underlie the western portion of the study area. They consist of various sandstones, limestones, and shales that formed in marine waters and where rivers, deltas, and shallow marine shelves existed. Minor volcanic activity also occurred during the late Cretaceous age. The rocks of the Cenozoic Era

were deposited by the environments characteristic of a retreating sea. Although there have been minor encroachments, the sea currently continues the slow southeasterly retreat toward the gulf (Sheldon, 1979, Baker and Penteado-Orellana, 1978, Brune and Duffin, 1983, and Sears, 1978).

Figure 2.18 is a more detailed geologic map of the study area. The map is extended to the west to include the Balcones Fault zone in order to emphasize the abrupt change in the geologic environment. The fault zone marks the eastern boundary of the hill country and the beginning of the transition into the coastal plains. The rocks in the Austin area and west include limestones, dolomites, marls (calcareous clays), and shales (compacted clays). East of Austin, clays, shales, silts, and sandstones dominate. East of the fault zone there is also a tremendous increase in the amount of Quaternary age fluvial sediments, i.e., alluvium and terrace deposits. The river deposits are a function of bed rock type and are direct evidence of the abrupt change in geological environments. West of the fault zone, the river travels through incised meanders along a path dictated by resistant bed rock,

Time*			LEGEND: <u>GEOLOGIC MAP</u>	
	SYSTEM	Series	<u>Group/Formation</u>	
0.01	QUATERNARY	Recent		Alluvium (gravel, sand, silt, clay)
		Pleis- tocene		Terrace deposits; includes Onion Creek Marl and high terrace deposits (gravel, sand, silt, clay; often calcareous)
38	TERTIARY	Eocene		Carrizo Sand (sandstone)
55				Wilcox Group (sand, sandstone, sandy clay, clay, shale)
65				Midway Group (clay, silt, sand)
101	CRETACEOUS	Gulf		Navarro and Taylor Groups (sandstone, silt, clay, marl)
				Austin Chalk (chalk and marl)
				Igneous rocks (basalt and tuff)
		Comanche		Eagle Ford Group, Buda Limestone, Del Rio Clay, Georgetown Formation (shale, limestone, clay, marl)
				Fredericksberg Group (limestone, dolomite, marl)
				Glen Rose Formation, upper member (limestone, dolomite, marl)

*(million years)

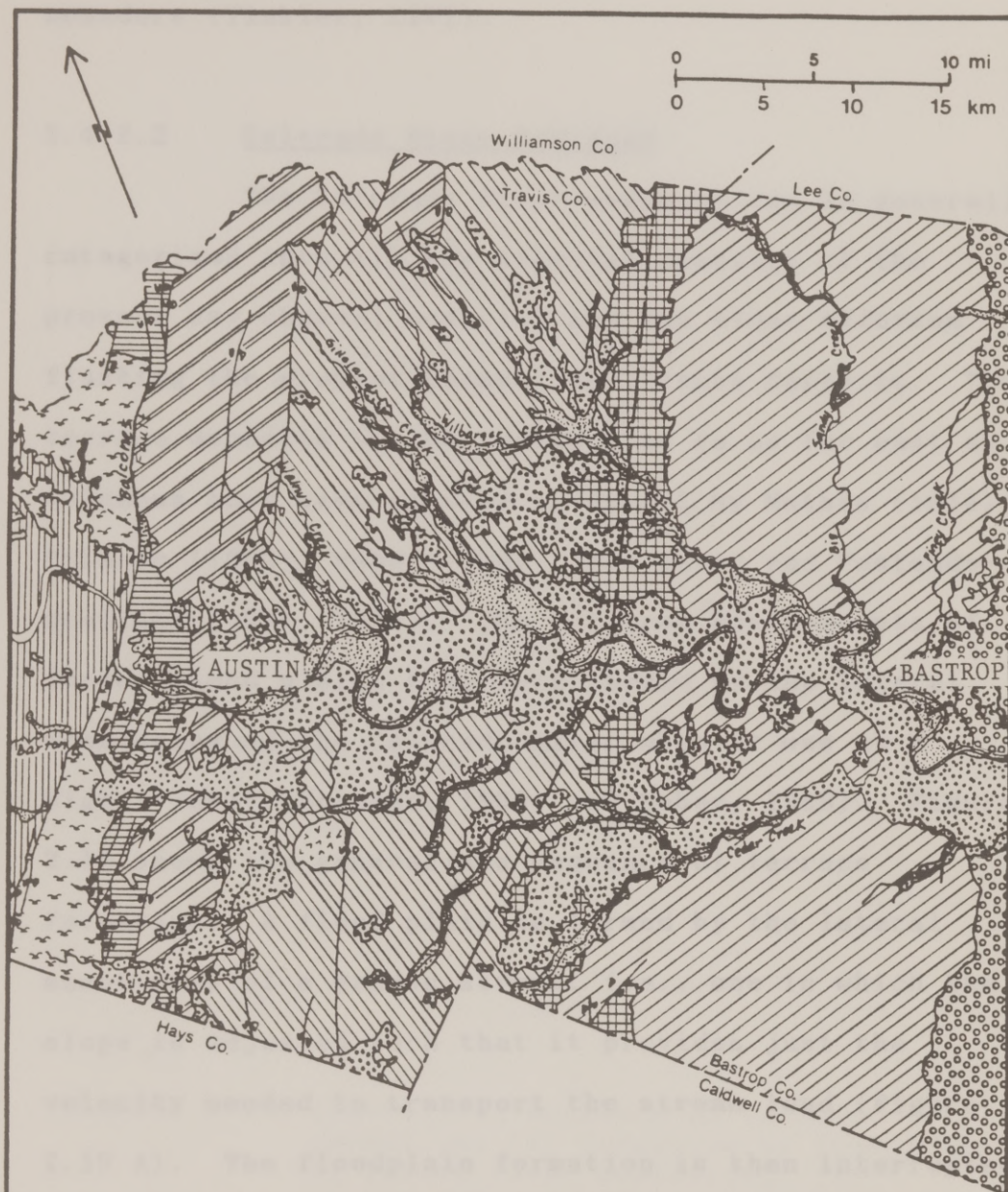


Figure 2.18: Geologic map of Travis and Bastrop counties between Austin and Bastrop. (Adapted from Brune and Duffin, 1983, Bureau of Economic Geology, 1974, Follett, 1970, and van Eysinga, 1978)

whereas to the east, the river is free to form alluvial meanders (Tinkler, 1971).

2.4.2.2 Colorado River Sediment

The Colorado River sediment can be generally categorized into (i) the alluvial deposits of the present day channel and (ii) and the older alluvium flanking the present channel as terrace deposits. The terrace deposits in the Austin area to as far east as Columbus have been studied in detail by Mathis (1944), Urbanec (1963), Weber (1968), and Baker and Penteado-Orellana (1977, 1978). The terraces are remnants of former flood plains that were formed by the lateral meandering of the Colorado River when it was at a higher level (Urbanec, 1963, and Weber, 1968). Figure 2.19 shows the generalized sequence of terrace formation. A flood plain is formed by the lateral meandering of a graded stream, i.e., one in which the slope is adjusted such that it provides just the velocity needed to transport the stream load (Figure 2.19 A). The floodplain formation is then interrupted by the river downcutting into the underlying sediments to a lower level. As the river becomes graded again, it cuts a broad valley as it meanders, leaving bench

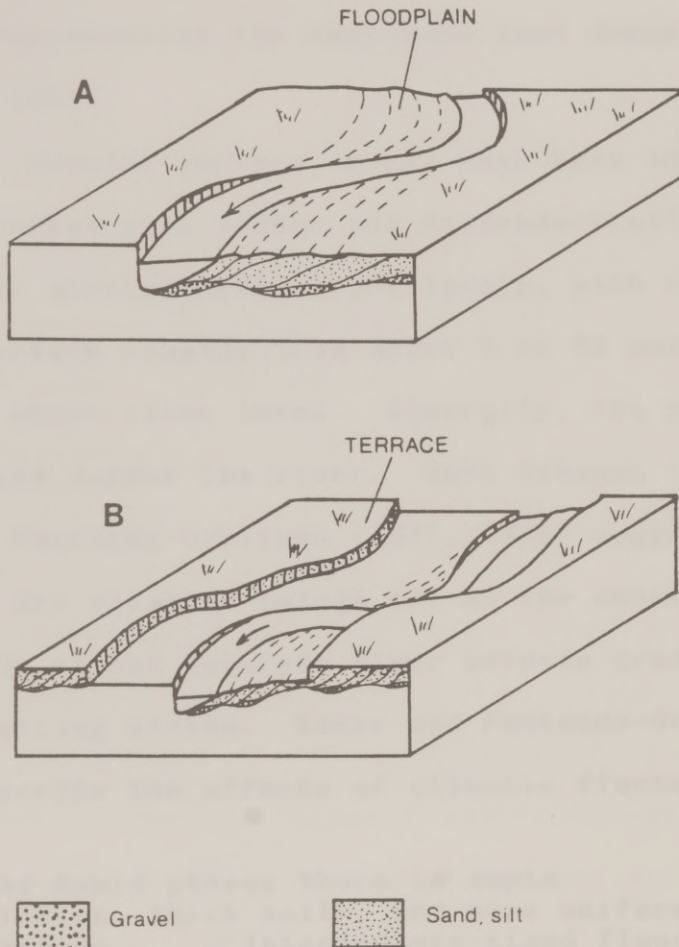


Figure 2.19: Generalized sequence of terrace formation: (A) formation of floodplain by graded river meandering, (B) terraces form as floodplain formation is interrupted by valley deepening; as the river becomes graded again, it cuts a broad valley as it meanders. (Adapted from Reinech and Singh, 1980, and Leopold et al., 1964)

type remnants at a higher elevation (Figure 2.19 B). The terraces consist of gravel overlain by sand and silt, the gravel representing the bedload, and the sand and silt representing the suspended load deposits (Urbanec, 1963).

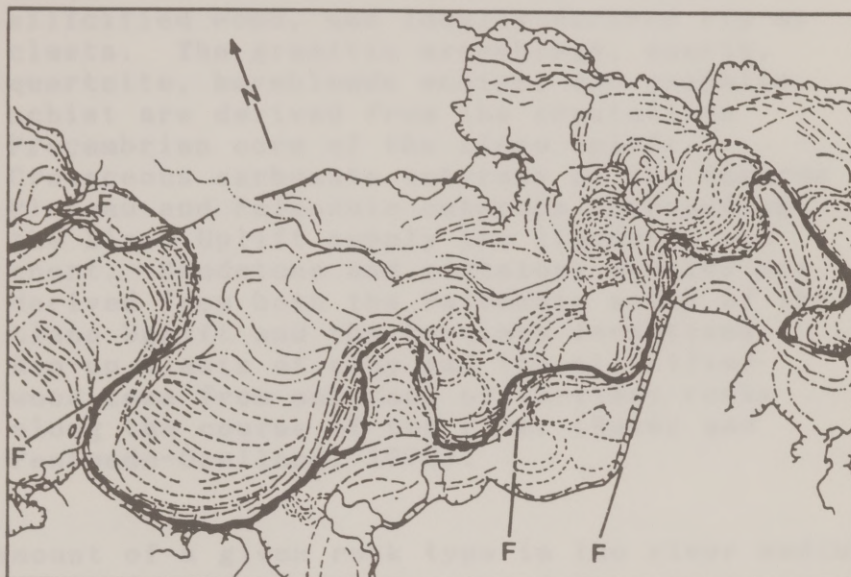
Several terrace levels have been identified. The most recent work (Baker and Penteadó-Orellana, 1977, 1978) distinguishes eight levels, with the terrace surface ranging from about 2 to 85 meters (6 to 280 feet) above river level. Generally, the younger terraces are nearer the river. Both Urbanec (1963) and Baker and Penteadó-Orellana (1977, 1978) suggest that humid and dry climatic swings may be the cause of the fluctuation of the Colorado River between graded stream and downcutting stream. Baker and Penteadó-Orellana (1978) describe the effects of climatic fluctuation:

During humid phases there is ample vegetation, thick soils, and more uniform streamflow . . . Intermediate-sized floods occur relatively frequently . . . Floods also tend to be longer in duration . . . All of these factors favor more continued transport of sediment and promote better sorting in fluvial environments. Sediment on interfluvies (i.e., the area between adjacent streams flowing in the same general direction) will generally be stabilized during such episodes, resulting in only finer sediment being introduced into the

A change to relatively arid conditions would involve increased dominance of the fluvial regimen by infrequent high-intensity thunderstorms. The xerophytic vegetation favored by such meteorological regimen will not retard active erosion of the interfluves by intense rainfall. The enhanced gullies and rills will introduce considerable coarse sediment into the nearby stream channels . . . The sediment . . . is likely to be both coarse and poorly sorted.

Figure 2.20 is a geomorphic map of the alluvial valley of the Colorado River between east Austin and Webberville, and is included as an illustrative example of the different cross-cutting channel assemblages. The assemblages were either incised into bedrock or superimposed on older alluvial deposits. The phases of floodplain development are numbered 2 to 7, with 2 and 7 representing the youngest and oldest, respectively. These numbers are not fully representative of terrace levels, however, because some of the early phases involved cutting without deposition (Baker and Penteadó-Orellana, 1977).

The sediments of the terrace and related river deposits are made up of mostly sand and gravel size grains (Urbanec, 1963 and Weber, 1968) and consist of a variety of lithologic types, including



- | | |
|---------------|-----------------|
| Valley Margin | Channel 4 |
| Channel 6 | Channel 3 |
| Channel 6A | Channel 2 |
| Channel 6B | Modern River |
| Channel 5 | Fault Control ? |

0 1 2 mi
0 1 2 3 km

Figure 2.20: Geomorphic map of the alluvial valley of the Colorado River between east Austin and Webberville. (After Baker and Penteado-Orellana, 1977)

. . . a granitic assemblage (granite, gneiss, aplite, pegmatite, and graphitic granite), quartz and quartzite, chert, limestone, sandstone, siltstone, schist, silicified wood, and locally-derived rip-up clasts. The granitic assemblage, quartz, quartzite, hornblende schist, and graphite schist are derived from the crystalline Precambrian core of the Llano Uplift. Cretaceous carbonate outcrops of the Edwards Plateau and Paleozoic outcrops surrounding the Llano Uplift supply the limestone and chert. Sandstone and siltstone pebbles are derived from both the Paleozoic units of the Llano Uplift and the Tertiary formations. . . Rip-up clasts of clay and the silicified wood come from outcrops of Tertiary rocks along the course of the river (Baker and Penteado-Orellana, 1978).

The amount of a given rock type in the river sediment depends on its availability from the upstream drainage area and its durability under the physical and chemical stresses that occur during transport and storage in the fluvial system (Baker and Penteado-Orellana, 1978).

Mathis (1944) examined the heavy minerals (specific gravity > about 2.9) of the Colorado River terraces between Mansfield Dam (Lake Travis) and Altair, Texas, about 209 river miles downstream. Most of the heavy minerals originated from the Central Mineral Region in central Texas. He found that certain distinctive mineral ratios could be used to identify and correlate the various terrace deposits.

The present day lower Colorado River is considered to be a bed-load stream which transports coarse sands and gravels throughout most of its extent (McGowen and Garner, 1970, and Morton and McGowen, 1980). In their studies of the Colorado River between Austin and La Grange, Baker and Penteado-Orellana (1977) classify the present day river to be a degradational coarse-grained meanderbelt, influenced by a climate considered transitional between arid and humid conditions. The channel bed sediments are poorly sorted, composed mostly of sand and gravel, with only about a 10 percent silt-clay fraction. Figure 2.21 shows cumulative frequency curves for grain size for the present day and older river phases. Data for the curves was based on sieve analysis of samples from 14 locations between Austin and La Grange (Baker and Penteado-Orellana, 1977), however, the locations of the sample sites were not specified. For the modern river channel, number 1, the curve shows a 10 percent silt-clay fraction, a 17 percent sand fraction, and a 73 percent fraction of gravel and coarser fragments. Most of the other channel phases follow this general trend, which is reflective of low sinuosity streams. The two outlying curves represent the finer sand and silt

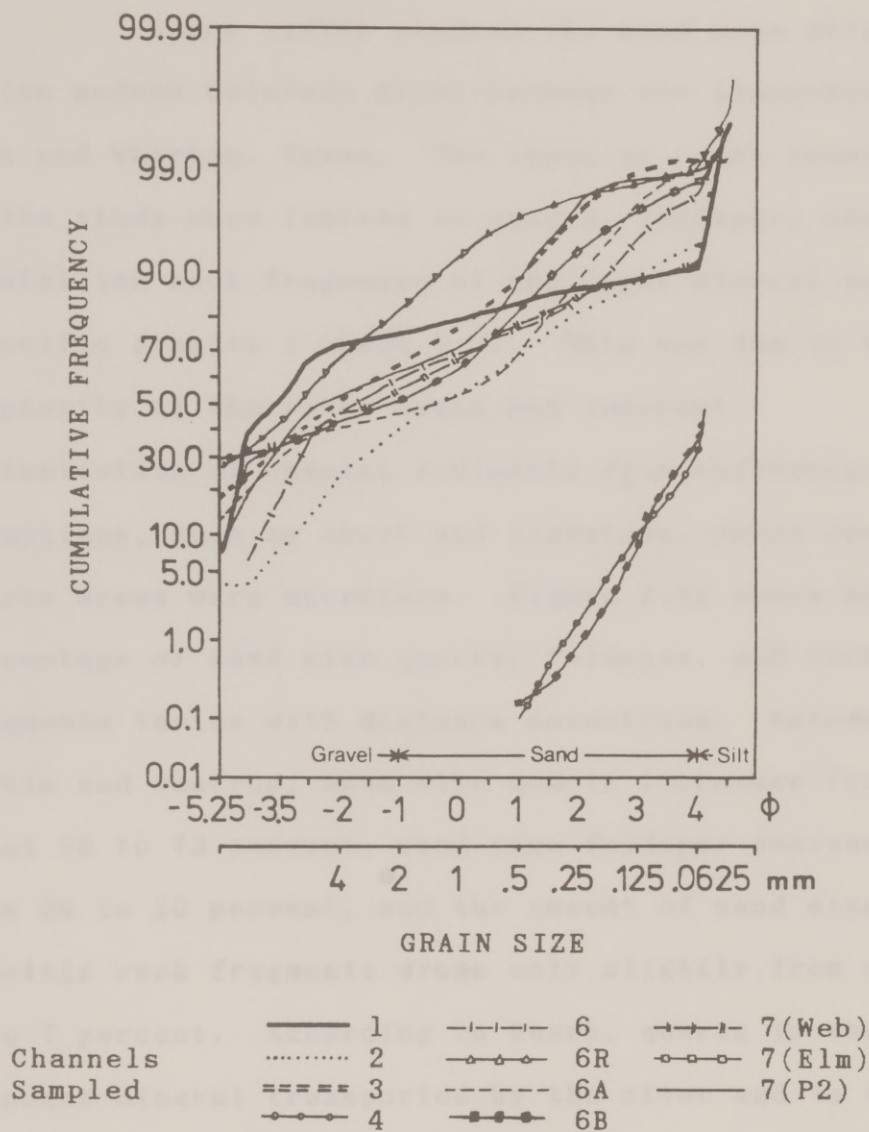


Figure 2.21: Cumulative frequency curve for grain size in the modern Colorado River channel bed (1) and the various older channel phases (2-7). (Modified from Baker and Pentead-Orellana, 1977)

phases transported by highly sinuous stream channels (Baker and Penteado-Orellana, 1977).

Sears (1978) studied the sand size alluvium of the modern Colorado River between the Llano-Burnet area and Wharton, Texas. The types of rocks examined in the study were limited to quartz, feldspar, and crystalline rock fragments of the light mineral suite (specific gravity < about 2.9). This was due to the complexity of the river basin and inherent contamination of channel sediments from sedimentary formations, such as chert and limestone, whose specific source areas were uncertain. Figure 2.22 shows how the percentage of sand size quartz, feldspar, and rock fragments varies with distance downstream. Between Austin and Bastrop, sand size quartz increases from about 68 to 73 percent, sand size feldspar decreases from 24 to 20 percent, and the amount of sand size granitic rock fragments drops only slightly from about 8 to 7 percent. According to Sears, quartz is the most abundant mineral transported by the river and is the most resistant to weathering. Feldspar is relatively unstable and deteriorates rapidly. Sears points out that at Kingsland, there is a 1:1 ratio of potassium feldspar to plagioclase (sodium and/or calcium rich)

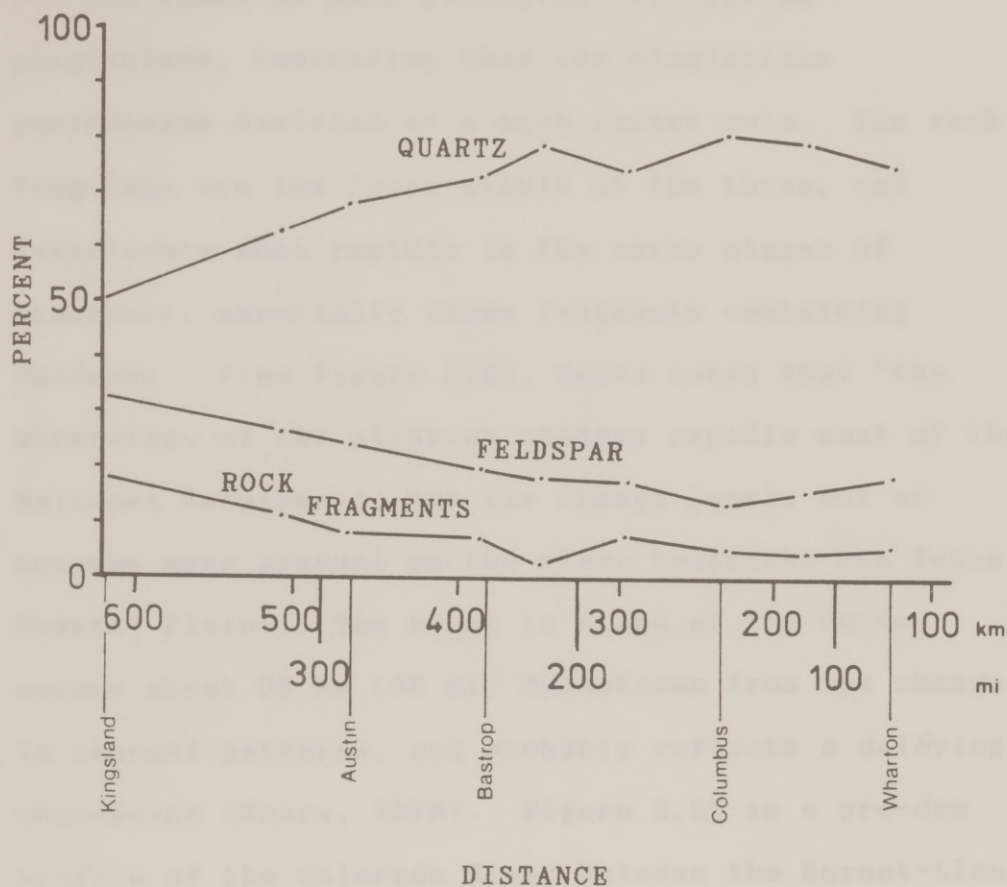


Figure 2.22: Graph of sand size quartz, granitic feldspar, and rock fragment percentages vs. distance from mouth of the modern Colorado River. (Modified from Sears, 1978)

feldspar. At Wharton, however, the alluvium sampled had 4.5 times as much potassium feldspar as plagioclase, indicating that the plagioclase percentages diminish at a much faster rate. The rock fragments are the least stable of the three, and deteriorate most rapidly in the early stages of transport, especially those fragments containing feldspar. From Figure 2.22, Sears notes that "the mineralogy of the alluvium changes rapidly west of the Balcones Escarpment, but the change levels out or becomes more gradual as the river transects the Texas Coastal Plain". The break in slope of the curves occurs about 35 km (56 mi) downstream from the change in channel patterns, and probably reflects a delaying phenomenon (Sears, 1978). Figure 2.23 is a pre-dam profile of the Colorado River between the Burnet-Llano region and Wharton. West of Austin and the Balcones Escarpment, the average channel gradient is 0.69 m/km (3.65 ft/mi) with a profile indicative of rugged topography. Between Austin and Wharton, the gradient greatly decreases to an average of 0.29 m/km (1.53 ft/mi) (Sears, 1978). Sears (1978) concludes:

Downstream changes in mineralogy correlate rather well with changes in channel hydrology. Rapid loss of unstable minerals

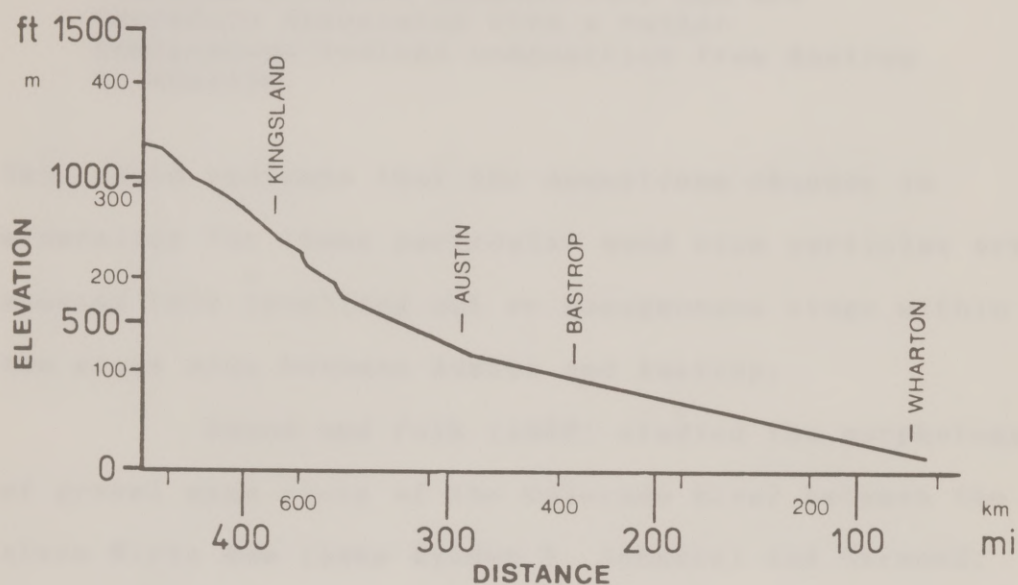


Figure 2.23: Colorado River pre-dam profile from the Burnet-Llano area to Wharton, Texas. Distance indicates distance upstream from mouth. (Modified from Sears, 1978)

is associated with the narrow, incised channel patterns of the Edwards Plateau and Llano Basin. The wide alluvial valley and the lower stream gradients east of the Balcones Escarpment seem incapable of changing sediment composition, and are therefore associated with a rather homogeneous bedload composition from Bastrop to Wharton.

This would indicate that the downstream changes in mineralogy for these particular sand size particles are nearing this levelling out or homogeneous stage within the study area between Austin and Bastrop.

Sneed and Folk (1958) studied the morphology of gravel size rocks of the Colorado River between the Alvin Wirtz dam (Lake Lyndon B. Johnson) and Garwood, Texas, 430 km (267 mi) downstream. To determine the variation of rock types with distance downstream, 250-300 gravel size rocks (>7mm) were collected at each station (Figure 2.24). Chert and limestone were the most abundant, followed by quartz, granite, and miscellaneous rocks (sandstones, gneisses, schists). It should be noted that the last source of granite and quartz is just downstream of the Alvin Wirtz dam, and the last source of limestone and chert lies just upstream of the Austin station (Montopolis bridge). The percentage of limestone increases rapidly between the Marble Falls dam and the Austin station, as the

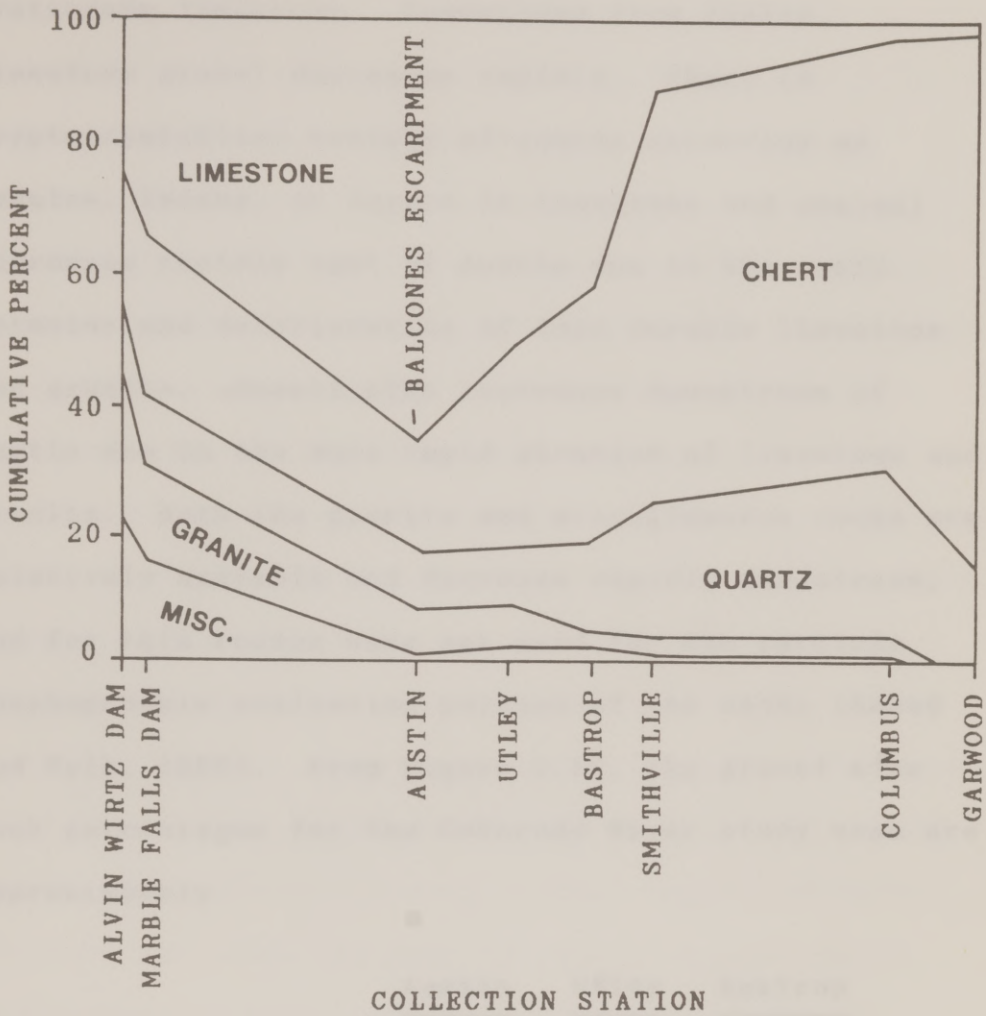


Figure 2.24: Graph of gravel size limestone, chert, quartz, granite, and miscellaneous (sandstone and metamorphic) rock percentages vs. location along the modern Colorado River. (After Sears, 1978, and Sneed and Folk, 1958)

river crosses a continuous outcropping of Paleozoic and Cretaceous limestone. Downstream from Austin, limestone gravel decreases rapidly. Chert (a cryptocrystalline variety of quartz occurring as nodules, lenses, or layers in limestone and shales) increases rapidly east of Austin due to the rapid abrasion and deterioration of less durable limestone and granite. Quartz also increases downstream of Austin due to the more rapid abrasion of limestone and granite. Both the granite and miscellaneous rocks are relatively unstable and decrease rapidly downstream, and for this reason were not used for the particle morphogenesis evaluation portion of the study (Sneed and Folk, 1958). From Figure 2.24, the gravel size rock percentages for the Colorado River study area are approximately:

	<u>Austin</u>	<u>Utley</u>	<u>Bastrop</u>
limestone	64	52	42
chert	19	30	38
quartz	8	8	15
granite	7	7	2
misc.	2	3	3

Sneed and Folk (1958) also studied the roundness and sphericity of gravels as possible indicators of transport distance. Fifty samples of

size range 32-64 mm from each station were examined, and on occasion some rocks slightly outside the specified range were included to obtain the desired total of fifty. It was found that quartz rounds appreciably during transport downstream, and three-fourths of the total change occurs in about half the distance from Alvin Wirtz dam to Garwood. Chert shows no significant change in rounding between the first stations and the midstream stations because of the continuous supply of fresh chert until just upstream of Austin. At the downstream stations, the roundness has increased significantly. Over the entire section of the river, quartz is more rounded than chert, and accomplishes the rounding at a faster rate. The reason for this is that chert is brittle and tends to spall off in large flakes, giving a sharp-edged conchoidal fracture and many new flat to gently concave faces, while quartz rounds smoothly and uniformly by the breaking away of minute chips. The limestone gravel shows no significant change in roundness over the entire reach of the river, suggesting that it is soft enough to reach maximum roundness in only a few miles. Within the specified size range, there is no significant change in roundness vs. size for any of the

rock types. Upon casual examination of rocks above and below this size range, it was found that the expected increase in roundness with increase in size was clearly evident. Also noted was a roundness reversal between Utley and Bastrop, i.e., gravels of all rock types were more angular at Bastrop than at Utley, 24 miles upstream. With bad sampling disregarded as a reason for this reversal, no valid explanation could be offered, and only a suggestion that it may be "due to a local variation in stream characteristics."

The sphericity and form of the gravels are also influenced by rock type, size, and travel distance, and it was found that:

Quartz and chert show generally parallel behavior. Quartz pebbles 54-70 mm. long tend to roll downstream like a rolling pin, hence become more rodlike but maintain fairly constant numerical sphericity. Quartz pebbles 30-54 mm. long appear to bounce randomly downstream, therefore wear on their two longer axes and sphericity increases significantly. Chert pebbles 38-70 mm. long seem to spall off chips parallel with the bedding and hence decrease markedly in sphericity downstream. Contrarily, chert pebbles of 30-38 mm. wear like the smaller quartz pebbles and increase in sphericity downstream. Limestone shows no systematic changes in sphericity (Sneed and Folk, 1958).

Sneed and Folk (1958) concluded that the comparison of sphericity and form in relation to specific gravel size is the best method for determining distance from source for the most durable rocks.

Besides those factors which influence the shape of an individual particle, the factors which affect the properties of an aggregate of particles can be combined under the term "selective sorting" or "bypassing":

. . . given a certain assemblage of pebble shapes on a bar, a river flowing over the bar may tend to pick up some shapes more easily than others, so that a downstream deposit may have a different mean sphericity or roundness from that of the lag deposit upstream, even though none of the individual particles has suffered any shape modification at all (Sneed and Folk, 1958).

Sneed and Folk (1958) determined, however, that this process is negligible for Colorado River gravels.

The preceeding discussion of the geology of the Colorado River indicates that the Austin area marks the beginning of a major change in the nature of the river. West of Austin, the river meanders are controlled by resistant bedrock and faulting patterns, whereas east of Austin, the river is free to form alluvial meanders. The source rocks of the alluvial

and terrace deposits are found as far upstream as the Llano-Burnet region. The percentages of rock types found in both the sand and gravel size material undergo the greatest changes between the Llano-Burnet region and the Bastrop/Smithville area. Downstream, the river reflects more homogeneous conditions. The Colorado River between Austin and Bastrop, then, is responding to geological transition.

2.4.3 GROUNDWATER HYDROLOGY

The relationship of the Colorado River study area to the major aquifer trends of Texas can be seen in Figure 2.25. As expected, the major aquifers closely parallel the geologic trends as seen in Figures 2.16 and 2.18. Within Travis County, the hydrologic units which yield fresh to moderately saline groundwater are, in order of production, the Edwards and associated limestones (Fredericksberg and Washita Groups), the Trinity Group (Lower Comanche Series, including the Glen Rose Formation), the alluvium and terrace deposits, the Austin Chalk, the Navarro and Taylor Groups, igneous rocks around Pilot Knob, and the Midway Group (Brune and Duffin, 1983). Within Bastrop County, those formations yielding moderate to large

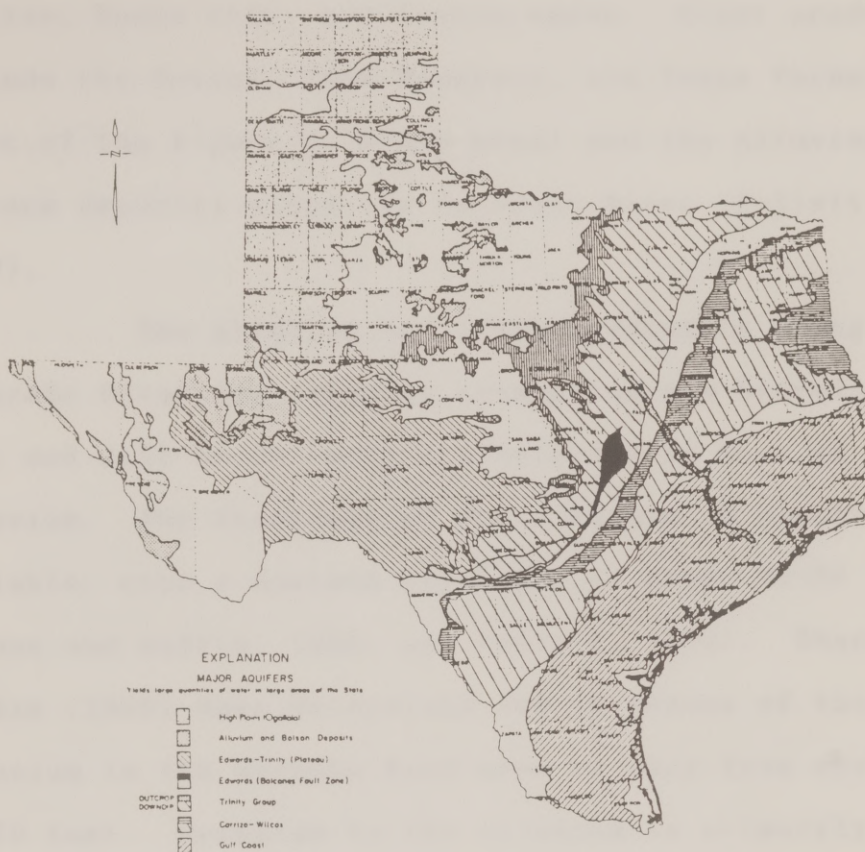


Figure 2.25: Major aquifers of Texas. (Texas Water Commission, 1984)

quantities of water include the Wilcox Group, and the Carrizo, Queen City, and Sparta sands. Minor producers include the Reklaw, Cook Mountain, and Yegua Formations (east of the Figure 2.18 map area) and the alluvium and terrace deposits along the Colorado River (Follett, 1970).

The alluvium and terrace deposits along the Colorado River are commonly treated as one hydrologic unit and will be collectively referred to here as alluvium. The thickness of the alluvium is highly variable, with a maximum thickness of about 50-60 feet (Brune and Duffin, 1983, and Follett, 1970). Sharp and Larkin (1988) have determined the thickness of the alluvium in the Hornsby Bend area to vary from about 30-70 feet. Recharge to the alluvium is primarily from infiltration of precipitation, with minor amounts from tributaries of the Colorado River and from subsurface flow from the north (Brune and Duffin, 1983, and Sharp and Larkin, 1988). The average annual recharge to the alluvium is estimated to be 5-8 percent of the mean annual rainfall. Sharp and Larkin (1988), Brune and Duffin (1983), and Follett (1970) all concluded that the groundwater in the alluvium is influent to the Colorado river during normal flow conditions. Springs

above river level may also appear where groundwater flows from the base of the alluvium into the river (Brune and Duffin, 1983, and Follett, 1970). During high river stages, however, the river may become temporarily influent.

Simons, Li, and Associates (1982) discuss the forces that cause the movement of water through alluvial bank material, in a general setting:

1. On the rising stage a gradient develops, sloping from the river channel into the bank material. On the falling stage, the energy gradient reverses direction and water moves through the banks toward the river channel, decreasing the stability of the bank.

2. If the water table is higher than water stage, flow will be from the banks into the river. The high water table may result from many conditions: (a) a wet period during which water draining from adjacent watersheds saturated the floodplain to a higher level, (b) poor drainage conditions resulting from deterioration or failure of drainage systems, (c) increased infiltration resulting from changes in land use causing an increase in water level, and (d) development of the adjacent floodplain for homes and businesses that utilize septic tanks and leach fields to dispose of waste water and sewage.

3. In general, the storage and release of water for hydropower generation causes numerous fluctuations in river stage. These changes in stage, even though relatively small, cause flow conditions in the banks as described in the first paragraph.

4. Wind waves cause local variations in stage that introduce inflow and outflow of water from the banks. However, because the duration of the change in stage is small, the inflow and outflow phenomena are usually concentrated locally in the surface of the banks.

5. Boat-generated waves have an effect similar to wind waves, but the characteristics of the waves generated are different.

Brune and Duffin (1983) inventoried approximately 177 wells and springs from alluvial deposits in Travis and adjacent counties. Most of the wells are used as a source for public supply, domestic water, and livestock supply. Pumping tests from wells in Travis County resulted in hydraulic conductivities ranging from 334,100-594,800 L/d/sq.m (8,200-14,600 gal/d/sq.ft) or 0.39-0.69 cm/s (0.15-0.27 in/s). Transmissivities may be expected anywhere from 0-4,967,200 L/d/m (0-400,000 gal/d/ft) due to the great range in permeability and thickness of the water-bearing alluvium. It should be pointed out that these wells were tested in thick, coarse gravel alluvium, and the resulting values should be treated as maximums. Hydraulic conductivity was also measured on soil samples collected in the Hornsby Bend area (Sharp and Larkin, 1987). The results showed that the hydraulic

conductivities varied from about 1.41 E-3 to 14.1 E-3 cm/s (0.556 E-3 to 5.56 E-3 in/s) in most soils along the river.

2.4.4 SEDIMENT SOURCES

2.4.4.1 Natural Sources

The sources of sediment to the Colorado River from upstream of the study area and the source rocks and soils within the study area have been discussed in general terms. In the course of the literature review, no references could be found pertaining to site specific sediment sources or sinks for the study area. Sears (1978) concludes that tributaries provide a continual supply of sediment to the river. Sediment sources include older stream terraces and a possibly significant contribution from the Tertiary age rocks. He cites an example at Smithville, about 39 km (24 mi) downstream from Bastrop, where an Eocene oyster reef exposed at the channel has resulted in the coarse channel sediment at this location to be made up entirely of broken mollusk fragments. Sears also attempted to determine how much of the modern channel alluvium is reworked from older terraces, however, the results were inconclusive.

McGowen and Garner (1970) studied the point bars of the Colorado River from Smithville to Matagorda. Although this reach of the river is located downstream of the study area, it does provide clues as to the physiographic features one would expect with coarse-grained point-bars. Figure 2.26 is a plan sketch similar to a typical lower Colorado River point bar, illustrating the principle physiographic features. The concave bank is densely vegetated, which tends to retard lateral cutting by the stream. Sediment (clayey silt to fine sand) is deposited here only during extreme flooding. Scour pools are found in the deeper part of the river adjacent to the concave bank. Maximum depths in the scour pools range from 0.9-1.8 m (3.0-6.0 ft). During low flow, bed-load sediment in the scour pool area is not usually transported. Scour troughs commonly develop downstream from large obstructions, such as trees that fall into the scour pools. They are typically scoured through pebbly coarse sand with a sandy pebble to cobble gravel bottom. The troughs have been observed to be about 0.3-0.6 m (1.0-2.0 ft) deep, 1.5-2.4 m (5.0-8.0 ft) wide, and up to 15.2 m (50 ft) long. The lower point bar includes the area between the low water level and

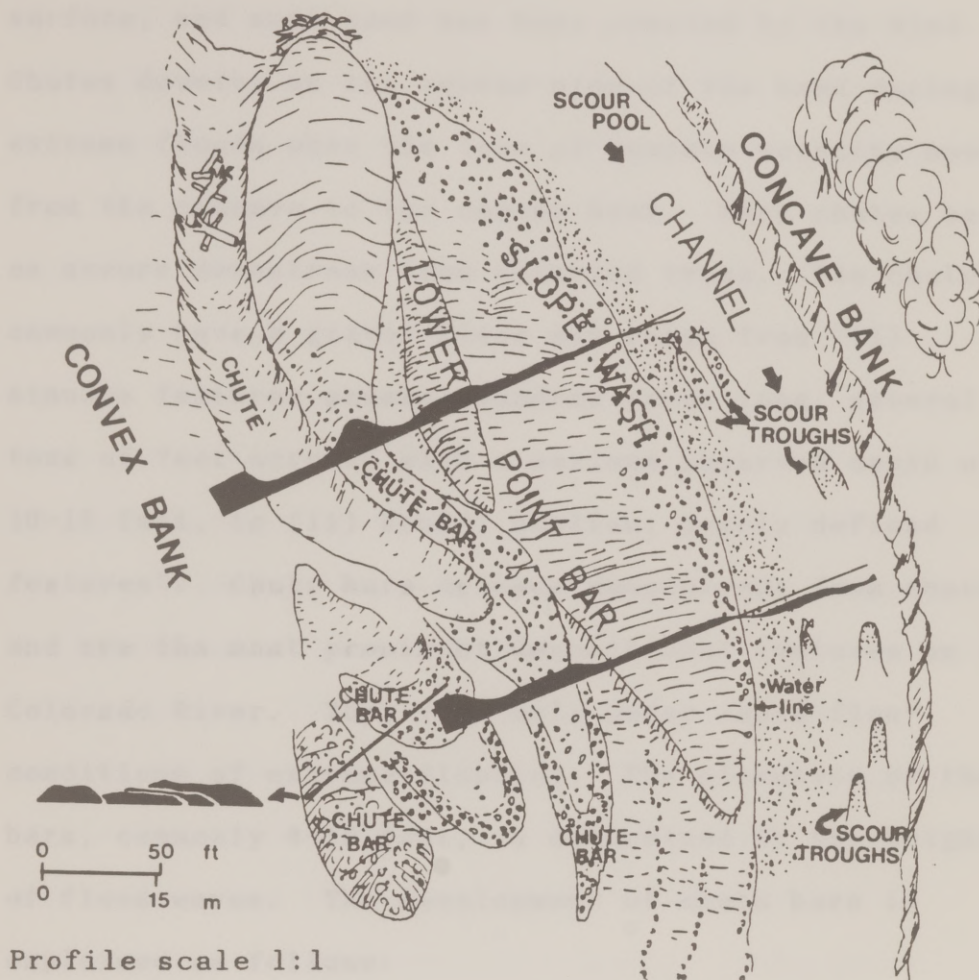


Figure 2.26: Coarse-grained point bar plan view and cross-sections illustrating principle physiographic features. (Modified after McGowen and Garner, 1970)

the chute bars, and is generally featureless, with no preserved bed forms. Local patches of gravel cover the surface, and some sand has been removed by the wind. Chutes develop on the convex side of the bend during extreme floods when the line of maximum velocity moves from the concave to the convex bank. Many chutes begin as scours downstream from uprooted trees. The chutes commonly have a gravel floor and range from "(i) sinuous features several hundred yards long, several tens of feet across, with a maximum observed depth of 10-15 feet, to (ii) broad, shallow, poorly defined features". Chute bars develop downcurrent from chutes and are the most prominent depositional features on the Colorado River. They form only under rapid-flow conditions of extreme flooding. The elevation of the bars, commonly 4-10 feet, is determined by the height of flood waves. The development of chute bars is explained as follows:

Scour of a chute and initial bar construction are contemporaneous. Gravel and coarse sand probably were transported as a heavy fluid layer where flow was confined to the chute. As chute depth decreases, in a downchannel direction, flow was no longer confined and much of the material carried in the heavy fluid layer was dropped (McGowen and Garner, 1970).

The sediment movement within the river is greatly influenced by river discharge. The discharge of the Colorado River is referred to as "flashy", reflecting intense, short duration flood events (McGowen and Garner, 1970, and Baker and Pentead-Orellana, 1978). These events provide rapid transportation of coarse sediment, followed by extremely rapid deposition in the waning flood stages, leaving little time for selective sorting (Baker and Pentead-Orellana, 1978). The Colorado River has an average (regulated) flow of $56.2 \text{ m}^3/\text{s}$ (1,986 cfs) at Austin (USGS gage no. 0815800) for 51 years of data, and an average flow of $61.9 \text{ m}^3/\text{s}$ (2,187 cfs) at Bastrop (USGS gage no. 08159200) for 27 years of data. An example of flood magnitudes for the Colorado River at Austin is included in Table 2.6. The peak discharge appears to have been greatly influenced by the construction of the reservoir system, given the dramatic drop in observed peak discharge rates beginning in 1952. Although the regulated rates are relatively lower than those unregulated in the past, they represent significant flood events capable of altering river features. The degree of scour and bed load transport during flood events depends upon the

TABLE 2.6
TEN HIGHEST FLOODS IN ORDER OF OCCURRENCE
(UP TO 1976)

Order No.	Date of Crest	Gage Height		Observed Peak Discharge $\frac{\text{m}^3}{\text{s}}$ (cfs)	Routed Peak Discharge $\frac{\text{m}^3}{\text{s}}$ (cfs)
		Stage ■ (ft)	Elevation ■ (ft)		
1	July 7, 1869	15.54 (1) (51.0)	138.16 (453.27)	—	—
2	Dec. 4, 1913	8.23 (4) (27.0)	136.81 (448.86)	4,644 (164,000)	—
3	June 15, 1935	15.24 (1) (50.0)	137.85 (452.27)	13,621 (481,000)	1,699 (3) (60,000)
4	Sept. 28, 1936	9.57 (4) (31.4)	138.16 (453.26)	6,626 (234,000)	4,248 (3) (150,000)
5	July 25, 1938	13.78 (1) (45.2)	136.39 (447.47)	7,816 (276,000)	4,446 (3) (157,000)
6	Sept. 17, 1952	2.92 (1) (9.59)	125.54 (411.86)	105 (3,720)	13,593 (2) (480,000)
7	June 4, 1957	6.89 (1) (22.60)	129.50 (424.87)	1,155 (40,800)	12,063 (2) (426,000)
8	Oct. 8, 1959	6.83 (1) (22.4)	129.44 (424.67)	1,070 (37,800)	7,079 (2) (250,000)
9	May 16, 1965	4.31 (1) (14.15)	126.93 (416.42)	456 (16,100)	5,182 (2) (183,000)
10	May 15, 1970	4.21 (1) (13.82)	126.83 (416.09)	433 (15,300)	4,531 (2) (160,000)

(1) Stage at present US Geological Survey gage located 305 ■ (1,000 ft) upstream from US Highway 183 (Montopolis bridge). Datum of gage is 122.61 ■ (402.27 ft) msl.

(2) Estimated discharges that would have occurred if the upstream Colorado River Basin reservoirs had not been constructed.

(3) Estimated discharges that would have occurred if the upstream Colorado River Basin reservoirs had been in operation at the time the flood occurred. Assumed that Lake Travis was operated according to Code of Federal Regulation, Title 33, paragraph 208.19, as revised January 1971.

(4) Stage at old Congress Avenue gage. Datum of gage was 128.58 ■ (421.86 ft) msl.

(Modified from U.S. Army Corps of Engineers, 1976)

flow velocity. As discussed in an earlier section, the transport rate of bed load is proportional to flow velocity with an exponent ranging from 3 to 5 ($q_s \propto \bar{u}^{(3-5)}$). Therefore, a small change in velocity results in a much greater change in the amount of bed load transported. The physiographic features noted in Figure 2.26 were observed during low flow conditions. Under these conditions, most of the erosion occurs on the concave bank where velocity and turbulence is greatest. Deposition along the lower point bar also occurs during low flow where velocity and turbulence are minimal. Under extreme flood conditions, chutes and chute bars may form, followed by chute fill accumulation during falling flood stage. In addition, most point bar deposition occurs during extreme floods (McGowen and Garner, 1970). No references could be found relating specific peak flood discharge to physiographic features formed in the lower Colorado River. Given the peak flows observed in Table 2.6, one can only suggest that flooding prior to dam construction had a much greater influence on the physiographic features of the river. The effects of floods on river features might be qualitatively ranked for comparison, assuming that magnitude of peak

discharge corresponds with degree of alteration. To determine the degree to which various flood magnitudes could affect river features would involve detailed observation and field work both before and after storm events.

2.4.4.2 Influence of Man

Man is capable of greatly altering the water and sediment supply within a watershed, which can result in significant and long term changes within a river system. In the study area, the principal man-made influences on the Colorado River sediment include stream regulation from the Highland Lakes dams, land use and management, and the sand and gravel mining operations along the river.

2.4.4.2.1 Stream Regulation

The construction of a dam or series of dams for the purpose of impoundment and water flow control can have an enormous effect on a river system. The impacts of impoundments can be analyzed by considering (Simons, 1979):

- (1) the response of the river channel and tributaries upstream from the impoundment,

(2) the physical processes within the impoundment, and

(3) the response of the river channel and tributaries downstream from the impoundment.

Dams and associated reservoirs function as excellent sediment traps, often trapping more than 90% of the sediment load, and effectively all of the coarser material, at least during the early years of operation (Petts, 1984). As earlier noted, the study area is located just downstream of Longhorn Dam and the Highland Lakes chain. Taylor (1910, 1930) provides good evidence of the history of the extensive sedimentation in Lake Austin. From the time it was initially completed in 1893 until the failure of the first dam during the 1900 flood, Taylor estimated that approximately 48% of the lake's original 6.12 E7 m^3 (49,600 acre-ft) capacity had been filled with silt. He conducted the survey using a "two-transit" method and sounding tape. A second dam was partially completed in 1913 and finished by 1915. Silt surveys were made in 1913, 1922, 1924, and 1926 and showed that from 1913-1926, the capacity of the lake was reduced from its original volume of 3.95 E7 m^3 (32,029 acre-ft) to 1.82 E6 m^3 (1,477 acre-ft), i.e., only 4.6% of the original capacity remained. This would certainly seem

to provide evidence to Weeks' (1941) assessment that the last time bedload sediment from the Central Mineral Region reached the Lower Colorado River was before the completion of the second dam on Lake Austin.

No specific information pertaining to the effects of the Highland Lakes system on the Colorado River sediment within the study area could be found from the literature review. However, Petts (1984) presents a detailed discussion of the effects of impoundments on river environments. He explains that upstream river impoundment will bring about a complete readjustment of channel morphology for a significant length of the river below the dam, and that tens to hundreds of years may be required for such a change to be completed. The most notable responses of a river undergoing post-dam adjustment include (i) accelerated erosion, (ii) sedimentation within the channel, and (iii) changes in channel form. Although discussed separately below, these responses are considered interdependent in nature.

The sustained outflow of relatively clear, sediment-free water from an upstream impoundment into a river channel composed of transportable bed and bank materials can result in rapid erosion of the channel,

especially near the dam, and can extend for many miles downstream. If this erosion results in a lowering of the channel bed, adjacent tributaries may become rejuvenated, i.e., respond with accelerated erosion of their channels. The rate and magnitude of erosion of a river channel are limited by the nature of the channel (bed and bank) material, i.e., size, cohesiveness, and degree of protection by vegetation, and by the local hydraulic conditions, e.g., low channel slope interaction, a large cross-section, or a rough boundary (Petts, 1984). In the case where non-transportable sediment is present in the bed material, such as gravel and coarse sand, selective transport of the smaller particles creates a coarse sediment layer at the bed surface which can protect the underlying material from erosion. This 'armor' layer requires only a small percentage of larger particles to be effective during normal flow; a single layer of grains or perhaps less than a single layer have been suggested (Petts, 1984, and Simons, Li, and Associates, 1982). Armoring tends to form in areas of natural scour in the river, such as on the upstream end of islands and bars (Simons, Li, and Associates, 1982). The armoring and erosion will "shift progressively downstream until channel

hydraulics are adjusted, or until the bed is protected by an 'armoured' layer" (Petts, 1984). The degree of effectiveness of the armor layer is dependant upon the magnitude of flow under which it developed. For example, an armor layer developed under moderate flow conditions can be disrupted during high flow, but may be restored as flows diminish (Simons, Li, and Associates, 1982). During field observation of the segment of the Colorado River between Longhorn Dam and Webberville, Armstrong (1989) noted evidence of channel armoring in riffle areas. In addition, Koenig (1987) stated that the densest stands of rooted vegetation in the river appeared to grow on sediment composed mostly of sand and gravel. He suggested that closer inspection would probably reveal a significant amount of silt between or beneath the sand and gravel.

Selective erosion and bed armoring can affect the size-frequency distribution of the channel sediments and result in an increase in the median grain size of the surface layer of the bed material. As with erosion, this change becomes less significant over time and with distance downstream. When armored channels have only minor bed erosion or a channel receives limited sediment from tributaries, the sediment load

may be derived from the erosion of the river banks, particularly from rivers with migrating meanders (Petts, 1984). The impoundment of a river can affect the character of a migratory river in several ways:

. . . flood regulation might reduce rates of erosion; sediment abstraction, on the other hand, could accelerate erosion rates, while the depletion of fine suspended solids would reduce the rate of over-bank accretion, so that new floodplains would take longer and longer to mature, and the soils would remain infertile (Petts, 1984).

The forces causing the movement of water through alluvial bank material discussed earlier as a part of groundwater hydrology also tend to decrease bank material stability and may cause accelerated bank erosion (Petts, 1984).

Petts (1984) discusses several mechanisms for sedimentation within an impounded river channel, including tributaries, redistribution of channel sediment and bank erosion, and the wind. He notes that the sedimentation is usually localized. The amount of wind blown sediment available to the river channel depends on environmental conditions, and may be especially significant in semi-arid areas. Channel erosion and scour below dams can be an important sediment source for the river downstream. Another

source is the redistribution of the channel boundary and floodplain sediments in a migratory channel. The more common source of sediment is the unregulated tributary. Sediment tends to accumulate at the confluence of a tributary with a river channel. Deposition occurs because "the regulation of high-magnitude floods artificially slows sediment transport, while the debris discharge from tributaries is of course unaffected or possibly increased." Tributaries with steep gradients can supply coarse sediments into the river which, because of a relatively lower slope and wider channel, is not able to transport the larger sediment, resulting in deposition. Stream regulation may result in rejuvenation of tributaries, causing an increase in sediment yield for several years after dam closure. Petts has observed that in gravel-bed channels, the formation of bars may result in a confining of the flow and thus an increase in velocity and consequently an increase in sediment transport through the reach.

The greatest change in channel form is commonly expected at those sites with the smallest channel dimensions prior to regulation. Local and short-term changes in channel form can be misleading

because the new channel equilibrium is achieved by changes resulting from alternating periods of erosion and deposition. Long-term variations in channel form are affected by relative changes of discharge and sediment load at any point on a river. Within meandering channels, slope may be reduced by erosion, but the formation of a new floodplain at a lower elevation can produce a channel with smaller dimensions. Different channel changes can also be found downstream along a single river. Just below a dam, the sediment supply is zero, and flow competence (the largest particle of a given specific gravity that a river can carry) rather than capacity (the quantity of material a stream can carry past a fixed point per unit time) determines the nature of the sediment transport, and consequently, channel change. Farther downstream, as the sediment load increases from channel erosion and tributary sources, control of sediment movement shifts from flow competence to capacity. Channel changes continue until the channel is adjusted such that flow competence and capacity are capable of transporting all supplied sediments. The rate at which the new channel is formed depends on the frequency of competent reservoir releases and the frequency of

sediment-loaded tributary events. Gravel-bed rivers may require extreme flood events for sediment transport, and consequently, morphologic change may be relatively slow (Petts, 1984).

2.4.4.2.2 Land Use and Management

The degree to which man alters the natural condition of the land within a watershed can greatly influence the amount of sediment available for transport into a river system. Land use is determined to some degree by the type(s) of soil present. It has been found that agricultural land, especially large areas, produces the most sediment, followed by grasslands and forested areas. For example, the conversion of grassland to cropland increases erosion 20-100 fold, while conversion of forest land to cropland can increase erosion 100-10,000 fold. Urbanization can also introduce significant sedimentation problems on a local level by increasing the total runoff volumes and peak flow rates (SCS, 1971).

In the Colorado River drainage basin between Austin and Bastrop, the land use is about 49% cropland, 29% rangeland, 20% forest, and 2% urban (Miertschin and

Armstrong, 1986). The city of Austin is the largest nearby urban center, with the eastern portion of the city lying within the study area. Bastrop, the second largest city, is located at the eastern extreme of the study area. The remainder of the area is sparsely populated.

Sutton (1980) studied the morphologic changes due to urbanization in five streams draining north Austin (Figure 2.27). Although two of these streams discharge into Town Lake upstream of Longhorn Dam, the dam is relatively small and used primarily to maintain a constant lake level, and is therefore not seen as a significant sediment trap. In his investigations, Sutton found that both deposition and erosion of channels and flood plains is occurring in the Austin area, with erosion as the more common and persistent process. When occurring together, deposition usually precedes erosion. The clearest evidence for morphologic change was found in channel dimensions. Channel width had increased in many reaches, resulting from lateral bank erosion and by vertical incision of flood plains adjacent to banks. The greatest widening had locally more than doubled channel widths. Sutton found changes in channel depth

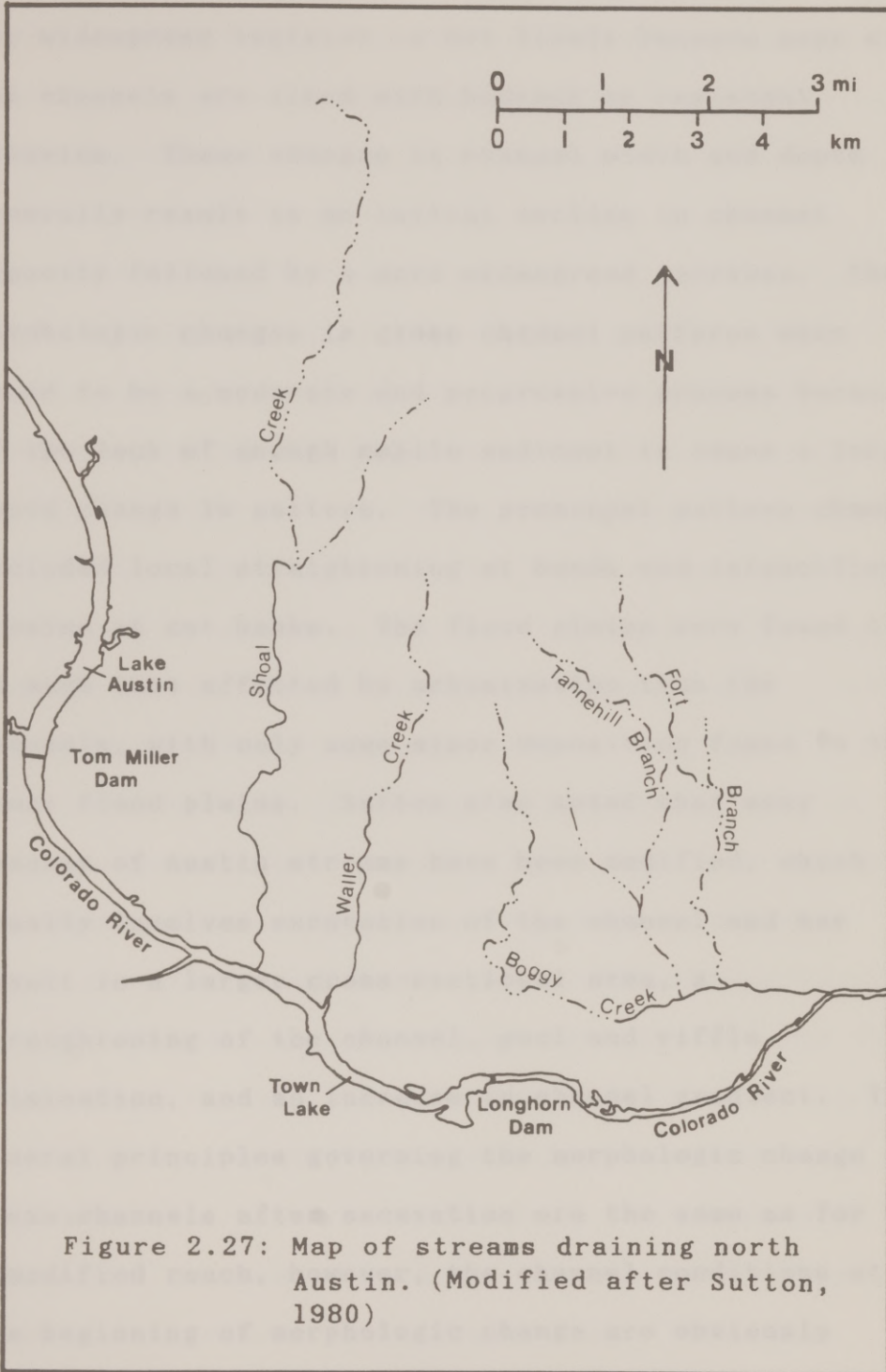


Figure 2.27: Map of streams draining north Austin. (Modified after Sutton, 1980)

difficult to estimate, concluding that the potential for widespread incision is not likely because many of the channels are lined with bedrock or resistant alluvium. These changes in channel width and depth generally result in an initial decline in channel capacity followed by a more widespread increase. The morphologic changes in gross channel patterns were found to be a moderate and progressive process because of the lack of enough mobile sediment to cause a large rapid change in pattern. The prominent pattern changes included local straightening at bends and intensified erosion at cut banks. The flood plains were found to be much less affected by urbanization than the channels, with only some minor deposition found in the lower flood plains. Sutton also noted that many reaches of Austin streams have been modified, which usually involves excavation of the channel and may result in a larger cross-sectional area, a straightening of the channel, pool and riffle elimination, and an increase in channel gradient. The general principles governing the morphologic change of these channels after excavation are the same as for an unmodified reach, however, the channel conditions at the beginning of morphologic change are obviously

different. If the modified reach has a greater capacity than needed for channel-forming discharges, then deposition will take place until the channel has reached maximum transporting efficiency. The amount of deposition depends on (i) the relative size of the excavated channel to discharge, (ii) the time elapse since excavation, (iii) the ability of the stream to react to principles governing stream flow, e.g., sediment supply and adequate discharge for sediment transport, (iv) the amount of stabilizing vegetation, and (v) the composition of the excavated bed and banks.

In studying the impact of suburbanization on fluvial geomorphology in a Denver suburb, Graf (1975) noted a significant sequence of events. Undisturbed land was initially cleared of vegetation over large areas, allowing for increased discharge, soil erosion, and wind effects. During construction, sediment production increased dramatically, introducing large amounts of sediment into the stream network. New flood plains were created and old flood plains were enlarged such that the total flood plain area increased significantly. After construction, the increase in impervious surfaces caused additional increases in runoff, but reduced the sediment load. This then

caused the streams to erode through the newly formed deposits.

Taylor (1977) investigated the effects of suburban development on the runoff response in a small basin in Peterborough, Ontario. It was found that seasonal variation in climate had a pronounced effect on the runoff response. This seasonal effect was felt much more strongly in the urban portion of the basin. Taylor concluded that the urban response is not merely a function of the amount of impervious surfaces or storm drains, and that antecedent moisture conditions which vary between seasons and individual storms may cause more variation in the runoff response in urban basins as opposed to natural basins.

2.4.4.2.3 Sand and Gravel Mining

As seen on the geologic map of the study area, alluvial deposits are abundant east of the Balcones fault zone. The Colorado River sediments and older terrace deposits are made up mostly of sand and gravel size sediment, as discussed earlier, and are a major source of sand and gravel for industry. Sand and gravel mining activities, however, can affect both the

sediment supply and the channel transport capacity in a river system.

Sand and gravel companies in the Austin area can be traced as far back as 1910 in the Austin telephone directory. In the last few decades, sand and gravel mining activities along the Colorado River have seen a significant and steady increase. Figures 2.28(a)-(e) show the progression of mining activity along the Colorado River from the years 1951, 1966, 1973, 1984, and 1987. The figures were compiled from the analysis of various aerial photographs and from information obtained from the U. S. Geological Survey (USGS) quadrangle maps. It should be noted that areas considered active may not be continually operating on a day-to-day basis; the degree of activity can depend on the immediate demand.

Figure 2.28(a) shows the sand and gravel operations active in 1951. Information was obtained from aerial photos taken for the Agricultural Stabilization and Conservation Service (ASCS) on January 16 and 18, 1951. Flow rates at the USGS stream gage at Austin (no. 08158000) for January 16 and 18 were $29 \text{ m}^3/\text{s}$ (1010 cfs) and $25 \text{ m}^3/\text{s}$ (886 cfs), respectively. The mining activities were located in

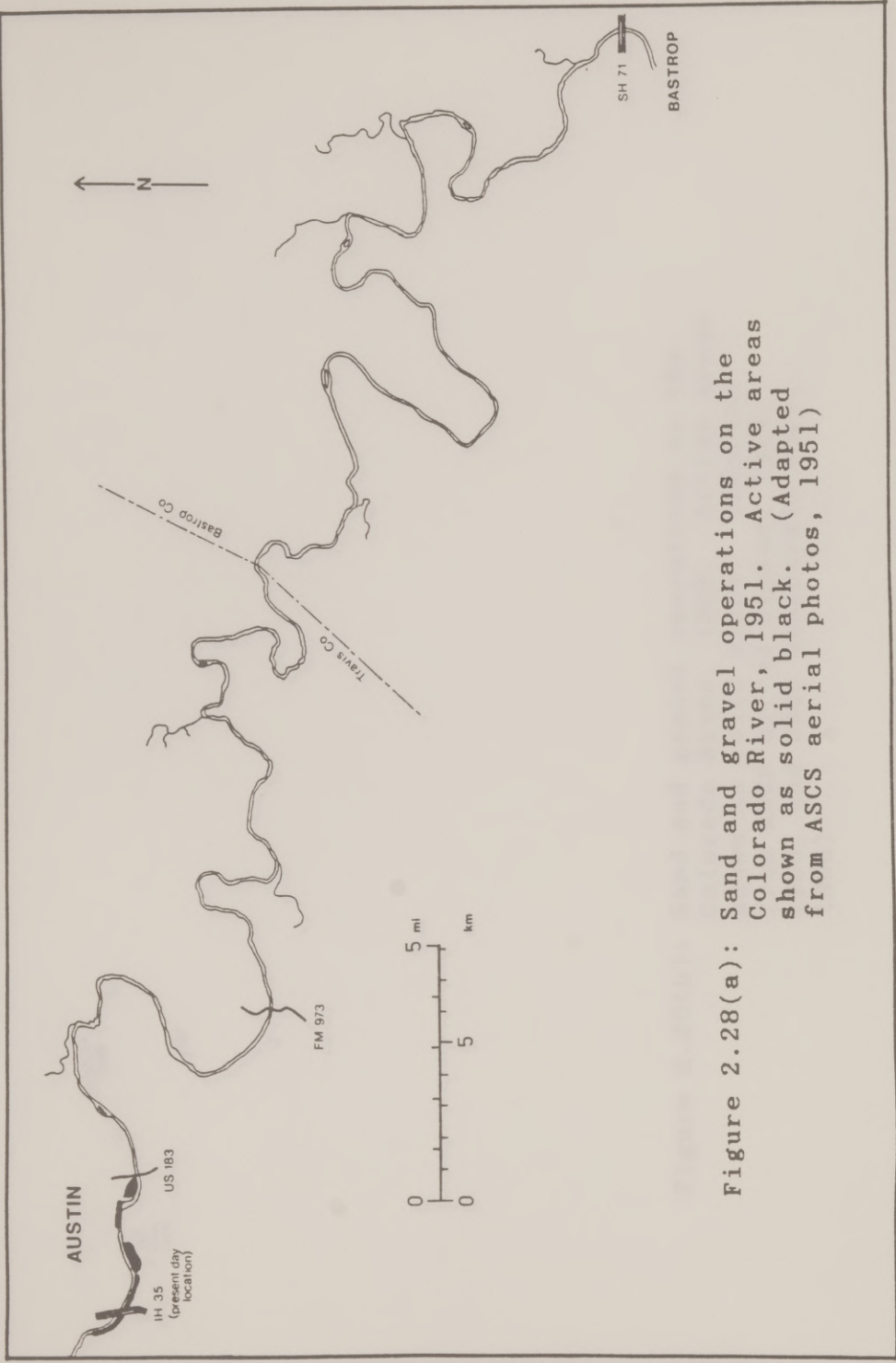


Figure 2.28(a): Sand and gravel operations on the Colorado River, 1951. Active areas shown as solid black. (Adapted from ASCS aerial photos, 1951)

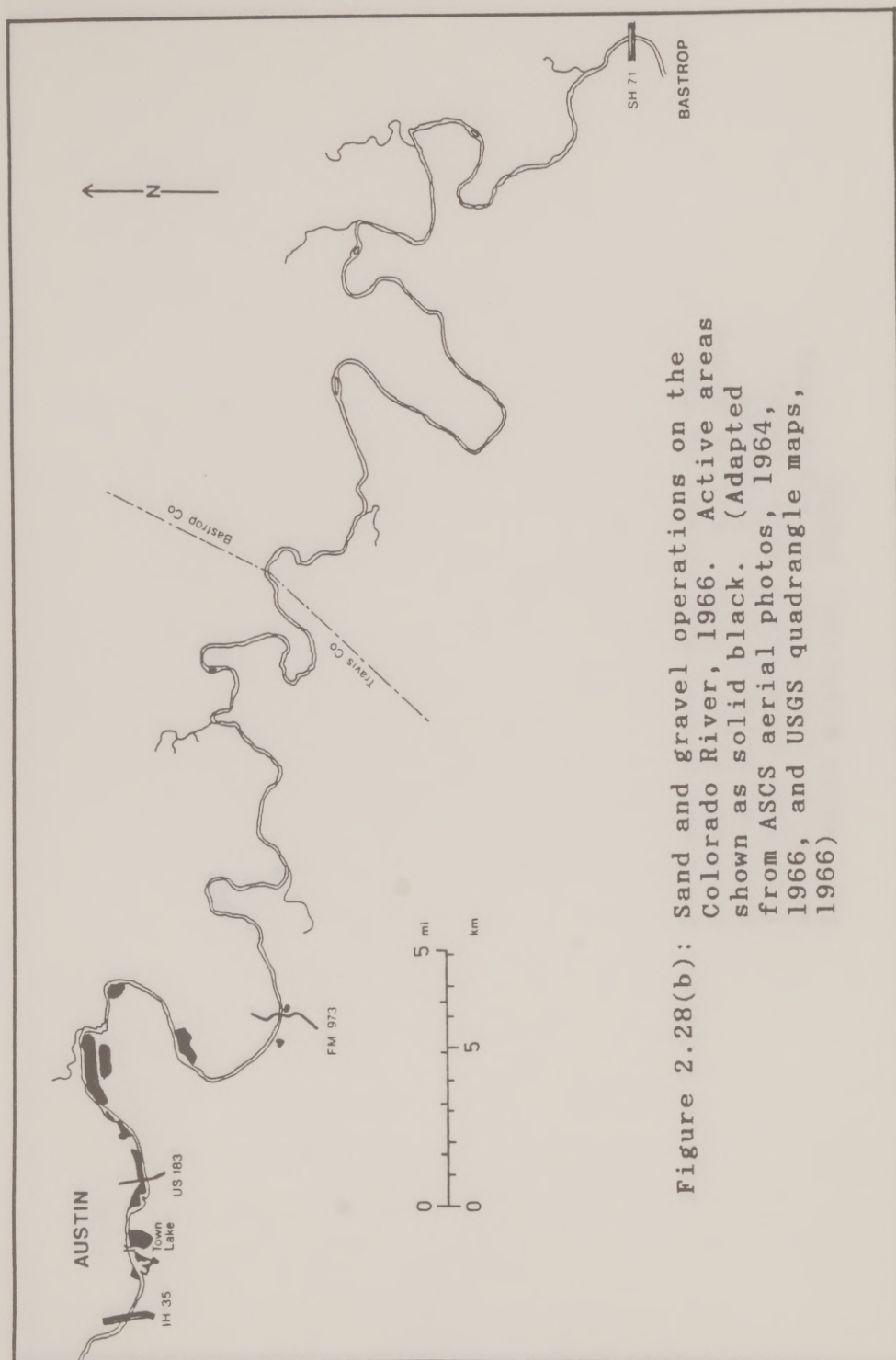


Figure 2.28(b): Sand and gravel operations on the Colorado River, 1966. Active areas shown as solid black. (Adapted from ASCS aerial photos, 1964, 1966, and USGS quadrangle maps, 1966)

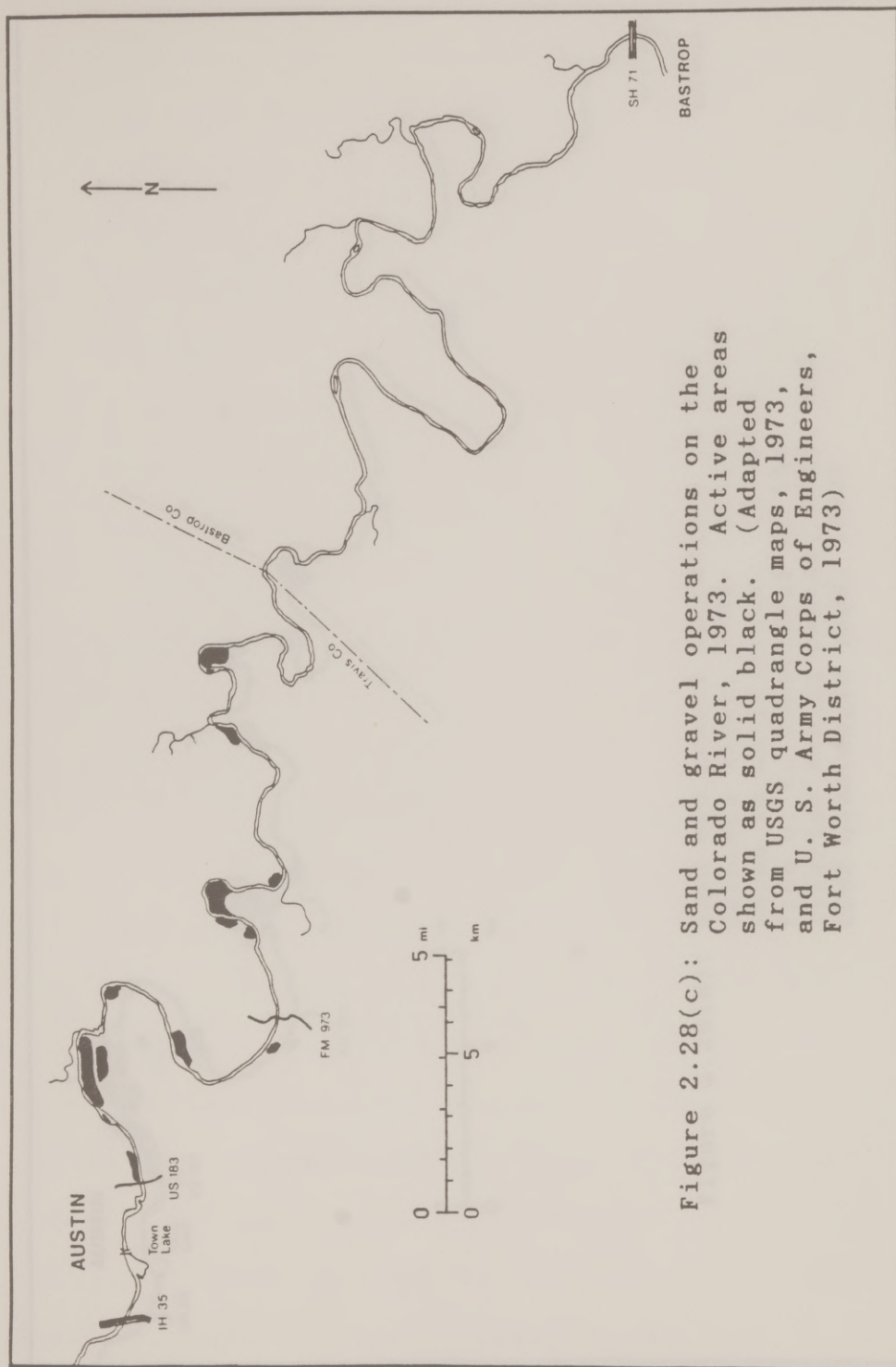


Figure 2.28(c): Sand and gravel operations on the Colorado River, 1973. Active areas shown as solid black. (Adapted from USGS quadrangle maps, 1973, and U. S. Army Corps of Engineers, Fort Worth District, 1973)

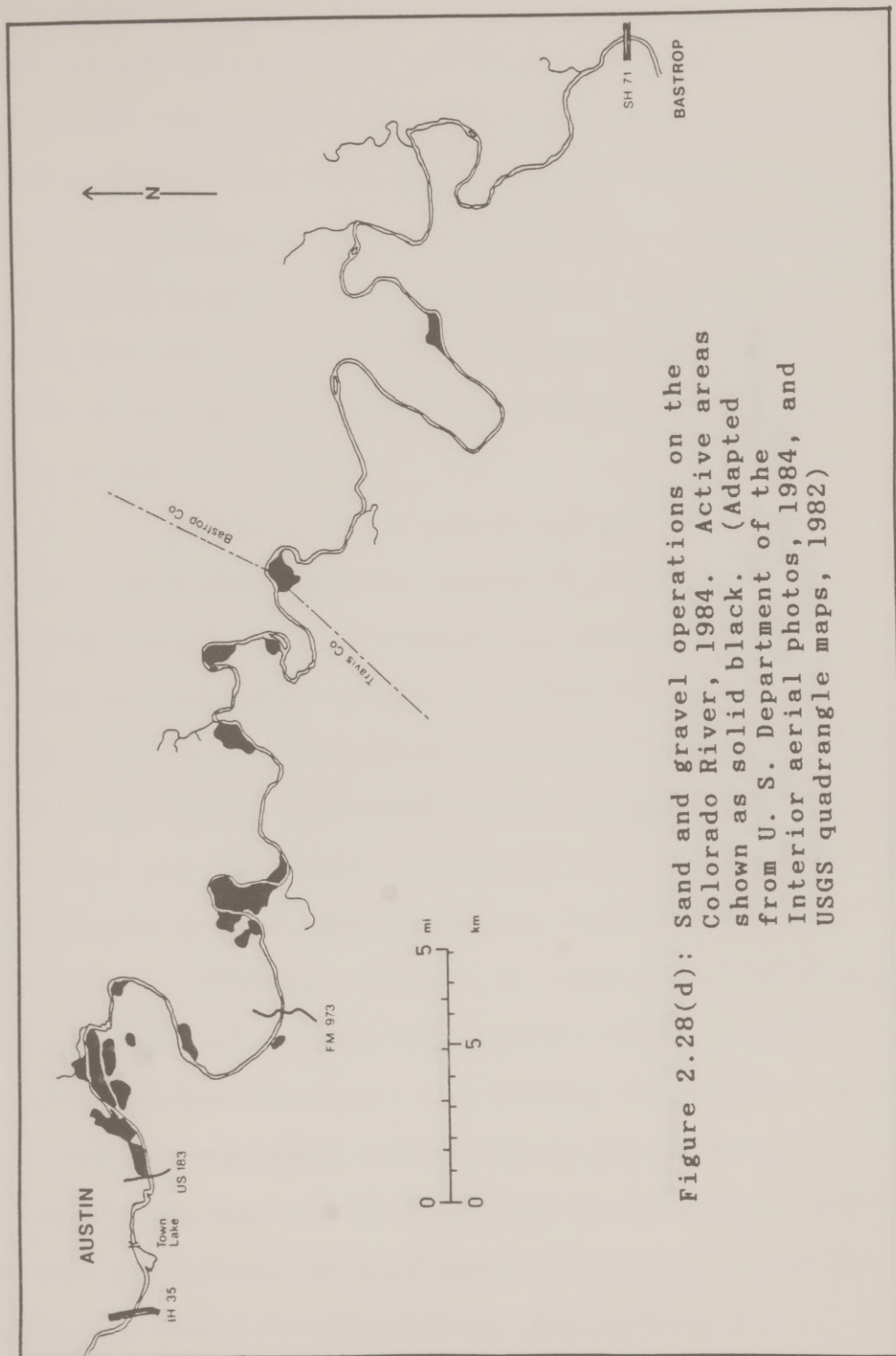


Figure 2.28(d): Sand and gravel operations on the Colorado River, 1984. Active areas shown as solid black. (Adapted from U. S. Department of the Interior aerial photos, 1984, and USGS quadrangle maps, 1982)

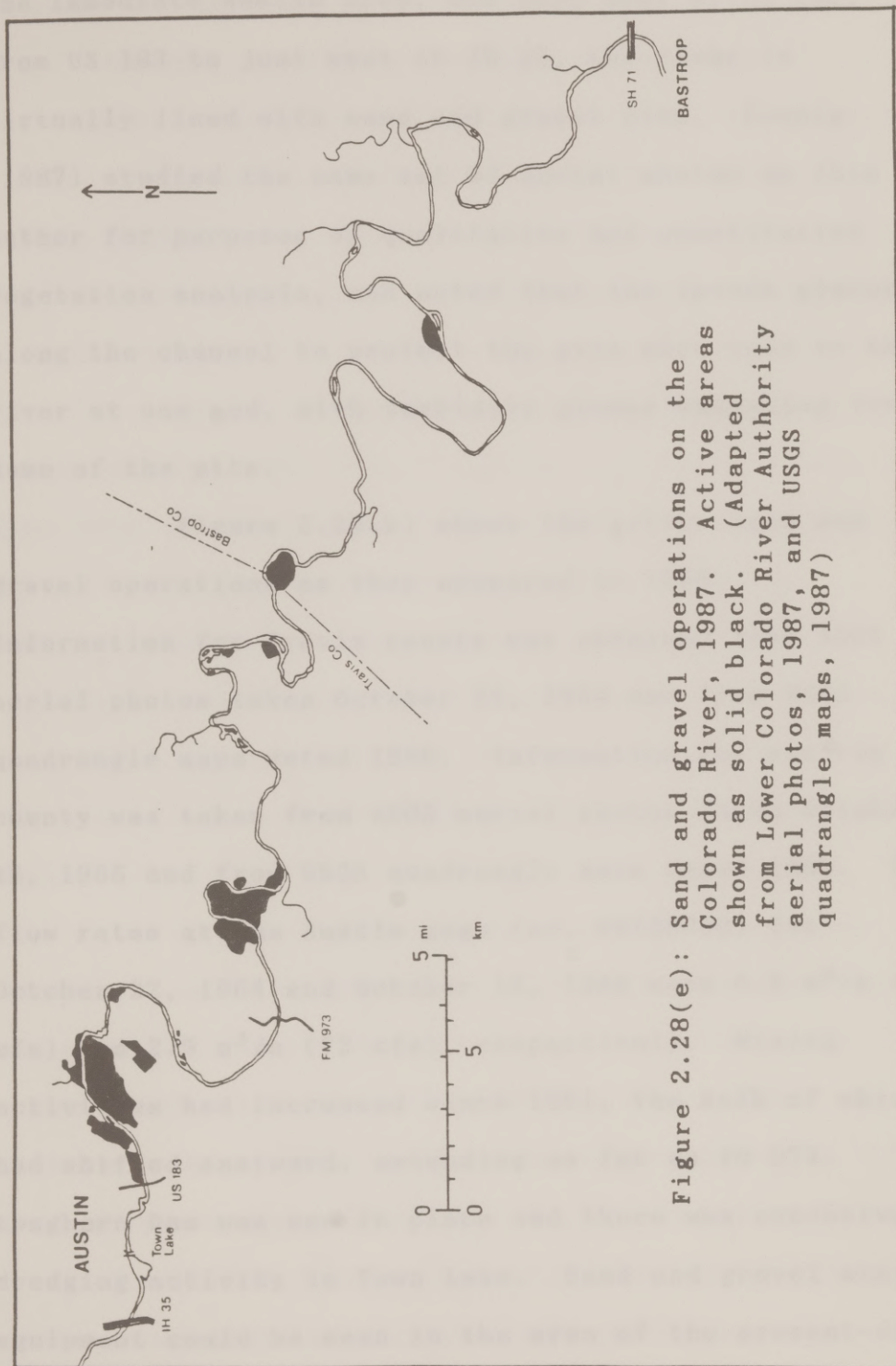


Figure 2.28(e): Sand and gravel operations on the Colorado River, 1987. Active areas shown as solid black. (Adapted from Lower Colorado River Authority aerial photos, 1987, and USGS quadrangle maps, 1987)

the immediate Austin area, and only west of US 183. From US 183 to just west of IH 35, the river is virtually lined with sand and gravel pits. Koenig (1987) studied the same set of aerial photos as this author for purposes of qualitative and quantitative vegetation analysis, and noted that the levees placed along the channel to protect the pits were open to the river at one end, with turbidity plumes emanating from some of the pits.

Figure 2.28(b) shows the active sand and gravel operations as they appeared in 1966. Information for Travis county was obtained from ASCS aerial photos taken October 22, 1964 and from USGS quadrangle maps dated 1966. Information for Bastrop county was taken from ASCS aerial photos taken October 15, 1966 and from USGS quadrangle maps dated 1966. The flow rates at the Austin gage (no. 08158000) for October 22, 1964 and October 15, 1966 were $0.9 \text{ m}^3/\text{s}$ (33 cfs) and $2.0 \text{ m}^3/\text{s}$ (72 cfs), respectively. Mining activities had increased since 1951, the bulk of which had shifted eastward, extending as far as FM 973. Longhorn Dam was now in place and there was extensive dredging activity in Town Lake. Sand and gravel mining equipment could be seen in the area of the present-day

softball fields just east of Longhorn Dam, on the south bank. In this area and other pits downstream, there was direct communication with the Colorado River, and the river appeared very cloudy along this reach. Koenig (1987) noted that the newer pits in Montopolis Bend were set back about 30-90 meters (100-300 feet) from the river.

Figure 2.28(c) shows the sand and gravel mining activity for 1973. Information was obtained from USGS quadrangle maps dated 1973 and from a report of the U. S. Army Corps of Engineers, Fort Worth District (1973), in which current sand and gravel operations were noted. The figure shows that mining activities continue to increase and spread eastward. The active areas now extend from just east of US 183 to Webberville, near Bastrop county.

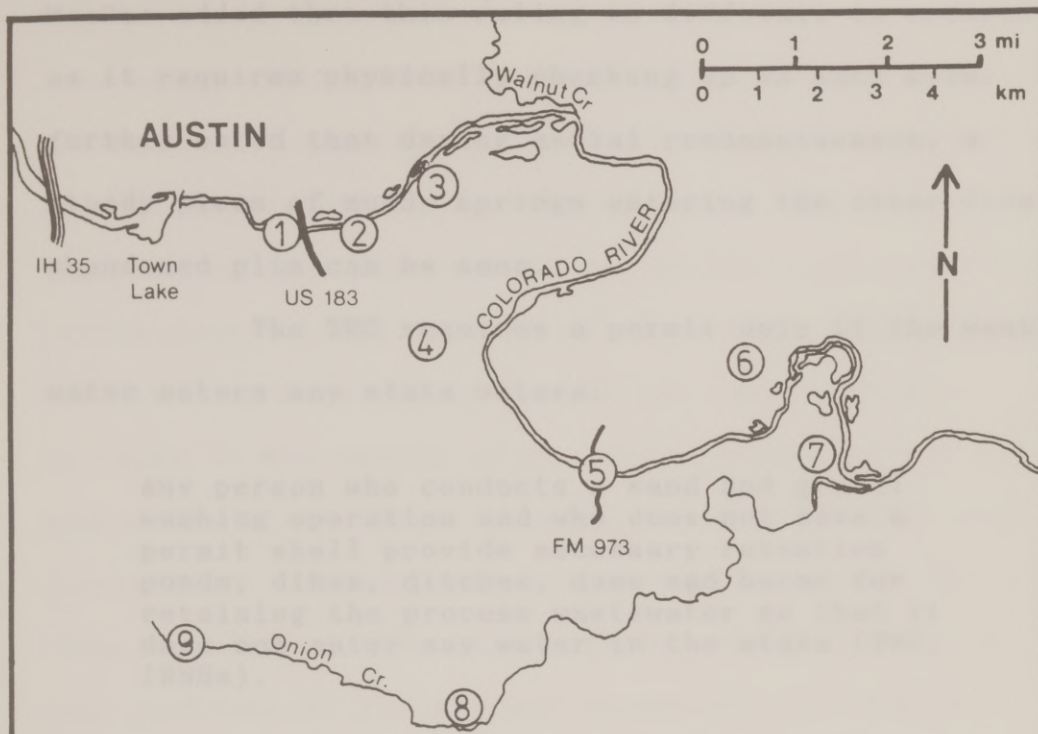
Figure 2.28(d) shows the sand and gravel operations active in 1984. Information for the figure was obtained from U. S. Department of the Interior aerial photos taken June 1, 1984 and from USGS quadrangle maps dated 1982. The flow rate at the USGS gage at Austin (no. 08158000) for June 1 was recorded as $72 \text{ m}^3/\text{s}$ (2540 cfs). The figure shows a very marked increase in activity in both newly active areas as well

as in previously active locations. The active areas now extend from US 183 across the Bastrop county line and into Wilbarger Bend. Again, many of the pits are in direct communication with the river by means of a break in levees located along the river.

Figure 2.28(e) shows the active sand and gravel operations in 1987. Information was obtained from LCRA aerial photos taken January 11, 1987 and from USGS quadrangle maps dated 1987. The flow rate of the river at the Austin gage (no. 08158000) for January 11 was $158 \text{ m}^3/\text{s}$ (5580 cfs). Although a few of the older areas had been abandoned, there was an overall noticeable increase in mining activity from only three years earlier. In some of the abandoned areas, the pits were in communication with the river, some becoming inundated, acting as part of the river channel.

Although some of the earlier mining took place within the modern river channel, the most recent sand and gravel operations are located adjacent to the river in the floodplains and terrace deposits. As expected, most of the mining takes place in the point bar deposits of the various river meanders, as can be seen in Figures 2.28(a)-(e).

A list of the currently active sand and gravel companies in the area and their locations can be found in the Bureau of Economic Geology (BEG) listing of active producers of non-petroleum mineral resources. The companies and their approximate locations as of March 1988 (BEG, 1988) are shown in Figure 2.29. Most of the active pits are located near or along the Colorado River, while two locations are found along Onion Creek. A listing of the quantity of materials extracted from the pits would be difficult to obtain, as most do not require regulation. If the mining activity takes place within the river, it falls under the jurisdiction of the Texas Parks and Wildlife Department. If the mining takes place on land, the Texas Water Commission (TWC) is the governing agency. According to Rollin MacRae (1988) of the Texas Parks and Wildlife Department, there are no current permits for in-stream mining in the study area, with all pits adjacent to the river considered to be on private property. He adds that the present ruling concerning berm openings on the Colorado River holds that in the case of one opening, the pit area is not considered as state waters. With two or more openings, however, the pit is considered state waters, as a part of the river.



1. Texas Industries Inc.
2. Naumann's Equipment Co.
3. Capitol Aggregates Inc.
4. Austin Sand and Gravel Co.
5. Texas Industries Inc.
6. J. V. Dirt and Loam
7. Centex Materials Inc., Colorado River terrace deposits
8. Onion Creek Sand and Gravel, Onion Creek terrace deposits
9. Colorado Materials Inc., Onion Creek terrace deposits

Other companies with non-specific locations:

- Southwest Materials Co., Travis County near Garfield, Texas
- Southwest Materials Co., Bastrop County, Birdall pit
- Y-B Dirt and Loam, Travis County

Figure 2.29: Locations of active sand and gravel producers as indicated by the Bureau of Economic Geology March 1988 listing.

MacRae added that this ruling is difficult to enforce as it requires physically checking up on each site. He further noted that during aerial reconnaissance, a steady plume of muddy springs entering the river from abandoned pits can be seen.

The TWC requires a permit only if the wash water enters any state waters:

Any person who conducts a sand and gravel washing operation and who does not have a permit shall provide necessary retention ponds, dikes, ditches, dams and berms for retaining the process wastewater so that it does not enter any water in the state (TWC, 1988a).

According to the TWC (1988b), there were no current permits as of August 3, 1988.

Simons, Li, and Associates (1982) discussed the potential impacts of sand and gravel mining in alluvial river systems. As a river constantly strives to attain equilibrium, the mining of sand and gravel from in-stream and in adjacent floodplains can effect the natural river processes both upstream and downstream of the mined area. When flood waters spill over into a floodplain gravel pit, there is potential for erosion and downcutting and ultimate breaching of the dike or buffer zone used to separate the pit from

the active river channel. Erosion through this buffer zone could alter local river channel characteristics and transport rates. If the reach of river adjacent to the pit is geomorphically active, e.g., the lateral migration of the Colorado River, it may also cause the buffer zone to fail in time if protective measures are not taken. An in-stream gravel pit can cause an increase in the energy slope just upstream of the pit, giving the river greater energy for bank erosion and downcutting. These processes could then upset the river's sediment transport balance, causing erosion just upstream of the pit and deposition in the pit, i.e., the pit would act as a sediment trap. Since the water leaving the pit may not be capable of carrying sand and gravel size material, clearer water will flow back into the main channel. The clearer water may, in turn, cause downstream scour (Simons, Li, and Associates, 1982).

The critical time for conditions favorable to bank erosion and downcutting depends on the volume of the pit and the inflow hydrograph. For an in-stream pit, a high flow event will fill the pit or reach equilibrium faster than a low flow event, thus drowning out the effect of the steeper energy slope much sooner.

For a floodplain pit, flooding only becomes a concern once water spills over into the pit. Once the pit is filled, it becomes merely a pool or slackwater area on the floodplain. Thus, the central portion of the hydrograph is critical for pit stability (Simons, Li, and Associates, 1982). These concepts are illustrated in Figure 2.30.

Jackson and Beschta (1984) conducted a flume study to examine the effects of increased sand delivery on the morphology of sand and gravel channels. As a result of this and previous studies, they suggested that a sand and gravel bed alluvial channel with pool and riffle sequences will respond to increased sand delivery by reducing bed roughness. This would be accomplished by filling in pools and by degrading riffles and would result in a decrease in the average channel depth. The study indicated that the increased sand concentrations in transport would enable lower stream discharges to transport riffle gravel materials, resulting in riffle degradation. As form roughness decreases, the average mean velocity and sediment transport capacity would increase and may result in an increase in width due to bank erosion. Jackson and Beschta (1984) further add that if the increase in sand

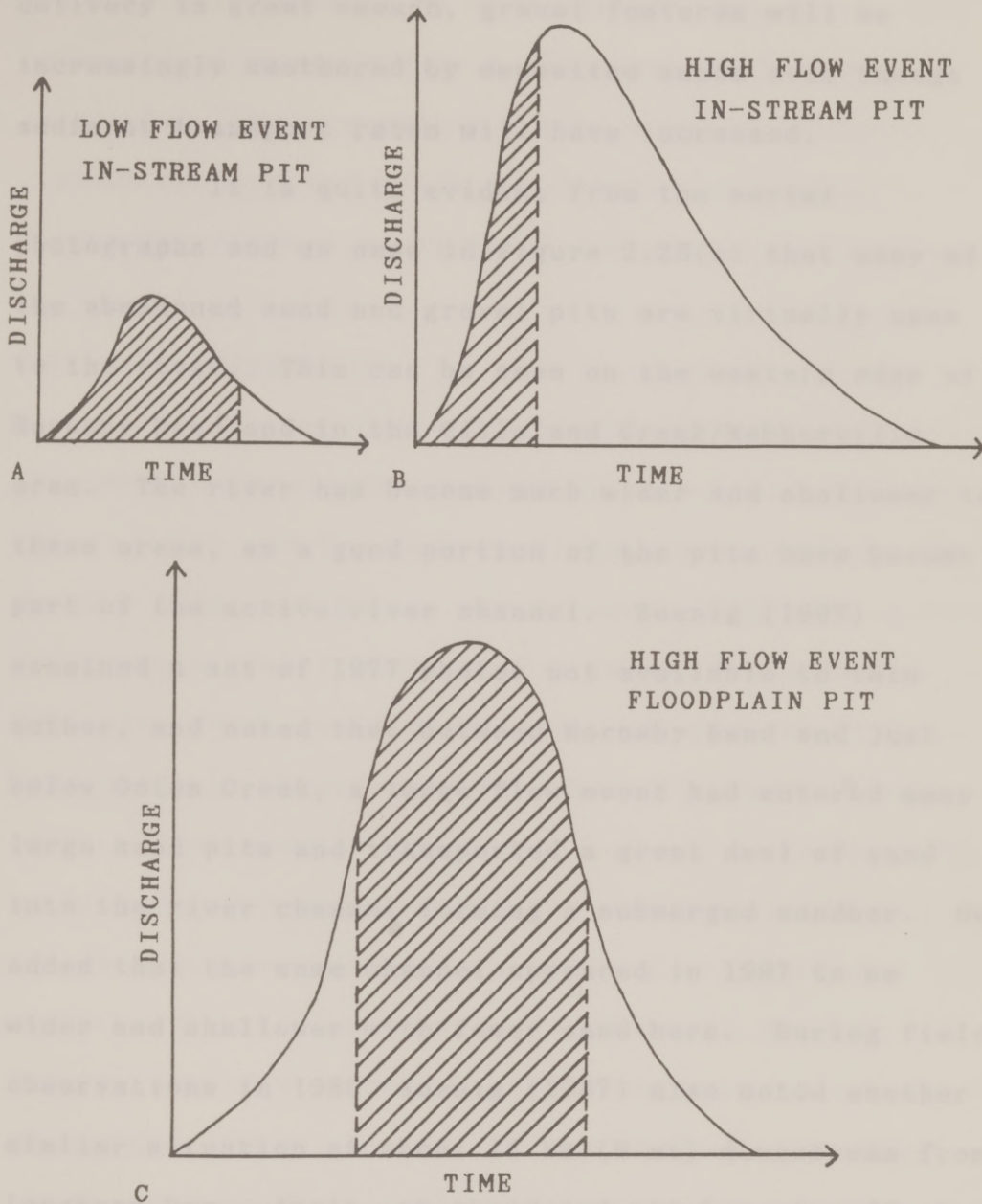


Figure 2.30: Relative time for (A) filling of in-stream gravel pit for a low flow event, (B) filling of in-stream gravel pit for a high flow event, and (C) critical time for erosion of a floodplain gravel pit. (After Simons, Li, and Associates, 1982)

delivery is great enough, gravel features will be increasingly smothered by deposited sands even though sediment transport rates will have increased.

It is quite evident from the aerial photographs and as seen in Figure 2.28(e) that many of the abandoned sand and gravel pits are virtually open to the river. This can be seen on the western edge of Hornsby Bend and in the Gilleland Creek/Webberville area. The river has become much wider and shallower in these areas, as a good portion of the pits have become part of the active river channel. Koenig (1987) examined a set of 1977 photos not available to this author, and noted that between Hornsby Bend and just below Onion Creek, a large flow event had entered many large sand pits and transported a great deal of sand into the river channel forming a submerged sandbar. He added that the same channel appeared in 1987 to be wider and shallower with fewer sand bars. During field observations in 1986, Koenig (1987) also noted another similar situation at about 14 km (9 mi) downstream from Longhorn Dam. Again, an abandoned pit has, in effect, widened the width of the river channel, with increased sand delivery resulting in a shallow channel depth. Koenig observed that in many parts of the river, the

channel form appeared to have changed from a somewhat asymmetrical trapezoid to a shallower but wider rectangle. The preceeding evidence would appear to support Jackson and Beschta's (1984) conclusions concerning channel response to increased sand delivery.

2.5 DISCUSSION

The modern Colorado river has been described as a meandering coarse-grained degradational bed load river (Baker and Pentead-Orellana, 1977, McGowen and Garner, 1970, and Morton and McGowen, 1980). According to Schumm's classification of alluvial channels (Table 2.1), the river would be catagorized as an eroding bed load channel. Erosion of the channel is most likely to occur where velocity and turbulence are greatest. The distribution of maximum velocity and turbulence in a meandering river system as presented in Figure 2.3 could be directly applied to the Colorado River. Erosion should then be expected along the outer banks of meanders (near the base of the channel) and along the channel margins in the straight reaches during normal flow. During flood flow, erosion is more likely to occur toward the convex banks (point bars), as the water takes a straighter path. McGowen and Garner's

(1970) study of point bars of the Colorado river confirmed that erosion along the outer banks of the river is taking place during normal flow. In addition, the presence of chutes and chute bars are evidence of point bar erosion during high flow events.

According to Petts (1984), the forces causing the movement of water through alluvial bank material also tend to decrease bank material stability and may cause accelerated bank erosion. These forces include influent groundwater flow, the rising and falling of flood stages, and the storage and release of water for specific purposes. The groundwater in the Colorado River alluvium is influent to the river during normal flow (Sharp and Larken, 1988, Brune and Duffin, 1983, and Follett, 1970). During flood flow, the river may become temporarily influent. This reversing of the energy gradient decreases bank stability. Although the Highland Lakes dam system has succeeded in greatly reducing the peak flood stage, the regulated peak flood stages should still be considered as very significant. The storage and release of water for irrigation purposes (rice farming) near the Texas gulf coast causes numerous fluctuations in river stage. While these changes may seem relatively small, they are

capable of causing the gradient reversing flow conditions in the river banks.

The peak flood discharge of the Colorado river appears to have been greatly influenced by the Highland Lakes dam system, evidenced by the dramatic drop in observed peak discharge rates beginning in 1952 (Table 2.6). Although the regulated rates are much lower than those of pre-dam conditions, they represent significant flood events capable of transporting tremendous quantities of sediment. The degree of scour and bed load transport during flood events depends upon the flow velocity. Since the transport rate of bed load is proportional to flow velocity with an exponent ranging from 3 to 5 ($q_s \propto \bar{u}^{(3-5)}$) (Komar, 1988), a small change in velocity results in a much greater change in the amount of bed load transported. Regulated peak flood discharges of the Colorado River near Austin (Table 2.6) ranged from about 2 to 20 times the average regulated flow rate. For a flood 2 times the average flow rate, then, $q_s \propto 8\bar{u}^3$ to $32\bar{u}^5$. For a flood 20 times the average flow rate, $q_s \propto 8000\bar{u}^3$ to $3,200,000\bar{u}^5$.

Considering Petts (1984) discussion of the effects of upstream impoundments on rivers, conclusions might be drawn concerning the expected responses of the

Colorado River. Accelerated erosion should occur within the channel, especially near the dam, and extend for many miles downstream. Since there is evidence of channel bed armoring, the sediments eroded from the channel are likely to be derived from the channel banks. Erosion may be locally limited by the resistant limestone channel material near Austin, which is in contrast to the more easily eroded sands, silts, clays, and older alluvial material east of Austin. Sediment may tend to accumulate at tributary confluences when flood flow from the unregulated tributaries enters the regulated river. Although a study of aerial photographs revealed that the morphology of the river has not changed too dramatically since the construction of the dams, it should be remembered that the readjustment of channel morphology may take up to hundreds of years.

The sand and gravel mining operations, both active and abandoned sites, have had and continue to have a significant effect on the Colorado river. A substantial amount of sediment appears to have entered the river due to inadequate barriers between pit areas and the river. Numerous breached berms and muddy plumes near pit areas were evident in aerial

photographs and have been noted by others (Koenig, 1987 and MacRae, 1988). Many of the abandoned pits were virtually opened to the river effectively widening the river channel. At some locations, the river has altered its course in favor of the pit. This influx of sediment to the river adds to its sediment load and may locally reduce the amount of channel erosion.

In conclusion, the Colorado river downstream from Austin is responding to both natural and man-made changes. Geologically, the river is adjusting from the bedrock-controlled channel west of Austin to the alluvial channel of the coastal plains. Hydrologically, the river seeks to attain equilibrium under the influence of man's interference.

CHAPTER 3

QUANTITATIVE ANALYSIS

3.1 INTRODUCTION

The literature survey of the previous chapter characterized the environment and the historical and present behavior of the Colorado River in the study area. It was desired to compare the expected and theoretical behavior of the river with the results of recent data analysis in order to establish trends and be able to predict the future responses of the river to its environment.

In keeping with the major objective of this study, the goal of this chapter was to determine the origin of the river sediment and relative percentage of sediment from each source.

The analysis of the study area has been divided into the upstream contribution, the study area and downstream loading estimation, and the resulting sediment budget.

3.2 UPSTREAM CONTRIBUTION

The sediment loading to the river within the study area from upstream of Longhorn Dam was estimated by two methods, the simple average method and the unbiased stratified ratio estimator method. Both methods use stream discharge and suspended sediment data from the USGS stream gaging station (Colorado River at Austin, no. 08158000) located 2.3 km (1.4 mi) downstream from Longhorn Dam.

3.2.1 SIMPLE AVERAGE

The first method involves multiplying the annual average daily discharge by the average suspended sediment concentration for a given year:

$$\bar{W} = 893 \bar{Q} \cdot \overline{TSS}$$

where \bar{W} = avg. yearly sediment loading (kg/yr)
 \bar{Q} = annual avg. daily discharge (cfs)
 \overline{TSS} = avg. suspended sediment concentration (mg/L)

This yearly sediment loading was calculated for the most recent five years of record, 1983-1987, and averaged over those five years as shown in Table 3.1.

TABLE 3.1
ANNUAL SUSPENDED SEDIMENT LOADING OF THE COLORADO RIVER
UPSTREAM OF THE STUDY AREA

Suspended Sediment Loading (kg/yr)		
Year	Method	
	$\bar{Q} \bar{TSS}$ (Simple avg.)	Unbiased strat. ratio est.
1987	4.61 E7	5.10 E7
1986	6.02 E6	8.32 E6
1985	1.44 E7	1.42 E7
1984	5.88 E6	4.80 E6
1983	8.88 E6	7.89 E6
Avg.	1.63 E7	1.72 E7

3.2.2 UNBIASED STRATIFIED RATIO ESTIMATOR

The loading estimation method (originated by Dolan, Yui, and Geist in 1981) as summarized by Thomann and Mueller (1987) uses the "unbiased stratified ratio estimator" as a means of calculating mass loading rates. It is intended to take into account that while extensive flow data may be available, certain water quality data may be analyzed only periodically. This was the case for suspended solids at the gages in the study area, which were sampled only four times per year. The mean load was calculated from

$$\bar{W} = \frac{\bar{Q} \bar{W}_c}{\bar{Q}_c} \left[\frac{1 + (1/N)(S_{qw} / \bar{Q}_c \bar{W}_c)}{1 + (1/N)(S_q^2 / \bar{Q}_c^2)} \right]$$

where \bar{W} = avg. yearly load (kg/yr)

\bar{Q} = mean annual flow (cfs)

\bar{W}_c = mean daily loading for the days that suspended sediment was sampled (kg/yr)

\bar{Q}_c = mean daily flow for the sampling days (cfs)

N = total number of sampling days for the year

Also,

$$S_{qw} = [1/(N-1)] \left[\left(\sum_{i=1}^N Q_{ci} W_{ci} \right) - N \bar{Q}_c \bar{W}_c \right]$$

and

$$S_q^2 = [1/(N-1)] \left[\left(\sum_{i=1}^N Q_{ci}^2 \right) - N\bar{Q}_c^2 \right]$$

where Q_{ci} = avg. daily flow for each sample day
(cfs)

W_{ci} = daily loading for each sample day
(kg/yr)

The resulting yearly loadings and five-year average are shown in Table 3.1. The computer program USTRAT used to solve the above equations is included in Appendix A.

3.2.3 RESULTS

Both methods were used to arrive at an expected yearly sediment loading for the Colorado River from immediately upstream of the study area. As shown in Table 3.1, the differences in loading between the methods were variable from year to year, probably due to the varying discharges on the selected sample days. The five-year averages were very close, showing only a 5% difference in loading. From this it was assumed that the \bar{Q} TSS simple average method was not significantly affected by the periodic sampling. Therefore, the resulting loading estimates from this method were used in later calculations.

3.3 STUDY AREA AND DOWNSTREAM LOADING ESTIMATION

Sediment sources within the study area were divided into the contributions from adjacent tributaries and the sediment eroded from the river channel itself. In order to calculate a sediment budget, it was also necessary to include sediment data collected downstream of the study area.

3.3.1 TRIBUTARY CONTRIBUTION

The model used to estimate the loading to the Colorado River from adjacent tributaries was adapted from the computer model HILOADS (Miertschin and Armstrong, 1986). Miertschin used the model in the Highland Lakes region of central Texas to estimate the phosphorus influx into the lake system from the tributaries within the watersheds. The model is based on the SCS method for estimating storm runoff (SCS, 1972) which is summarized by Chow, Maidment, and Mays (1988). Direct runoff or excess precipitation, P_e , is calculated as

$$P_e = \frac{(P - 0.2S)^2}{P + 0.8S}$$

where P = depth of precipitation (in)

S = potential maximum retention (in)

The potential maximum retention is a function of the curve number CN:

$$S = \frac{1000}{CN} - 10 \quad .$$

The curve number is a dimensionless indicator of the relationship between cumulative rainfall and cumulative runoff, with $0 \leq CN \leq 100$ and impervious surfaces indicated by $CN = 100$. The SCS has tabulated curve numbers based on hydrologic soil group and land use. These curve numbers apply to normal antecedent moisture conditions. For wet or dry conditions, the curve numbers must be adjusted.

3.3.1.1 SSLOAD Model

The SSLOAD computer program used in this study was developed from the Miertschin and Armstrong (1986) HILOADS model and from departmental work on the Lower Colorado River drainage basin between Austin and the Gulf of Mexico (Armstrong, 1989). Previous workers had divided the river basin into smaller subbasins or watersheds as shown in Figure 3.1. A subbasin description by tributaries/outfalls is included in Table 3.2. Each subbasin was then analyzed for land use and soil type. The land use categories applied to

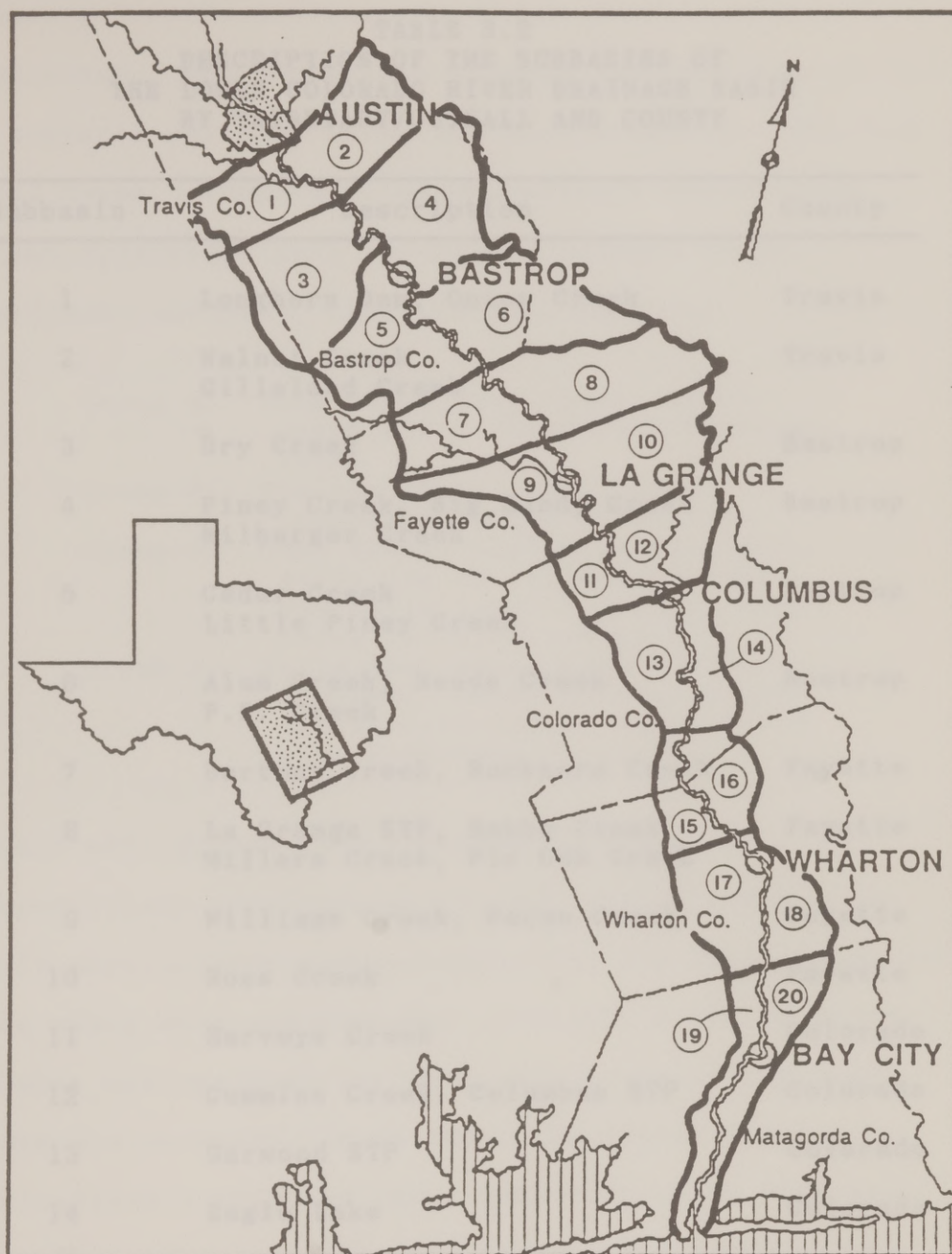


Figure 3.1: The twenty subbasins of the lower Colorado River drainage basin between Austin and the Gulf of Mexico.
(Adapted from previous departmental work)(Armstrong, 1989)

TABLE 3.2
DESCRIPTION OF THE SUBBASINS OF
THE LOWER COLORADO RIVER DRAINAGE BASIN
BY TRIBUTARY/OUTFALL AND COUNTY

Subbasin	Description	County
1	Longhorn Dam, Onion Creek	Travis
2	Walnut Creek Gilleland Creek	Travis
3	Dry Creek	Bastrop
4	Piney Creek, Big Sandy Creek Wilbarger Creek	Bastrop
5	Cedar Creek Little Piney Creek	Bastrop
6	Alum Creek, Reeds Creek P.D. Creek	Bastrop
7	Bartons Creek, Buckners Creek	Fayette
8	La Grange STP, Rabbs Creek Millers Creek, Pin Oak Creek	Fayette
9	Williams Creek, Pecan Creek	Fayette
10	Ross Creek	Fayette
11	Harveys Creek	Colorado
12	Cummins Creek, Columbus STP	Colorado
13	Garwood STP	Colorado
14	Eagle Lake	Colorado
15-18	Gulf of Mexico	Wharton
19-20	Gulf of Mexico	Matagorda

these subbasins include rangeland, forest, cropland, and urban. The percentage of each land use type within a subbasin was determined for each subbasin. The four soil types, groups A-D, were similarly apportioned. These hydrologic soil groups are defined (Chow, Maidment, and Mays, 1988 and SCS, 1972) as

- Group A: Deep sand, deep loess, aggregated silts (high infiltration rate)
- Group B: Shallow loess, sandy loam (moderate infiltration rate)
- Group C: Clay loams, shallow sandy loam, soils low in organic content, and soils usually high in clay (slow infiltration rate)
- Group D: Soils that swell significantly when wet, heavy plastic clays, and certain saline soils (very slow infiltration rate).

These soil groups were assigned to the soil associations according to the SCS soil surveys. The soil associations and corresponding SCS soil groups for the study area are included in Figure 2.14. A curve number was assigned for each soil group within each land use category. From this, the SSLOAD program calculated a weighted curve number for each land use category in each subbasin. Since curve numbers are also a function of the antecedent moisture conditions, and because the lower Colorado River basin includes

several different physiographic regions, these varying moisture conditions were also taken into account.

The precipitation for each subbasin was determined by its proximity to one of three gaging stations. The Austin gage was used for subbasins 1-4, the Columbus gage for subbasins 5-14, and the Matagorda gage for subbasins 15-20. In order to enter the precipitation data into the HILOADS program, the rainfall was grouped into a series of average precipitation depths (Miertschin and Armstrong, 1986):

1.5 in.	(1.0" < rainfall < 2.0")
2.5 in.	(2.0" < rainfall < 3.0")
4.0 in.	(3.0" < rainfall < 5.0").

Using these precipitation depths, Miertschin and Armstrong concluded that the annual frequency distribution of rainfall was reasonably represented since the smaller, more frequent storms did not result in significant runoff. The rainfall data from the three rain gages for 1984 was collected and grouped according to precipitation depth by previous workers, and was used as the input precipitation for the SSLOAD program. The program computed the storm event runoff in inches for each subbasin using the SCS method as

examined earlier. The flows for each subbasin were computed from the runoff, given the surface area.

The suspended sediment concentration for each subbasin was estimated based on data collected from various tributaries by Armstrong et al. (1987). SSLOAD calculates the mass loading from the suspended sediment concentration and flow for each subbasin. The SSLOAD computer program used in this study and the resulting calculations are included in Appendices B and C, respectively.

The SSLOAD program was run using precipitation and land use data for 1984. To estimate the tributary contribution for the sediment budget analysis, only subbasins 1-16 (Austin to near Wharton) were considered, due to limitations in data. This resulted in a suspended sediment loading of 3.26 E7 kg/yr from all subbasins between Austin and Wharton. This loading estimate will be included in the sediment budget calculations.

As a check to the SSLOAD program, a flow analysis was conducted between Austin and Bastrop. This check was not run between Austin and Wharton as there were too many abstractions (e.g., withdrawals for rice farm irrigation) to account for within that reach.

The SSLOAD program was run for subbasins 1-4 to obtain a value of the total flow input from adjacent tributaries. This value was added to the discharge at the Austin gage (no. 08158000) and compared with the discharge at the Bastrop gage (no. 08159200). Precipitation data for the years 1964, 1974, and 1984 had previously been previously used in other departmental work and was used as input for SSLOAD to compare flow data. The results are shown in Table 3.3. The percent difference between the actual vs. calculated flow values for the three years are an indication of the variability of the data and method used to estimate these values. It should be noted that the river discharge can also be affected by upstream LCRA dam releases.

3.3.1.2 Sediment Rating Curve

Another method used to estimate suspended sediment load requires the development of a sediment rating curve (SCS, 1971). The daily sediment load is plotted vs. average daily flow rate on a log-log scale. The data will often approximate a straight line. Given daily discharge data, it is possible to calculate the

TABLE 3.3
A COMPARISON OF SSLOAD CALCULATED FLOW VS.
ACTUAL FLOW AT THE USGS BASTROP GAGE
(NO. 08159200)

Year	Flow Data (m^3)		% Diff.
	Upstream + SSLOAD	Bastrop Gage	
1964	1.03 E9	7.57 E8	36
1974	2.83 E9	3.18 E9	11
1984	1.01 E9	1.26 E9	20

daily suspended sediment yield. From this, the average annual suspended sediment yield can be estimated.

Between Austin and Bastrop, sufficient suspended sediment concentration data was available for constructing suspended sediment rating curves for Walnut Creek, Onion Creek, and Big Sandy Creek. The USGS gaging station on Walnut Creek at Webberville Road (no. 08158600) is located 4.5 km (2.8 mi) upstream from the Colorado River. The Onion Creek gaging station (no. 08159000) is located on the downstream side of the US 183 bridge, about 17.1 km (10.6 mi) upstream from the Colorado River. Both Walnut Creek and Onion Creek were sampled from 1976-82. The Big Sandy Creek gaging station (no. 08159170) is located on the downstream side of SH 95 bridge, approximately 17.2 km (10.7 mi) north of Bastrop and 17.4 km (10.8 mi) from the Colorado River confluence. The creek was sampled from 1979-81. The sediment rating curves for the three creeks are shown in Figures 3.2 (a)-(c). All three curves show good line approximation, with the Onion Creek data showing excellent line fit. A composite graph of the three rating curves is shown in Figure 3.2(d). The Onion Creek and Walnut Creek curves are remarkably similar, while Big Sandy Creek shows

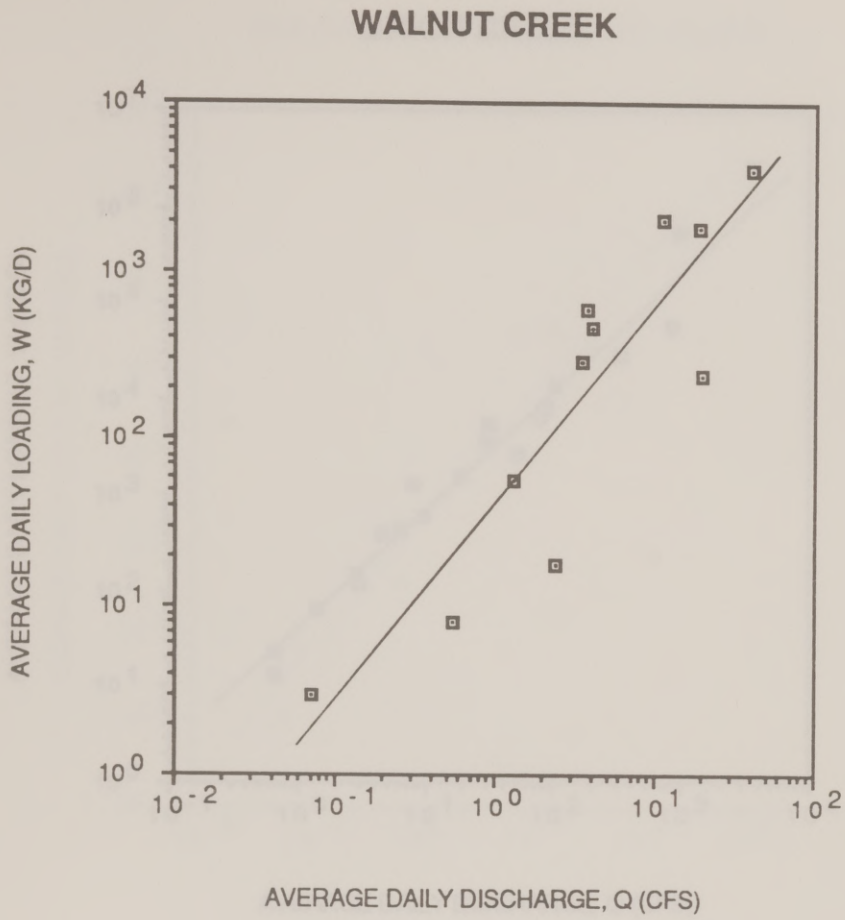


Figure 3.2(a): Sediment rating curve for Walnut Creek.

ONION CREEK

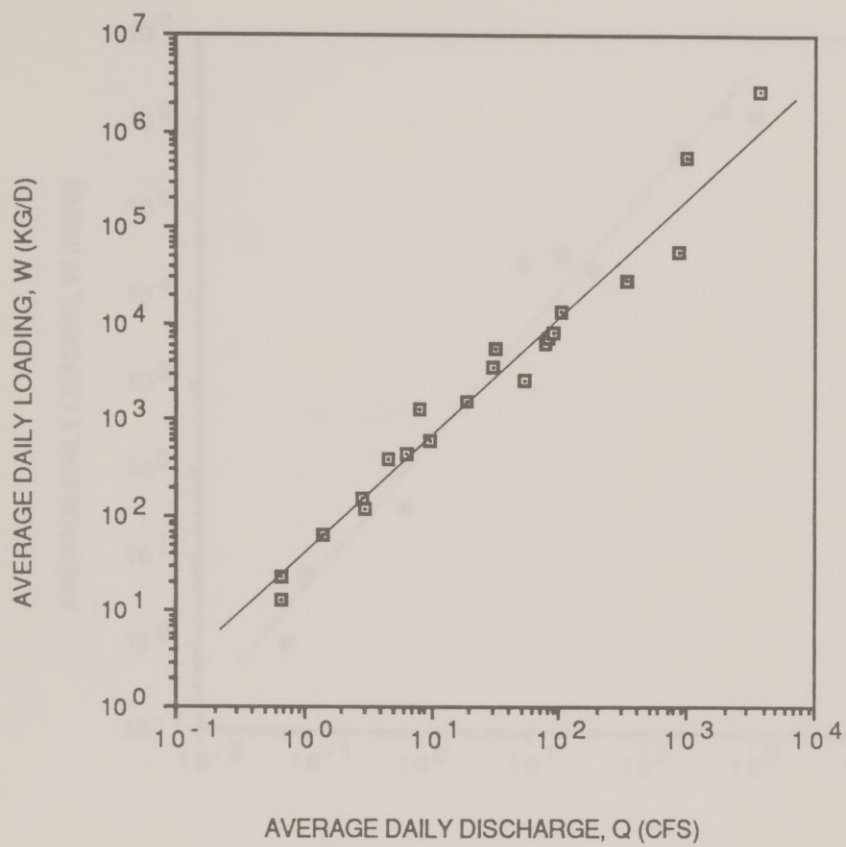


Figure 3.2(b): Sediment rating curve for Onion Creek.

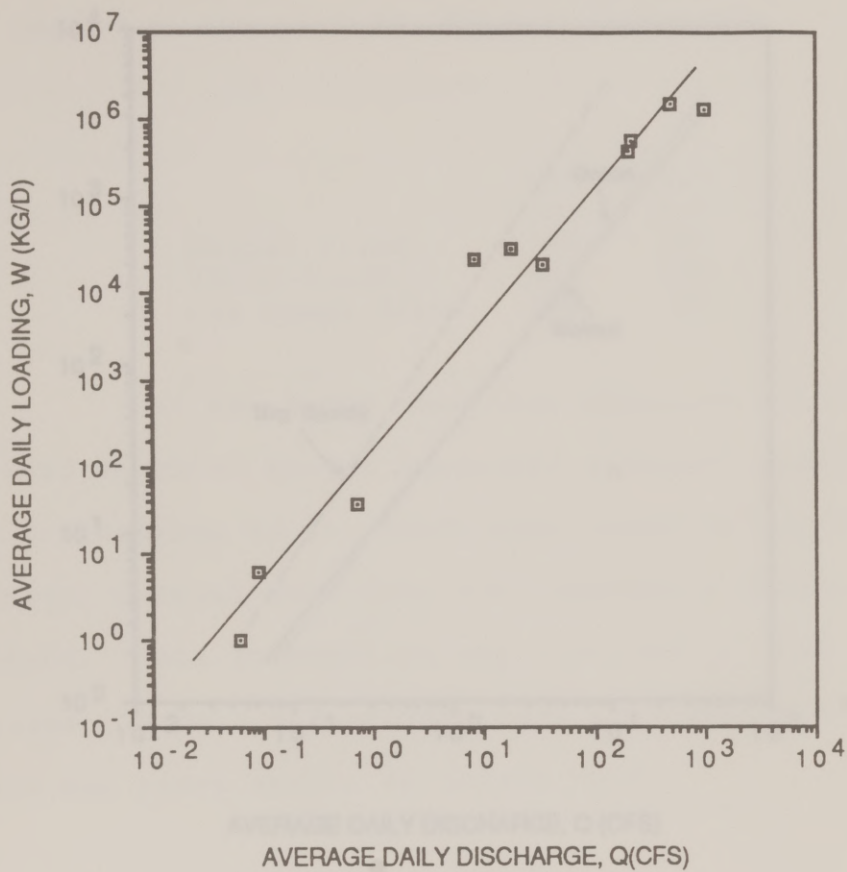
BIG SANDY CREEK NEAR ELGIN

Figure 3.2(c): Sediment rating curve for Big Sandy Creek near Elgin

COMPOSITE

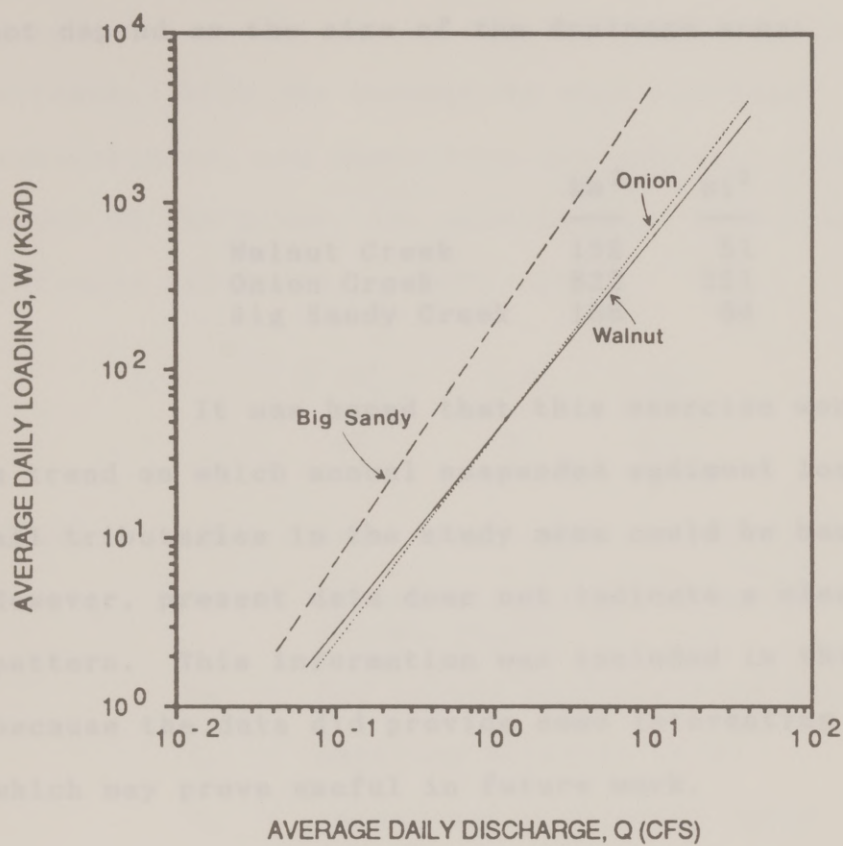


Figure 3.2(d): Composite graph of the Walnut Creek, Onion Creek, and Big Sandy Creek sediment rating curves.

significantly higher suspended sediment loading for a given discharge. It is evident that the loading does not depend on the size of the drainage area:

	km ²	mi ²
Walnut Creek	132	51
Onion Creek	832	321
Big Sandy Creek	166	64

It was hoped that this exercise would yield a trend on which annual suspended sediment loadings for all tributaries in the study area could be based. However, present data does not indicate a clear pattern. This information was included in this study because the data did provide some interesting results which may prove useful in future work.

3.3.2 RIVER CHANNEL EROSION

The suspended solids in the water column of a river represent a balance between settling and resuspension. The erosion of bed sediment results in an increase in solids in the water column downstream, and is capable of greatly affecting this balance.

3.3.2.1 Solids Balance

Thomann and Mueller (1987) present a discussion on the solids balance within rivers and streams. With the assumption that settling, resuspension, and deposition are constant along the reach of the river, the mass balance is represented (Thomann and Mueller, 1987) by

$$U \frac{dM_1}{dX} = - \frac{V_s M_1}{H} + \frac{V_u M_2}{H}$$

where

- U = mean river velocity (m/s)
- M_1 = solids concentration in the water column (mg/L)
- M_2 = bed solids concentration (mg/L)
- V_s = settling velocity (m/s)
- V_u = resuspension velocity (m/s)
- H = water column depth (m)
- X = distance downstream (m)

These parameters are graphically illustrated in Figure 3.3. For a spatially constant value of M_2 , the solution to this equation becomes

$$M_1(X) = M_1(0) \exp\left(-\frac{V_s X}{H U}\right) + \frac{V_u M_2}{V_s} \left[1 - \exp\left(-\frac{V_s X}{H U}\right)\right]$$

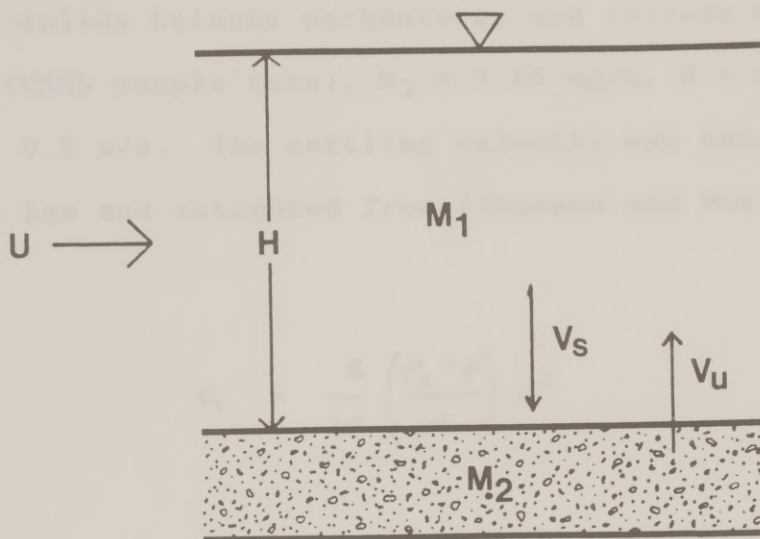


Figure 3.3: Cross-section of a stream, illustrating key parameters of the solids balance equation.

where $M_1(X)$ = solids concentration (mg/L) in the water column for a given X

$M_1(0)$ = solids concentration (mg/L) at $X=0$

Average values typical of the Colorado River were used for the solids balance parameters, and include $M_1(0) = 5$ mg/L (USGS sample data), $M_2 = 7 \text{ E}5$ mg/L, $H = 0.5$ m, and $U = 0.2$ m/s. The settling velocity was based on Stoke's Law and estimated from (Thomann and Mueller, 1987)

$$v_s = \frac{g}{18} \left(\frac{\rho_s - \rho}{\mu} \right) d^2$$

or

$$v_s = 0.033634 (\rho_s - \rho) d^2$$

which assumes

g = acceleration due to gravity
(981 cm/s²)

μ = dynamic viscosity (0.014 g/cm·s)

ρ_s = particle density (g/cm³)

ρ = water density (g/cm³)

d = particle diameter (μ m)

The solids were estimated to be 50% silt and 50% clay and the settling velocity was calculated separately for

each. These two settling rates were then averaged by calculating the harmonic mean, resulting in $V_s = 0.13$ m/d. The resuspension velocity was estimated from the solids concentration equation discussed earlier with the assumption that if $M_1(0)$ is small, the solids concentration increases to a steady value at $X = \infty$ of

$$M_1(\infty) = \frac{V_u M_2}{V_s}$$

or

$$V_u = \frac{M_1(\infty) V_s}{M_2}$$

The value of $M_1(\infty)$ was estimated using data from Armstrong et al. (1987) by plotting annual average suspended sediment concentration against distance downstream and noting where the concentration approached an asymptotic value (Figure 3.4). It should be noted that the two stations with annual average suspended sediment concentrations of greater than 300 mg/L were taken downstream of old sand and gravel operations, and are considered outliers. From the graph, the suspended sediment concentration leveled off at an average value of 123 mg/L = $M_1(\infty)$. The

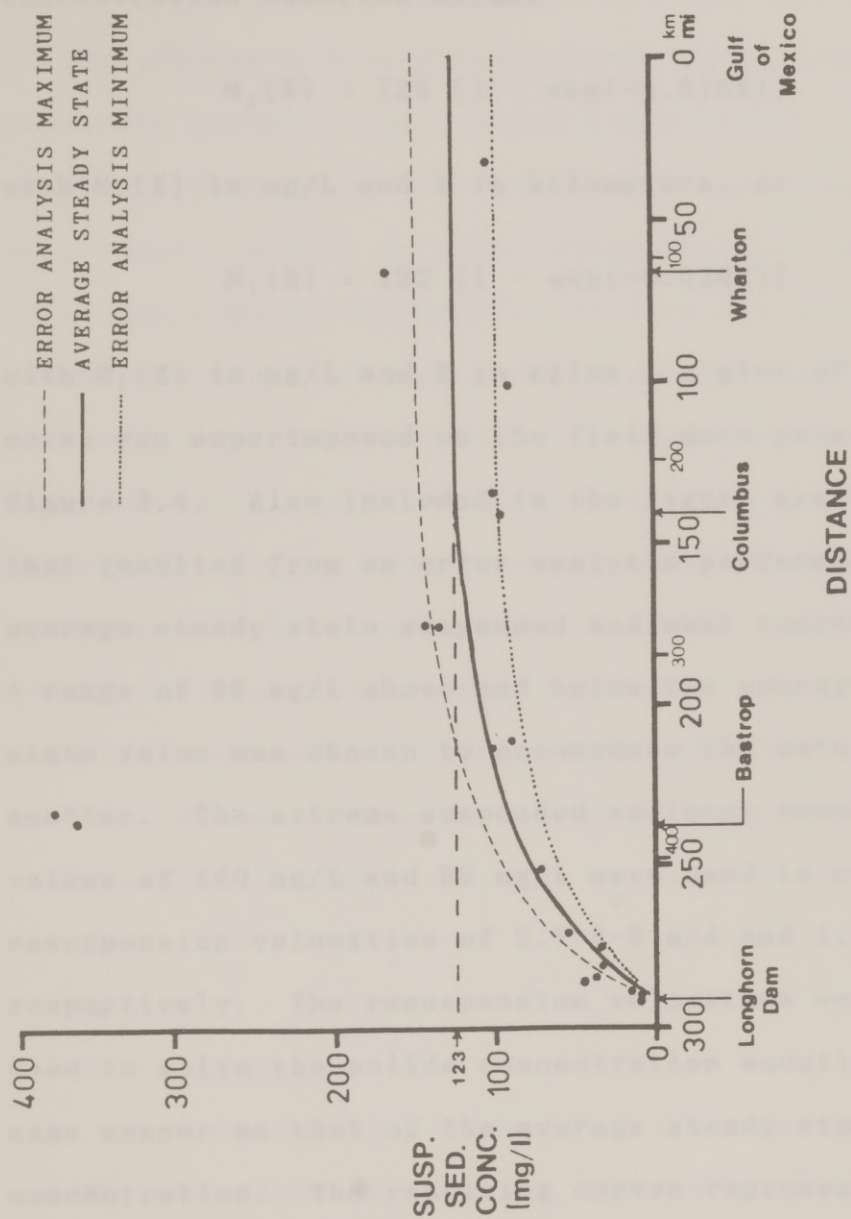


Figure 3.4: Average annual suspended sediment concentration as a function of distance downstream. The superimposed curves were derived from the solids balance equation.

resuspension velocity was then calculated to be $2.3 \text{ E-}5$ m/d. With the above known parameters, the solids concentration equation became

$$M_1(X) = 123 [1 - \exp(-0.015X)]$$

with $M_1(X)$ in mg/L and X in kilometers, or

$$M_1(X) = 123 [1 - \exp(-0.024X)]$$

with $M_1(X)$ in mg/L and X in miles. A plot of this curve was superimposed on the field data points in Figure 3.4. Also included in the figure are the curves that resulted from an error analysis performed on the average steady state suspended sediment concentration. A range of 25 mg/L above and below the average steady state value was chosen to accomodate the data point scatter. The extreme suspended sediment concentration values of 148 mg/L and 98 mg/L were used to calculate resuspension velocities of $2.7 \text{ E-}5$ m/d and $1.8 \text{ E-}5$ m/d, respectively. The resuspension velocities were then used to solve the solids concentration equation in the same manner as that of the average steady state concentration. The resulting curves represent the maximum and minimum suspended sediment concentration curves of the error analysis (Figure 3.4). All three

curves show the greatest increase in concentration near Longhorn Dam and approach an asymptotic value near Columbus. Error propagation in both the maximum and minimum curves occurs upstream from the steady state condition between Longhorn Dam and Columbus, with the greatest increase in error occurring near Longhorn Dam. As a result, errors in delineating the average suspended sediment concentration from the field data points and the consequent effects on the calculated suspended sediment concentration curve could produce some degree of overestimation or underestimation of the suspended sediment concentration. The error analysis did show, however, that the curves that would occur within the suggested range of error all represent the same basic set of conditions. That is, the suspended sediment concentration curve shows the greatest increase near Longhorn Dam and approaches an asymptotic value near Columbus.

3.3.2.2 Results

As shown in Figure 3.4, the plot of the solids concentration equation against the field data points results in a close curve fit. It follows, then, that the assumptions of steady state conditions and

constant parameters (i.e., U , H , M_2 , V_s , V_u) and the values estimated for the model presented by Thomann and Mueller are valid. The graph can then be used to estimate the suspended sediment concentration at any point within the reach while the river is flowing at normal conditions.

3.4 SEDIMENT BUDGET

In order to determine the percentage of sediment originating from each source area, that is, upstream of the study area, from adjacent tributaries, and from river channel erosion, both a short term and a long term sediment budget were calculated. Since the USGS suspended sediment data was only available for the Austin gage (no. 08158000) and the gage at Wharton (no. 08162000), this reach of the river was used to develop the sediment budget.

The short term sediment budget was calculated for September 1985 - August 1986 and is shown in Table 3.4. This is the period in which departmental data on the adjacent tributaries was collected. This data was used in the SSLOAD program to estimate loading from tributaries, as discussed earlier. The loadings from subbasins 1-16 were

TABLE 3.4
THE SHORT TERM AND LONG TERM SEDIMENT BUDGETS
FOR THE LOWER COLORADO RIVER DRAINAGE BASIN

	Short Term Sediment Budget (9/85-8/86)		Long Term Sediment Budget (1983-87)	
	W (kg/yr)	Source (%)	W (kg/yr)	Source (%)
INPUT				
Upstream	5.90 E6	1.9	1.63 E7	3.2
Adjacent Tributary	3.26 E7	10.6	3.26 E7	6.5
OUTPUT				
Downstream	3.07 E8	—	5.04 E8	—
Erosion = Output-Input	2.69 E8	87.5	4.55 E8	90.3

calculated using SSLOAD to obtain a total tributary loading between Austin and Wharton. The loading from upstream of the study area and the downstream loading at Wharton were estimated by the $\bar{Q} \overline{\text{TSS}}$ simple average method, using USGS data, as discussed in a previous section. The loading due to erosion was calculated by subtracting the upstream and tributary loading from the downstream loading. The percentage of sediment from each of the three sources could then be calculated.

The long term sediment budget was estimated based on five years of data (1983-1987), and is also included in Table 3.4. The upstream loading was estimated using the $\bar{Q} \overline{\text{TSS}}$ method by arithmetically averaging the resulting five annual loading rates. The downstream loading was calculated in the same manner. The annual loading from adjacent tributaries was estimated from the SSLOAD program, as with the short term budget. The loading due to erosion was, again, the difference between the upstream and tributary loading and the downstream loading.

Table 3.4 shows that in both cases, the overwhelming majority of the sediment originated from channel erosion. The contribution from the adjacent tributaries is significant but minor, and the loading

from upstream is almost negligible. The short term sediment source percentages agree fairly well with the long term percentages. The differences between them are probably more due to the particular short term period that was chosen than being a case of long term vs. short term percentages, as weather patterns may have a more pronounced effect on the short term results.

3.5 RESULTS

The Colorado River east of Austin flows within an alluvial channel. The sediment available to a particular reach must be derived from upstream, from the adjacent drainage basin, and from within the channel itself. Upstream from the study area, the contribution of sediment was shown to be negligible, evidenced by the suspended sediment sampling data and the sediment budget. The series of dams upstream from Austin have served to remove all of the coarse grained particles and most of the suspended sediment from the water.

3.5.1 DRAINAGE BASIN SEDIMENT

The influx of sediment to the river from tributaries of the adjacent drainage basins is relatively minor based on the data obtained from the SSLOAD program and the sediment budget. The sediments transported by the tributaries originate from the bedrock and/or associated soils within the drainage basin. As seen in the geologic map in Figure 2.18, the bedrock ranges from the calcareous units (limestones, marls) in the western portion of the study area to the sands, silts, and clays of the central and eastern portions. The soils are loamy throughout the study area and generally become deeper, more sandy, and less calcareous east of Austin (SCS, 1974, 1979). The tributaries may also pass through older tributary and Colorado River terrace deposits, supplying sediment from either local bedrock or from upstream sources (LLano-Burnet area, Cretaceous limestones) no longer supplying the present day river.

The sediment loading rates from the various subbasins were calculated in the SSLOAD program based on the SCS method for estimating runoff. The sediment yield for each subbasin was calculated by dividing the sediment loading by the corresponding drainage area.

Figure 3.5 shows the distribution of the drainage areas for each subbasin. Subbasins 1-4 represent the primary study area in and around Austin to near Bastrop.

Considering the method of subbasin numbering, there is a general decrease in the drainage area downstream.

Figure 3.6 shows the relationship between sediment yield and subbasin location. Subbasin location, or distance from mouth, was based on the points of influence of major streams with the Colorado river, giving a more or less geographical perspective. Except for a slight decrease in sediment yield for subbasin 7, the graph shows a marked increase in sediment yield downstream to subbasin 10. At this point, the sediment yield declines and then again increases to a second peak at subbasins 14 and 15. With the exception of subbasin 16, subbasins 1-4 have the lowest sediment yields of all subbasins, primarily due to land usage and to geologic and soil cover conditions. These factors and their distribution between Austin and Wharton are described below.

When the sediment flux, or loading for each subbasin is compared with the corresponding drainage area, there does appear to be a correlation (Figure 3.7). If subbasins 1-4 are not considered, a trend is

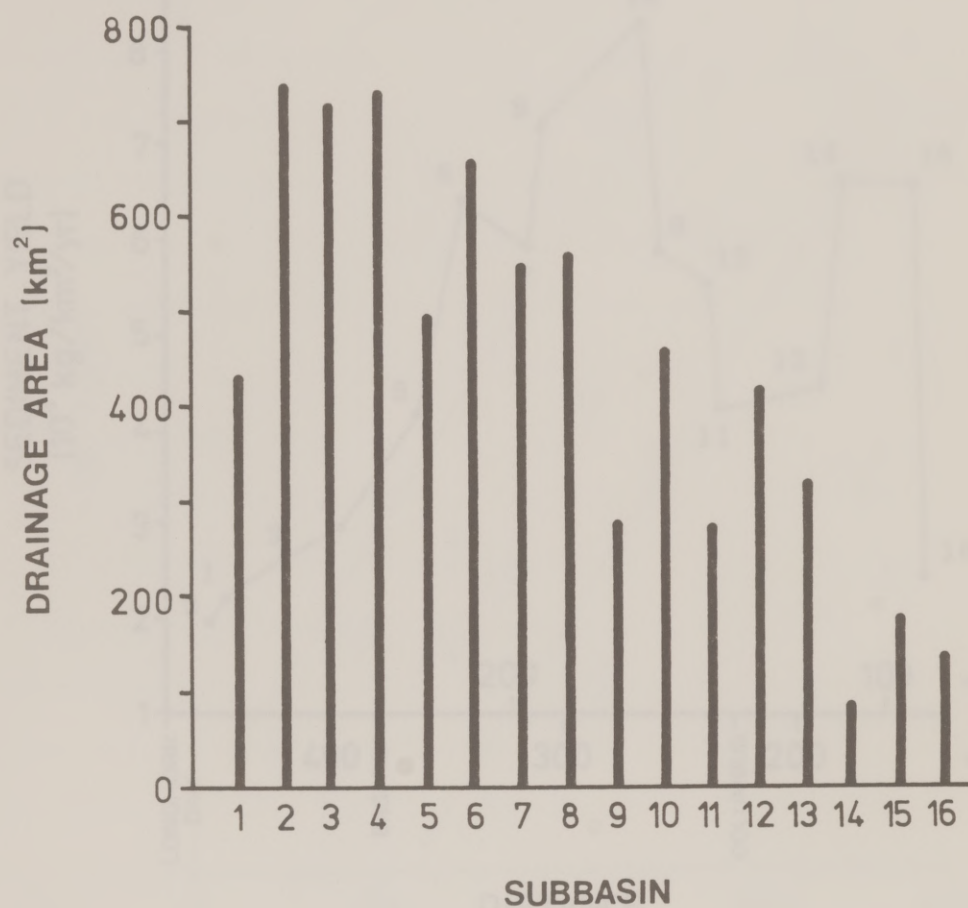


Figure 3.5: Distribution of drainage area for each subbasin between Austin and Wharton.

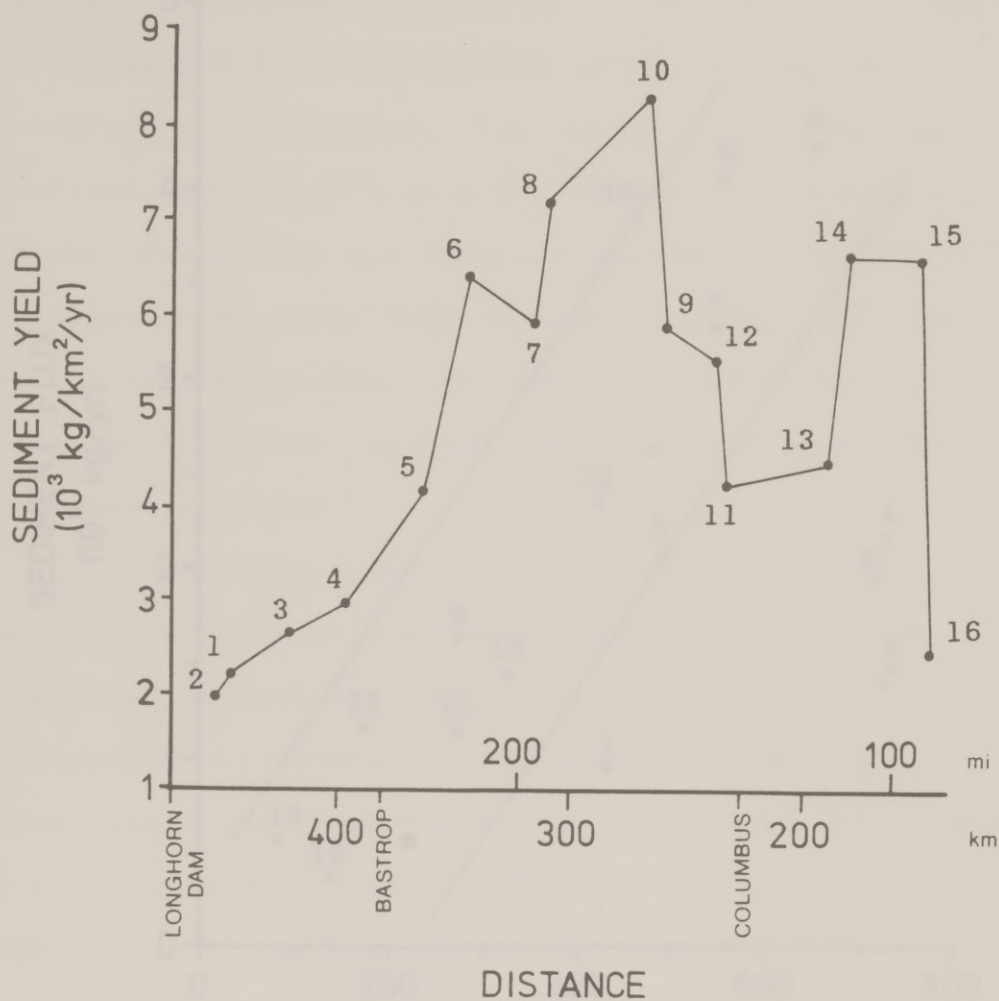


Figure 3.6: Relationship between sediment yield and subbasin distance from mouth. (Subbasins are indicated by number on graph).

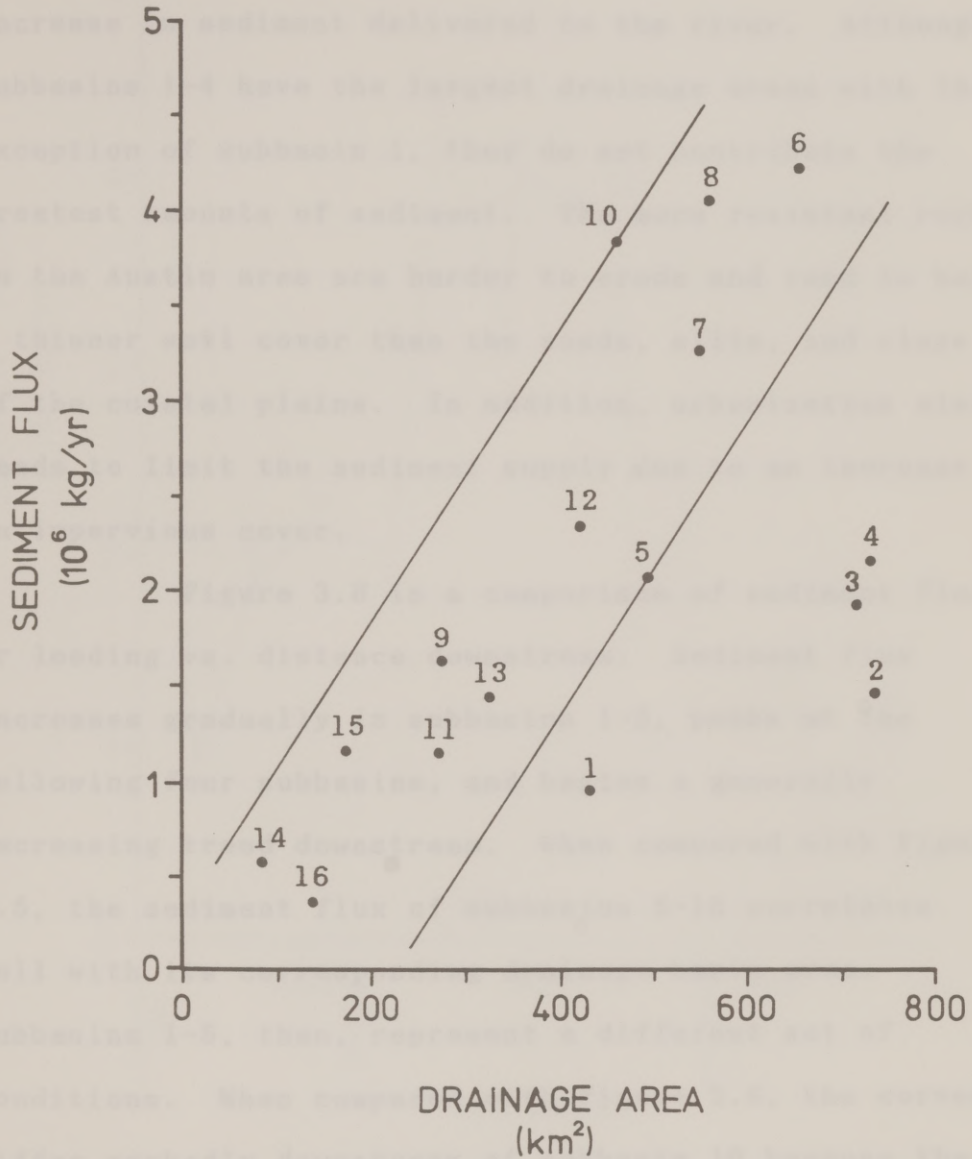


Figure 3.7: Relationship between sediment flux and drainage area. (Subbasins are indicated by number on graph; boundaries are arbitrarily drawn)

obvious among the remaining data points. As one would expect, an increase in drainage area results in an increase in sediment delivered to the river. Although subbasins 1-4 have the largest drainage areas with the exception of subbasin 1, they do not contribute the greatest amounts of sediment. The more resistant rocks in the Austin area are harder to erode and tend to have a thinner soil cover than the sands, silts, and clays of the coastal plains. In addition, urbanization also tends to limit the sediment supply due to an increase in impervious cover.

Figure 3.8 is a comparison of sediment flux or loading vs. distance downstream. Sediment flux increases gradually in subbasins 1-5, peaks at the following four subbasins, and begins a generally decreasing trend downstream. When compared with Figure 3.5, the sediment flux of subbasins 6-16 correlates well with its corresponding drainage basin area. Subbasins 1-5, then, represent a different set of conditions. When compared with Figure 3.6, the curves differ markedly downstream of subbasin 10 because the sediment flux curve reflects the decreasing drainage subbasin area downstream.

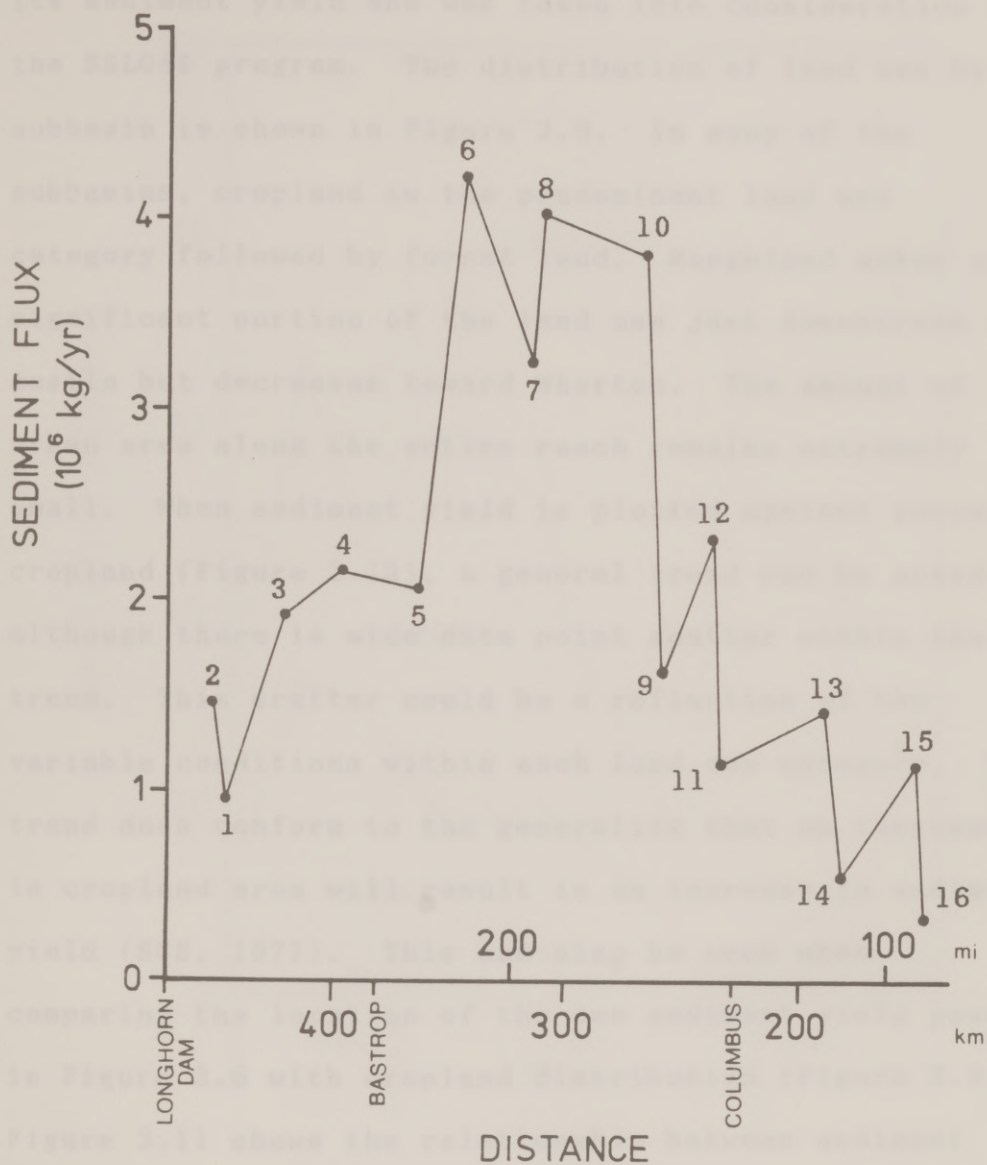


Figure 3.8: Relationship between sediment flux and subbasin distance from mouth. (Subbasins are indicated by number on graph).

The land usage of a basin can greatly impact its sediment yield and was taken into consideration by the SSLOAD program. The distribution of land use by subbasin is shown in Figure 3.9. In many of the subbasins, cropland is the predominant land use category followed by forest land. Rangeland makes up a significant portion of the land use just downstream of Austin but decreases toward Wharton. The amount of urban area along the entire reach remains extremely small. When sediment yield is plotted against percent cropland (Figure 3.10), a general trend can be noted, although there is wide data point scatter within the trend. This scatter could be a reflection of the variable conditions within each land use category. The trend does conform to the generality that an increase in cropland area will result in an increase in sediment yield (SCS, 1971). This can also be seen when comparing the location of the two sediment yield peaks in Figure 3.6 with cropland distribution (Figure 3.9). Figure 3.11 shows the relationship between sediment yield and percent rangeland. According to the graph, there is a general decrease in sediment yield with increase in percent rangeland, with some degree of scatter within the trend. It is interesting to note

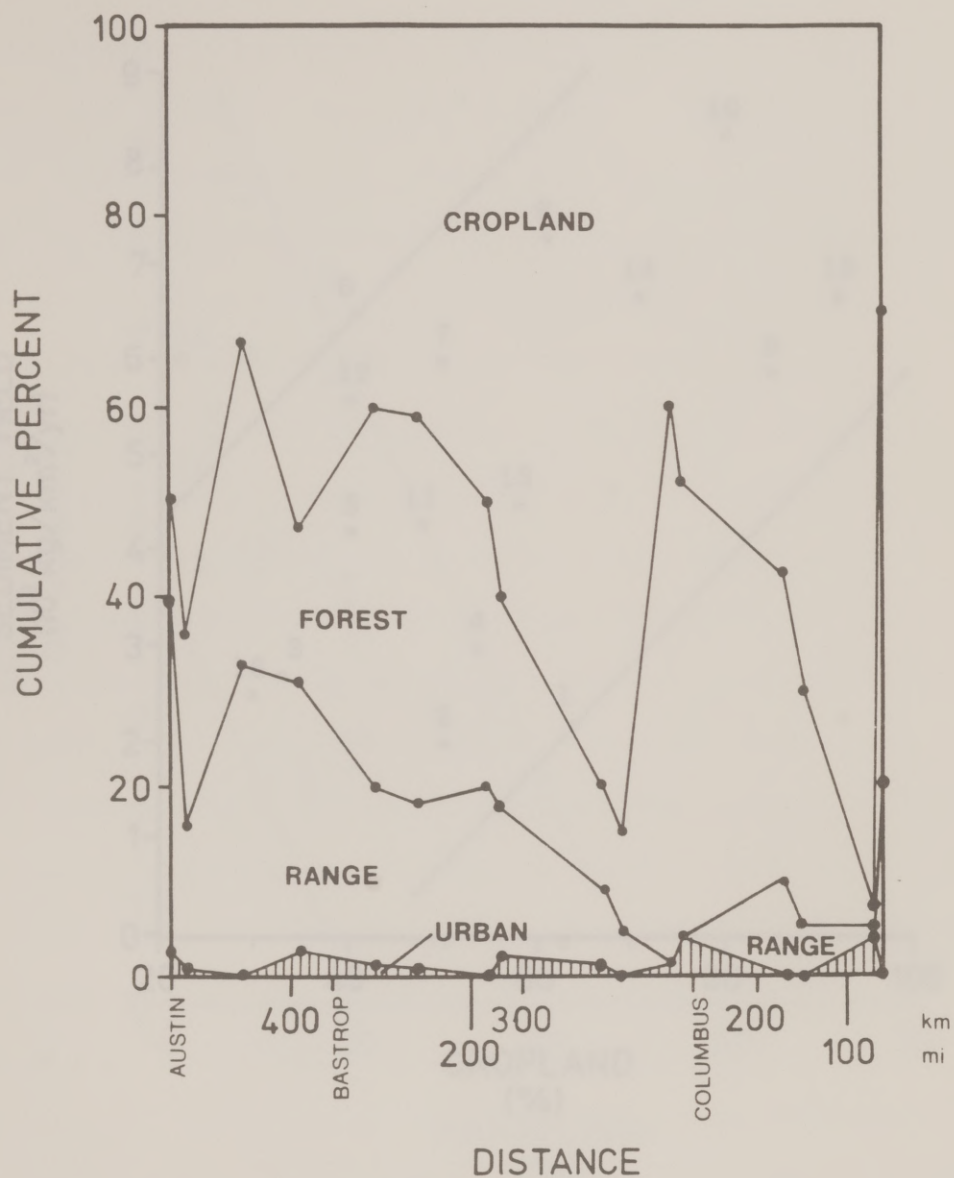


Figure 3.9: Distribution of land use based on subbasin distance from mouth.

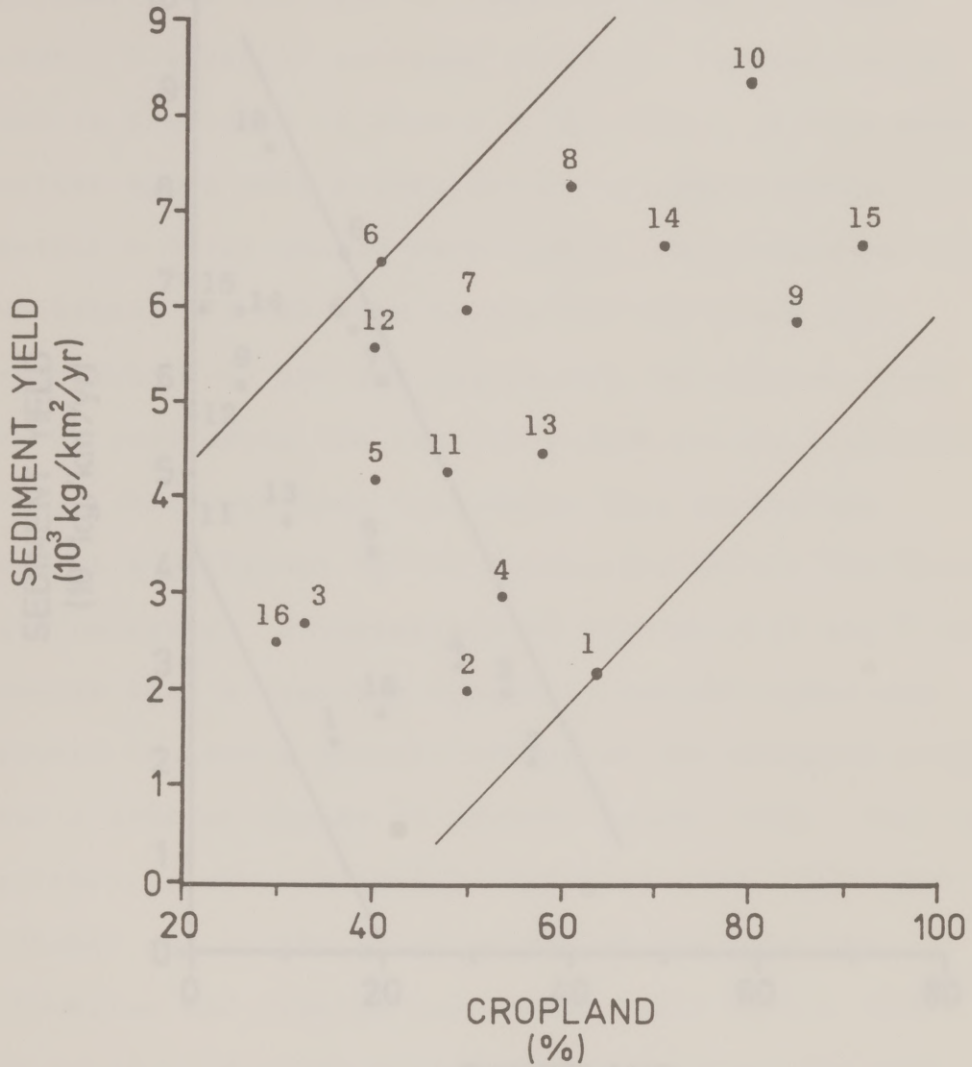


Figure 3.10: Sediment yield vs. percent cropland between Austin and Wharton. (Subbasins are indicated by number on graph; boundaries are arbitrarily drawn)

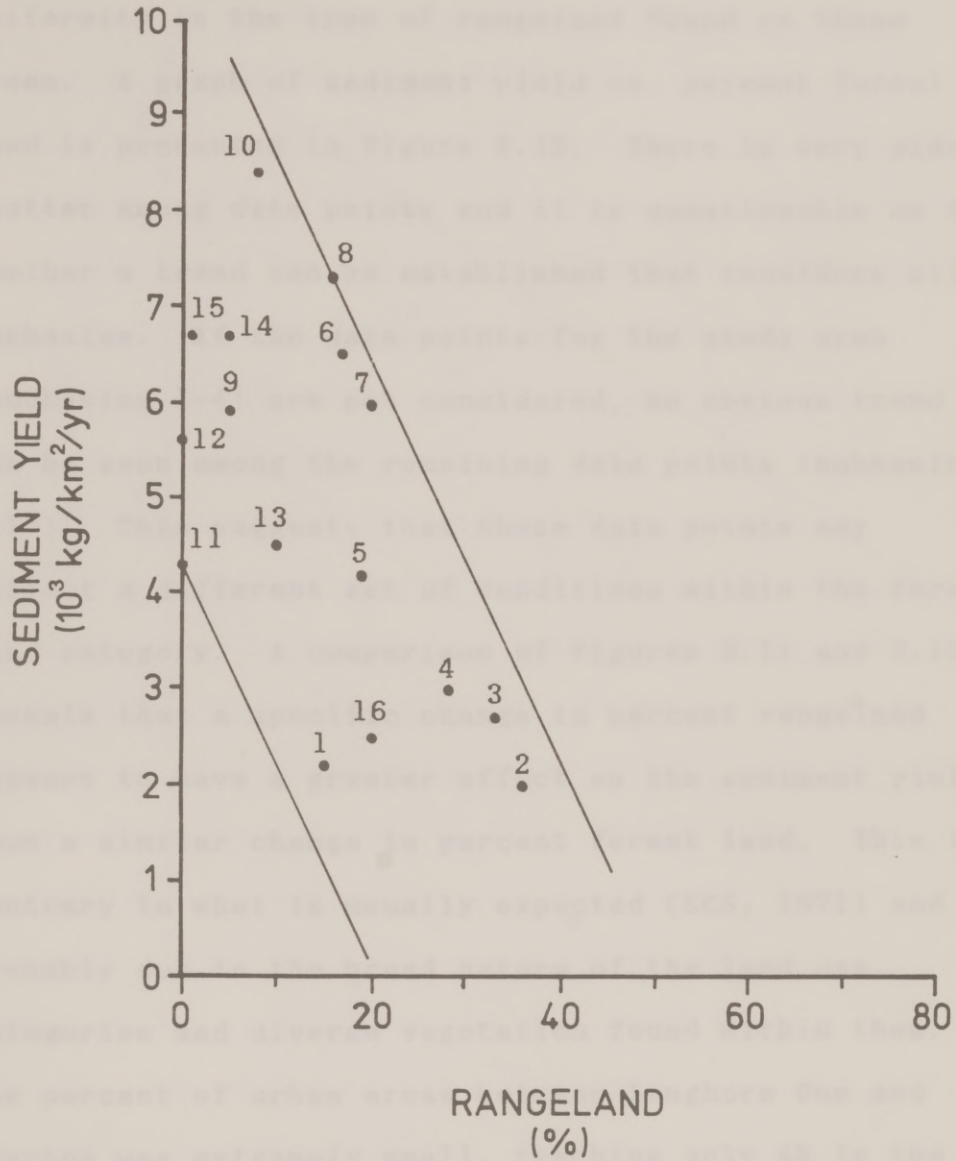


Figure 3.11: Sediment yield vs. percent rangeland between Austin and Wharton. (Subbasins are indicated by number on graph; boundaries are arbitrarily drawn)

that the data points from subbasins 2-8 and 10 seem to align in a very narrow band. Perhaps this suggests a uniformity in the type of rangeland found in these areas. A graph of sediment yield vs. percent forest land is presented in Figure 3.12. There is very wide scatter among data points and it is questionable as to whether a trend can be established that considers all subbasins. If the data points for the study area (subbasins 1-4) are not considered, an obvious trend can be seen among the remaining data points (subbasins 5-16). This suggests that these data points may reflect a different set of conditions within the forest land category. A comparison of Figures 3.11 and 3.12 reveals that a specific change in percent rangeland appears to have a greater affect on the sediment yield than a similar change in percent forest land. This is contrary to what is usually expected (SCS, 1971) and is probably due to the broad nature of the land use categories and diverse vegetation found within them. The percent of urban areas between Longhorn Dam and Wharton was extremely small, reaching only 4% in two of the subbasins (11 and 15). Consequently, a graph of sediment yield vs. percent urban revealed no significant information. Figures 3.10-3.12 indicate

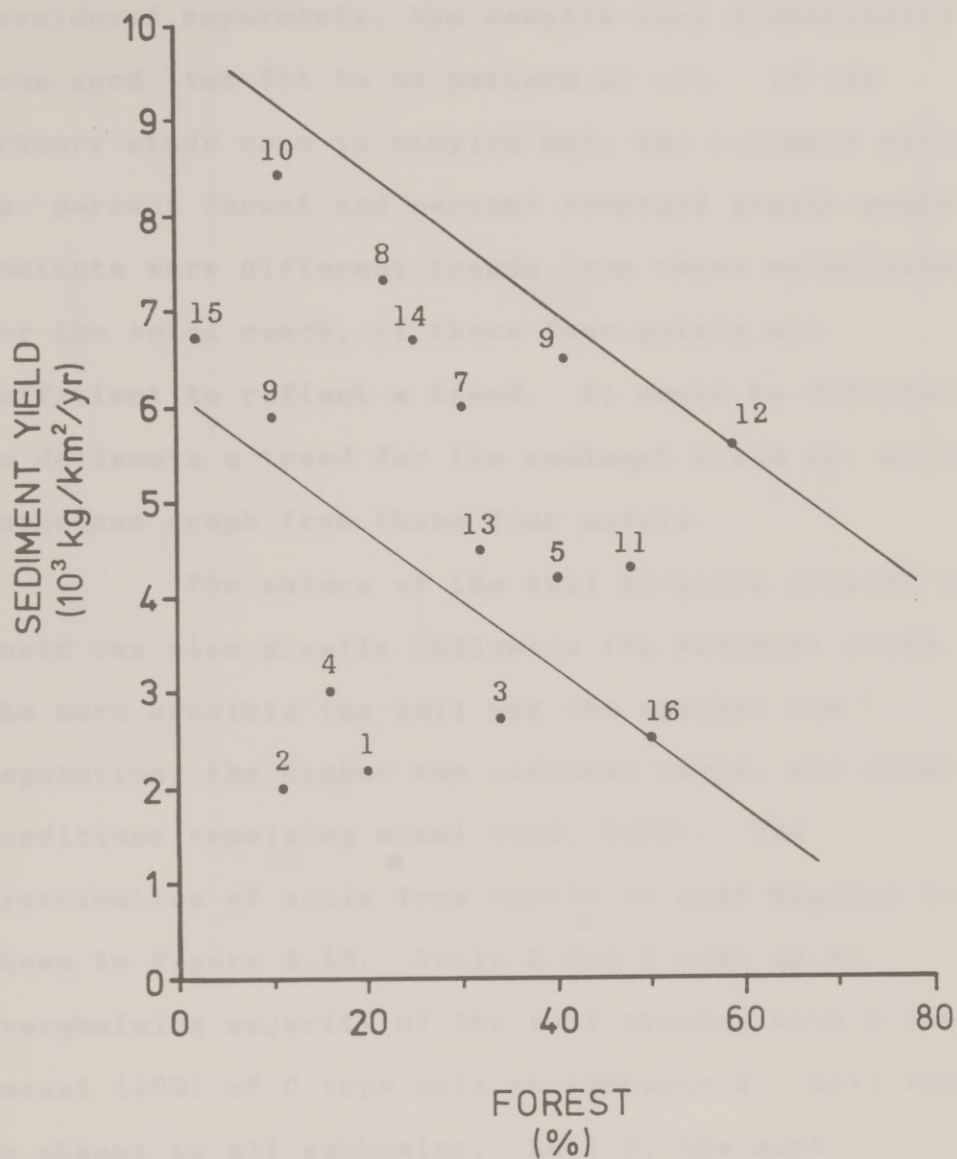


Figure 3.12: Sediment yield vs. percent forest between Austin and Wharton. (Subbasins are indicated by number on graph; boundaries are arbitrarily drawn)

that only very general trends can be established for the entire 16 subbasin reach. If smaller reaches are considered separately, the results vary dramatically from good line fit to no pattern at all. If the primary study area is singled out, the sediment yield vs. percent forest and percent cropland graphs would indicate very different trends from those established for the total reach, if these four points are sufficient to reflect a trend. It would be difficult to delineate a trend for the sediment yield vs. percent rangeland graph from these four points.

The nature of the soil or soils present in a basin can also greatly influence its sediment yield. The more erodible the soil and the sparser the vegetation, the higher the sediment yield, all other conditions remaining equal (SCS, 1972). The distribution of soils from Austin to near Wharton is shown in Figure 3.13. Soils B and D make up an overwhelming majority of the soil groups, with a small amount (10%) of C type soil in subbasin 2. Soil type A is absent in all subbasins. Soil D, the most predominant soil type, is characterized by very slow infiltration rates and therefore has a very high runoff potential. B soils have moderate infiltration rates,

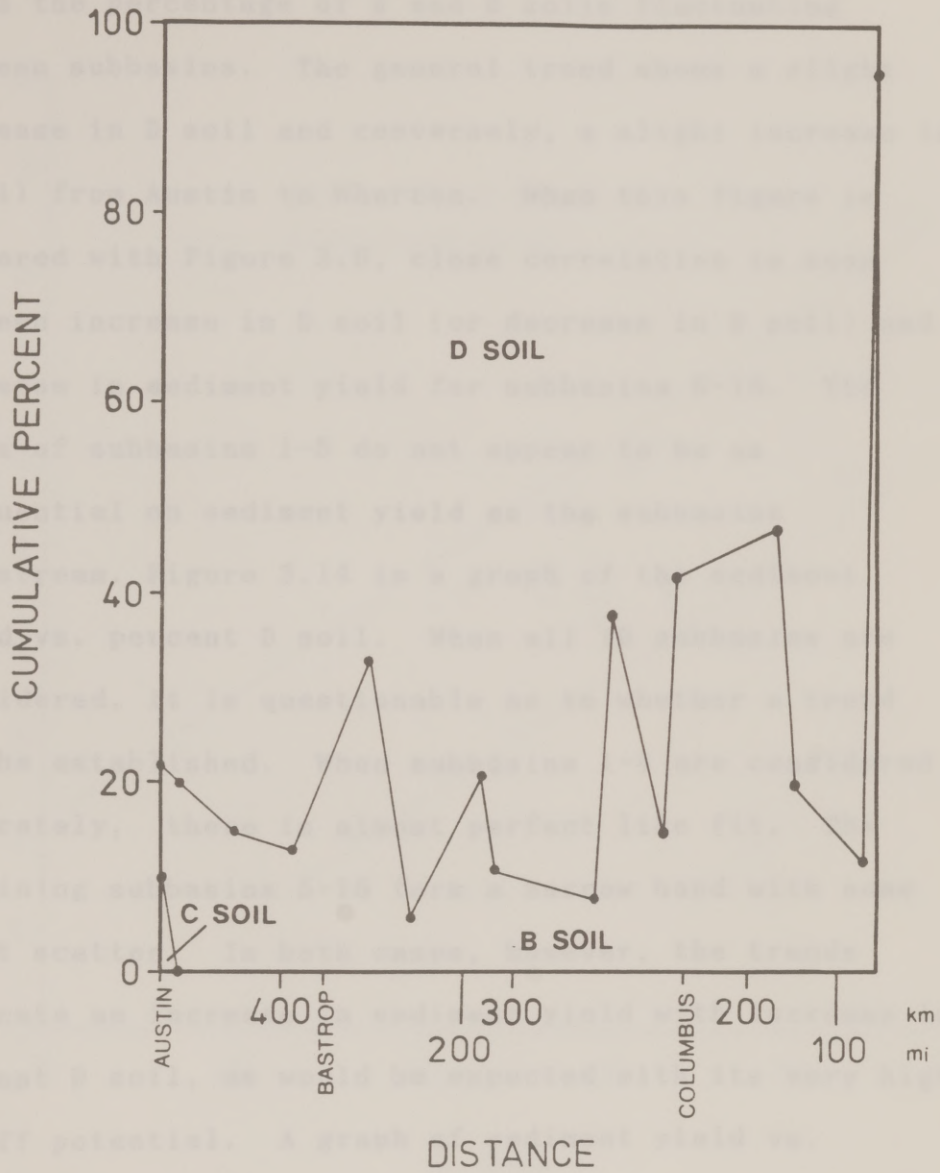


Figure 3.13: Distribution of soil type based on subbasin distance from mouth.

indicating moderate runoff potential. Figure 3.13 shows the percentage of B and D soils fluctuating between subbasins. The general trend shows a slight decrease in D soil and conversely, a slight increase in B soil from Austin to Wharton. When this figure is compared with Figure 3.6, close correlation is seen between increase in D soil (or decrease in B soil) and increase in sediment yield for subbasins 6-16. The soils of subbasins 1-5 do not appear to be as influential on sediment yield as the subbasins downstream. Figure 3.14 is a graph of the sediment yield vs. percent D soil. When all 16 subbasins are considered, it is questionable as to whether a trend can be established. When subbasins 1-4 are considered separately, there is almost perfect line fit. The remaining subbasins 5-16 form a narrow band with some point scatter. In both cases, however, the trends indicate an increase in sediment yield with increase in percent D soil, as would be expected with its very high runoff potential. A graph of sediment yield vs. percent B soil (Figure 3.15) resembles a mirror image of the previous graph as expected, given that B and D are the only soils present in all but one subbasin. Again, all 16 subbasins suggest only a questionable

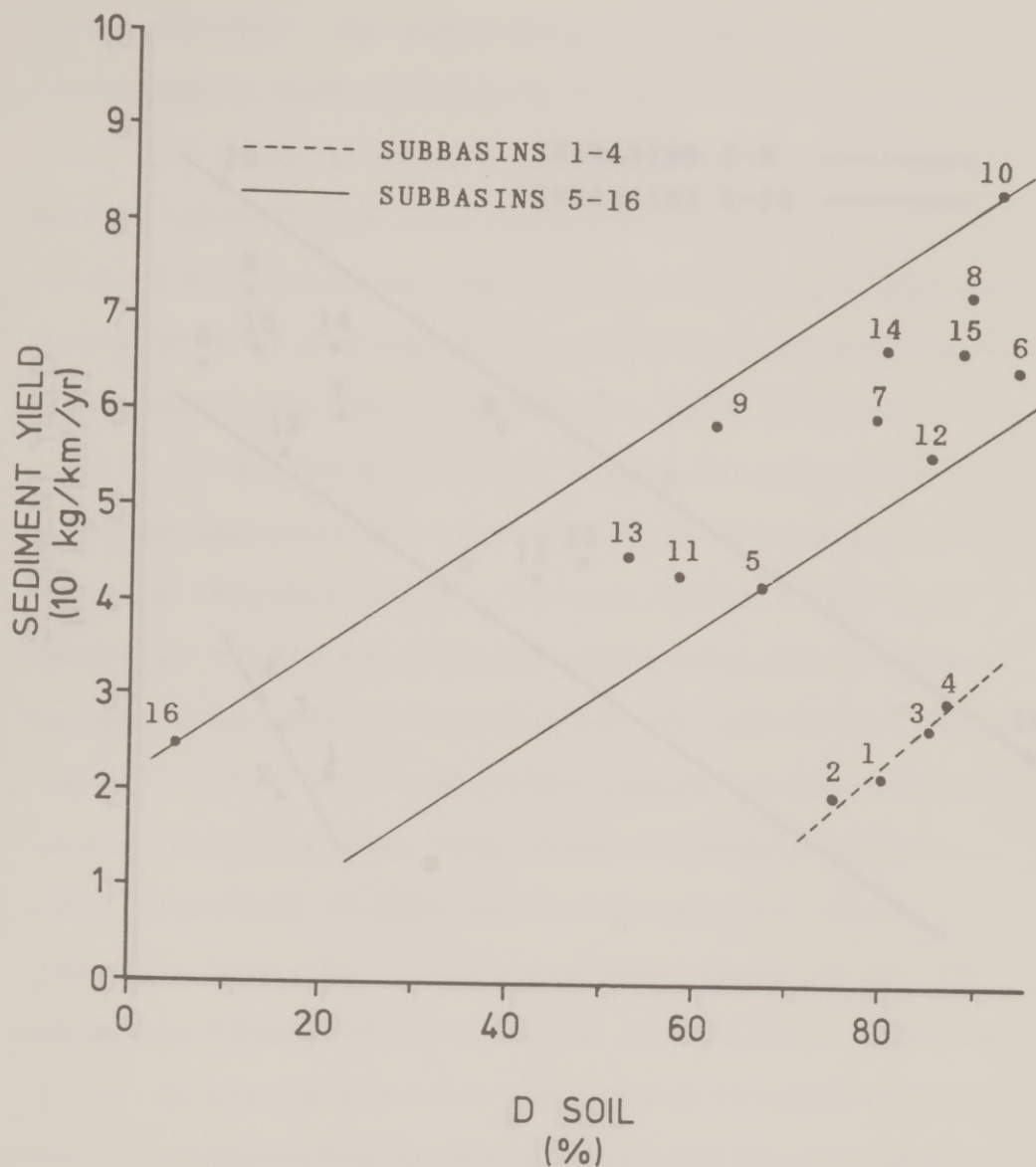


Figure 3.14: Sediment yield vs. percent D soil between Austin and Wharton.
(Subbasins are indicated by number on graph; boundaries are arbitrarily drawn)

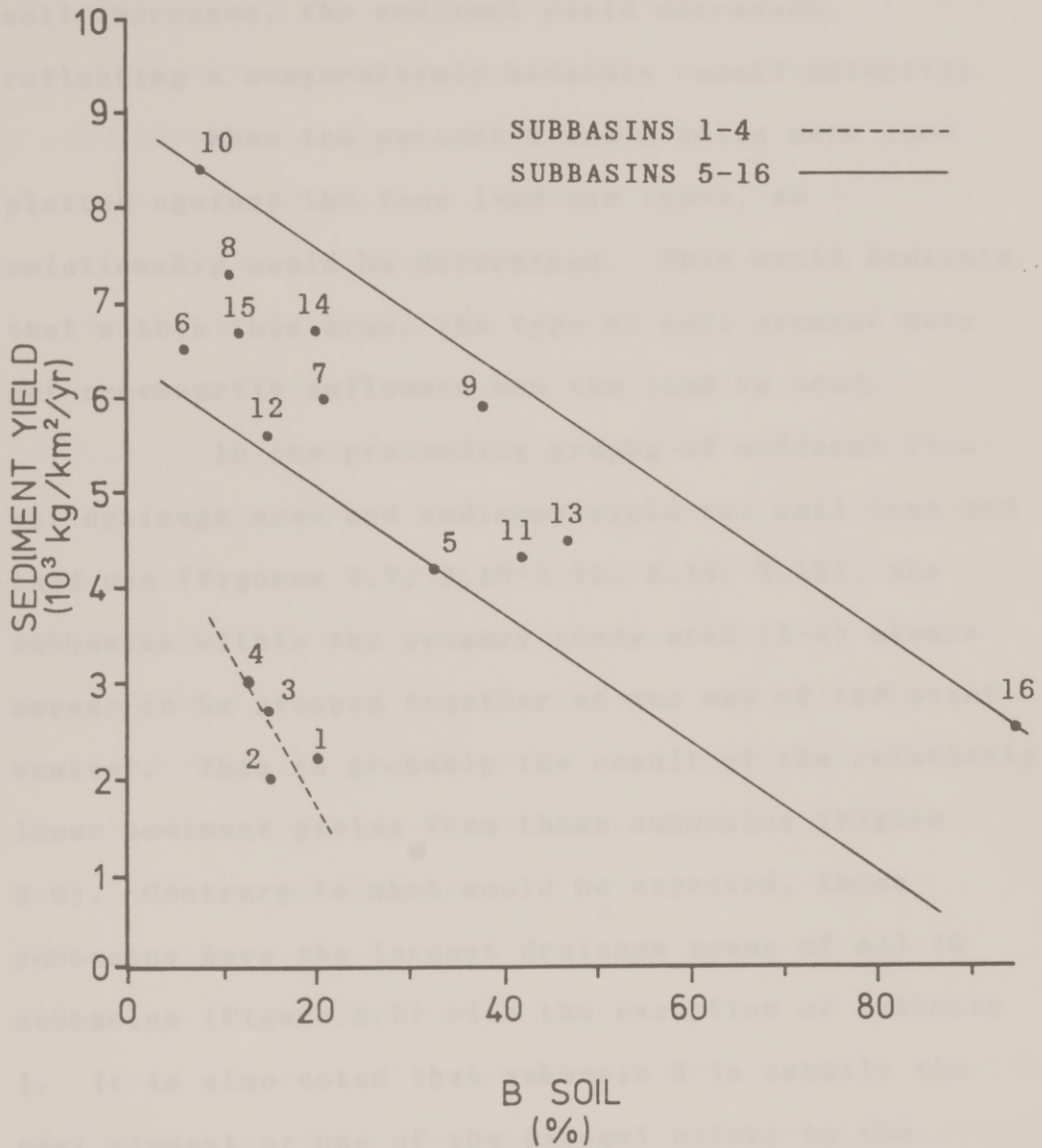


Figure 3.15: Sediment yield vs. percent B soil between Austin and Wharton. (Subbasins are indicated by number on graph; boundaries are arbitrarily drawn)

trend, while subbasins 1-4 and 5-16 seem to indicate two individual trends. In both cases, as percent B soil increases, the sediment yield decreases, reflecting a comparatively moderate runoff potential.

When the percent B and D soils were each plotted against the four land use types, no relationship could be determined. This would indicate that within this area, the type of soil present does not necessarily influence how the land is used.

In the preceeding graphs of sediment flux vs. drainage area and sediment yield vs. soil type and land use (Figures 3.7, 3.10-3.12, 3.14, 3.15), the subbasins within the primary study area (1-4) always appear to be grouped together at one end of the point scatter. This is probably the result of the relatively lower sediment yields from these subbasins (Figure 3.6). Contrary to what would be expected, these subbasins have the largest drainage areas of all 16 subbasins (Figure 3.5) with the exception of subbasin 1. It is also noted that subbasin 5 is usually the next closest or one of the closest points to the subbasin 1-4 grouping. This could indicate changing conditions between subbasins 1-4 and 5-16 with subbasin 5 reflecting the transition. This may be explained in

part by the increase in impervious cover due to urbanization in the first four subbasins, especially subbasins 1 and 2. In addition, there is more cropland downstream from Bastrop combined with a predominance of D soil throughout the entire reach. Other contributors to increased sediment yield downstream include depth of soil cover and average annual precipitation. The soils in the Austin area are relatively thin, generally deepening southeastward, reflective of the change in bedrock from the relatively hard, dense carbonates in Austin to the more easily erodible sands, silts, and clays of the Coastal Plain. In addition, as one nears the Gulf Coast, there is more precipitation available to erode and transport the sediment. The average annual precipitation in Austin is 85.1 cm (33.5 in), whereas near Wharton, the average annual rainfall is about 104 cm (41 in)(Figure 2.12).

3.5.2 CHANNEL SEDIMENT

As indicated by the sediment budget, erosion of the channel itself supplies an overwhelming majority (about 90%) of the river sediment. Within a meandering river, erosion is most likely to occur in areas of maximum velocity and turbulence. During normal flow,

the greatest velocity and turbulence, and therefore greatest erosion occurs along the outer concave banks near the base of the channel. Because of the helical flow pattern, some of this sediment is deposited on the next downstream point bar as it builds toward the channel. During flood flow, the water takes a straighter path as the greater velocity moves toward the inner bank, sometimes cutting across the point bar (Galloway and Hobday, 1983). This type of behavior for both normal and flood flow is expected for the lower Colorado River, as evidenced by the description of a coarse grained point-bar typical of the river between Smithville and Matagorda (McGowen and Garner, 1970). This reach of the river is located just downstream of the primary study area, however, it provides clues as to the physiographic features to be expected further upstream, although they may be less pronounced. Aerial photographs of the area between Austin and Bastrop revealed evidence of point bar buildup which could be seen quite easily along the meanders. Although it was difficult to distinguish smaller physiographic features due to the scale of the photos, several small chutes on minor meanders could be seen.

along the In a meandering river system, sediment can be eroded from the banks as well as the bed of the channel. The lateral meandering of the Colorado river is evidence of extensive erosion along its banks. Erosion occurs mainly along the concave banks, but can also occur on both banks along the straight reaches. During extreme flooding, there can also be extensive erosion and deposition along the point bar, or convex bank. Chutes and chute bars are direct evidence of these rapid flow conditions (McGowen and Garner, 1970). The stability of the bank material may be weakened by floods in that an increase in river stage can temporarily reverse the energy gradient, causing rising river water to flow into the banks. During the falling stage, the groundwater flow changes directions, and again becomes influent to the river. Even smaller fluctuations in river stage, such as the release of water for hydroelectric power generation, can decrease the stability of the banks by this same mechanism (Simons, Li, and Associates, 1982).

Erosion of the bed of the channel can occur adjacent to the eroding banks during normal flow, i.e., the bed areas near the concave banks and the banks of the straight reaches. There is evidence of armoring

along the Colorado River bed between Longhorn Dam and Webberville (Armstrong, 1989) and it is assumed that it extends further downstream, given that typical beds downstream of Smithville have been described as having a sandy and gravelly bottom (McGowen and Garner, 1970). Since armor layers form in areas of natural scour in a river, they protect the underlying finer layer from erosion. During flood events, however, the armor layer can be scoured away, given the increased competence of the river, but may be restored as the flow returns to normal levels (Simons, Li, and Associates, 1982).

Assuming that channel armoring is reasonably effective in riffle areas and considering the limited supply of sediment from its tributaries, it may be concluded that the majority of the river sediment is derived from the erosion of the river banks. During flood flow, scouring of the channel bed and erosion of the point bar would also add to the sediment load.

From the upstream channel, from the adjacent drainage basin, and from within the channel itself. For the Colorado river study area, the upstream contribution was calculated to be 7.0 percent and 3.3 percent for the short term and long term sediment budgets, and was

CHAPTER 4

DISCUSSION

The present day Colorado River has been characterized as a meandering coarse-grained degradational bed-load river (Baker and Penteado-Orellana, 1977, McGowen and Garner, 1970, and Morton and McGowen, 1980). Downstream from Austin, the river is responding to both natural and induced changes: (1) geologically, the river flows through the predominantly limestone bedrock in the Austin area into the sands, silts, and clays of the Coastal Plains, and (2) hydrologically, the river seeks to attain equilibrium under the influence of man's interference.

The sediment supply to a river system can be affected by and is a reflection of these changes. The sediment available to a reach of river can originate from the upstream channel, from the adjacent drainage basin, and from within the channel itself. For the Colorado river study area, the upstream contribution was calculated to be 1.9 percent and 3.2 percent for the short term and long term sediment budgets, and was

considered to be negligible when compared with other sources. An extremely low suspended sediment concentration was also noted at Longhorn Dam in Figure 3.4. Petts (1984) explained that river impoundments act as sediment traps, resulting in an outflow of relatively clear, sediment free water. Taylor's (1910, 1930) records of the historical silting of Lake Austin provided evidence that the dams of the Highland Lakes system do serve as excellent sediment traps. A very low suspended sediment concentration and therefore a negligible upstream sediment contribution is then the expected result downstream of the Highland Lakes impoundments.

The contribution of sediment to the river from the adjacent drainage basin for the short term and long term sediment budgets was 10.6 percent and 6.5 percent of the total river sediment. This significant but relatively minor sediment supply appears to be affected by the drainage basin area and the land use and soil type within the drainage basin. As expected, an increase in sediment loading corresponds well with an increase in drainage area, as seen in Figure 3.7. This is only true, however, for subbasins 5-16. Subbasins 1-4 have the largest drainage areas, with the

exception of subbasin 1, but do not contribute the greatest amounts of sediment. This appears to be due primarily to geological conditions and land use. The limestone rocks in the Austin area are more resistant to erosion and have thinner soils than the sands, silts, and clays of the coastal plains. Urbanization in the Austin area also tends to limit the sediment supply due to an increase in impervious cover. For these same reasons, the effects of land use and soil type on sediment yield are also more pronounced in subbasins 5-16. When sediment yield and sediment flux vs. distance downstream are compared (Figures 3.6 and 3.8), the downstream half of the sediment flux curve reflects decreasing drainage subbasin areas, while the downstream half of the sediment yield curve is influenced by land use and geologic and soil cover conditions. The relatively lower sediment yield from subbasins 1-4 (Figure 3.6) is also attributed to these conditions. Figure 3.10 illustrates that an increase in cropland results in an increase in sediment yield, as expected (SCS, 1971). An increase in forest and rangeland corresponds with a decrease in sediment yield (Figures 3.11 and 3.12). It should be noted that a specified change in percent rangeland appears to have a

greater effect on the sediment yield than a similar change in percent forest land. This is contrary to what would generally be expected (SCS, 1971), and is perhaps due to the broad nature of the categories and the wide variety of vegetation found within them. An increase in D type soil resulted in an increase in sediment yield due to its very high runoff potential (Figure 3.14). Conversely, an increase in B soil resulted in a decrease in sediment yield, reflecting a relatively moderate runoff potential (Figure 3.15).

The channel itself supplied the overwhelming majority of sediment to the river. The short term and long term sediment budgets indicated 87.5 percent and 90.3 percent channel contribution. Observations by Armstrong (1989) and Koenig (1987) led to the assumption that the channel bed has an effective armor layer. From this, the conclusion was drawn that the majority of the channel sediment would be derived from the channel banks. Petts (1984) explains that given these conditions, i.e., armored channel bed and limited sediment supply from tributaries, bank erosion would be the expected response, particularly from a river with migrating meanders.

The effects of the Highland Lakes dam system on the sediment load between Longhorn Dam and the Gulf of Mexico were seen in Figure 3.4. The greatest increase in concentration occurred just downstream from the dam as Petts (1984) indicated should be expected for an impounded river. Much of this increase occurred between Austin and Bastrop. The curve approached an asymptotic value near Columbus, and remained at that value downstream. It appears, then, that during normal flow, the effects of the dams on the suspended sediment concentration are felt downstream as far as Columbus. Petts (1984) explained that upstream river impoundments will bring about a complete readjustment of channel morphology for a significant length of river below the dam. He indicated that the most notable river responses should include accelerated erosion, sedimentation within the channel, and changes in channel form. Downstream from Longhorn Dam, then, one should expect accelerated erosion of the channel due to the clarifying effect of the dams on river water. Due to lack of pre-dam data, the degree of present day erosion could not be compared to that of pre-dam conditions. Erosion may be locally limited by resistant limestone channel material near Austin, which

is in contrast to the more easily eroded sands, silts, clays, and older alluvial material east of Austin. The dense vegetation along the Colorado River tends to hinder erosion along the river banks (McGowen and Garner, 1970). Localized sedimentation should be expected at tributary confluences with the Colorado river. Regulation of flood waters artificially slows the sediment transport within the river, whereas the sediment load from the tributaries is unaffected or possibly increased if rejuvenation is occurring (Petts, 1984). Field observations and measurements would be required to estimate the amount of sedimentation at these confluences. Although a study of aerial photos revealed that the channel form of the Colorado river does not appear to have changed too dramatically since the construction of the dams, it should be remembered that readjustment of channel morphology below an impoundment is a very long term process, taking perhaps up to hundreds of years. This change can be especially slow in gravel bed rivers because they require extreme flood events for sediment transport (Petts, 1984).

The sand and gravel mining operations, both active and abandoned sites, have had and continue to have a dramatic effect on the river sediment. Numerous

breached berms and muddy plumes near pit areas were evident in the aerial photographs and have been noted by others (Koenig, 1987 and MacRae, 1988). Some of the abandoned pits have been inundated by the river, effectively widening the river channel. This has resulted in an increase in channel bed sediment and therefore a decrease in channel depth near the pit and downstream as the sediment is gradually transported. An increase in channel width may also occur due to bank erosion which could result when the velocity and sediment transport capacity of the river are increased due to a decrease in bed roughness as pools fill and riffles degrade (Jackson and Beschta, 1984). The suspended sediment concentration in the river also increases downstream of the pits as the finer material from sand and gravel washing operations is transported. An example of this increase was seen in Figure 3.4. Recall that the two stations on the graph that were considered outliers were taken downstream of old sand and gravel operations. The values of average annual suspended sediment concentration at these stations were approximately four times that of the undisturbed portions of the river. The amount of sediment transported from these sand and gravel pits depends

upon the location and volume of the pit, i.e., is the pit considered to be in-stream or in the adjacent floodplain, and what volume of water is required to fill the pit. It is also dependent upon the stream discharge and the magnitude and frequency of flood events (Simons, Li, and Associates, 1982).

The amount of each rock type present in river sediment depends on when it entered the river, its condition upon entering, and its physical and chemical durability during transport and storage in the river system (Baker and Penteado-Orellana, 1978). The lithology of a rock can be a clue to its origin. Sears (1978) studied the sand size quartz, feldspar, and granitic rock fragments originating in the Llano-Burnet area. Quartz proved to be the most durable while granitic rock fragments were the least durable. Sears attempted to determine how much of the modern channel alluvium is derived from older terrace deposits, with inconclusive results. The study of gravel size rocks (Sneed and Folk, 1958) included all rock types found in the river. Limestone and chert were the most abundant rocks between Austin and Bastrop due to close proximity to a source. Limestone erodes relatively quickly, however, resulting in a greater percentage of chert

downstream. The gravel size quartz, granite, and miscellaneous rocks (sandstone, gneiss, schist) originated from the Llano-Burnet area. A minor amount of the sandstone may originate from the bedrock east of Austin. The best method for determining distance from source for the more durable rocks (quartz, chert) appears to be the comparison of sphericity and form in relation to specific gravel size. Near the source, all sizes of gravel have similar form and sphericity, whereas, far from the source, smaller and larger gravels differ in sphericity and form due to different weathering mechanisms.

As evidenced by the above discussion, some degree of comparison could be made between expected conditions and responses, as gathered from the literature review, and actual calculated results. However, a more detailed and localized analysis of sediment sources could not be made due to limited sediment data. In addition, a lack of previous work within the study area concerning the effects of the Highlands Lakes dam system and the sand and gravel mining operations also prevented data comparison.

CHAPTER 5

CONCLUSIONS AND RECOMMENDATIONS

From the results of the quantitative analysis coupled with the information gathered from the literature review, the following conclusions have been drawn:

1. The flux of suspended solids in the Colorado River at Austin and Wharton from September 1985 through August 1986 was found to be 5.9 E6 kg/yr and 307 E6 kg/yr , respectively, while the long term flux was estimated to be 1.6 E7 kg/yr and 50.4 E7 kg/yr , respectively.

2. Between Austin and Wharton, the subbasin tributaries were estimated to contribute only about 10.6 percent and 6.5 percent of the suspended solids gained between the two cities over the 1985-1986 and long term periods, respectively. The balance of the sediment is derived from the erosion of the river channel.

3. The amount of sediment derived from the drainage basin of the lower Colorado river is influenced by both land use and soil type. It was clearly evident that, in general, an increase in cropland and in D type soil resulted in an increase in sediment yield, while an increase in forest, rangeland, and B soil resulted in a decrease in sediment yield. In addition, the largest subbasins, located between Austin and Bastrop, did not contribute the greatest amount of sediment. This appears to be due to a combination of factors including geological and soil cover conditions, land use, and climatic conditions.

4. Given that the Colorado River receives a limited supply of sediment from its tributaries and assuming that channel armoring is effective at protecting the channel bed sediments in riffle areas, one can deduce that the majority of the river sediment is being derived from the erosion of the river banks.

5. The sand and gravel mining operations along the Colorado River between Austin and Bastrop are also significantly effecting the behavior of the river. A substantial amount of sediment has entered the river due to inadequate barriers between pit areas and the

river. These pits are a source of both fine and coarse sediment, the finer sediment being transported downstream as suspended sediment while the coarser sediment is gradually transported downstream as bedload. In some locations, as the river flows through flooded pits, it alters its course in favor of the pit. This influx of sediment to the river adds to its sediment load and may locally reduce the amount of channel erosion.

6. The series of dams making up the Highland Lakes system appear to have had and continue to have an enormous effect on the Colorado River below Austin. The dams act as sediment traps, removing all the coarse grained material and most of the suspended sediment, thereby clarifying the water downstream. Rapid channel erosion is then the expected response as the river regains its sediment load. The dams also help maintain flood control, often greatly reducing the peak discharge of the river. This lowers the erosive capability and transport capacity of the river during flood events, altering the natural course of the river.

The following recommendations for future work could further enhance the results of this study:

1. One recommendation would be to consider smaller segments of the river for suspended sediment analysis. This would involve taking water samples for suspended sediment analysis at intermediate stations of known discharge, such as Bastrop and Columbus. These three segments, Austin to Bastrop, Bastrop to Columbus, and Columbus to Wharton, could then be individually analyzed for change in suspended solids concentration and flux. One would expect a very small flux at Longhorn Dam. At Bastrop, the flux should be much higher, resulting from a slight increase in flow, but a tremendous increase in suspended solids. An even higher flux would be expected at Columbus from an increase in suspended solids and a slight increase in flow. At Wharton, the flux is expected to be higher, but only as a result of additional flow. This type of analysis could help in determining the source of sediments on a smaller scale.

2. Another recommendation would be to explore the possibility of determining the river discharges necessary to erode and transport the various sizes of sediment. A site specific model might be patterned after the Shield's relation, in which the beginning of particle motion is a function of the Shield's parameter

and the Reynold's number (Simons, Li, and Associates, 1982). A model might also be adapted from Hjulstrom's work in which erosion, transportation, and deposition of a particle are related as a function of grain size and the critical velocity of grain movement (Reineck and Singh, 1980). This type of study could help predict the sediment load of the river downstream, the rate of movement and distribution of bed sediments, and help determine when scouring of the armor layer will most likely occur.

APPENDIX A

PROGRAM USTRAT

C This program determines tributary mass loading rates using the
 C "unbiased stratified ratio estimator". The user will input values
 C of mean annual discharge, mean daily discharge for sample day, and
 C selected sample data for sample day. A minimum of 2 sample days
 C is required.

```

INTEGER    I, J, N, QP, SAMPLE(100), DAYFLO(100)
REAL       W(100), WSUM, WC, QSUM, QC, QCIWCI, QCIQCI, SQW, SQQ,
          RNUM, DENOM, WP
CHARACTER  DATYP*20, LOCATN*25, YEAR*25

```

```

WRITE(6,*) 'ENTER TYPE OF SAMPLE DATA IN APOSTROPHES (MAX. 20
.CHARACTERS): '
READ*, DATYP
WRITE(6,*) 'ENTER LOCATION IN APOSTROPHES (MAX. 25 CHARACTERS): '
READ*, LOCATN
WRITE(6,*) 'ENTER WATER YEAR OR EQUIVALENT IN APOSTROPHES --
.EX: WATER YEAR 1986 (MAX. 25 CHARACTERS): '
READ*, YEAR
WRITE(6,*) 'ENTER MEAN ANNUAL DISCHARGE (CFS): '
READ*, QP
N = 1
10 WRITE(6,*) 'ENTER SAMPLE DATA FOR ONE DATE (MG/L): '
READ*, SAMPLE(N)
WRITE(6,*) 'ENTER CORRESPONDING MEAN DAILY FLOW (CFS): '
READ*, DAYFLO(N)
WRITE(6,*) 'MORE SAMPLE DATA? YES = 1 NO = 2 '
READ*, I
IF(I.EQ.1) THEN
  N = N + 1
  GOTO 10
ENDIF

DO 20 J = 1,N
  W(J) = DAYFLO(J) * SAMPLE(J) * 893
20 CONTINUE

WSUM = 0.0
DO 30 J = 1,N
  WSUM = WSUM + W(J)
30 CONTINUE
WC = WSUM / N

QSUM = 0.0
DO 40 J = 1,N
  QSUM = QSUM + DAYFLO(J)
40 CONTINUE
QC = QSUM / N

QCIWCI = 0.0
DO 50 J = 1,N

```

PROGRAM USTRAT

C This program determines tributary mass loading rates using the
 C "unbiased stratified ratio estimator". The user will input values
 C of mean annual discharge, mean daily discharge for sample day, and
 C selected sample data for sample day. A minimum of 2 sample days
 C is required.

```

INTEGER    I, J, N, QP, SAMPLE(100), DAYFLO(100)
REAL       W(100), WSUM, WC, QSUM, QC, QCIWCI, QCIQCI, SQW, SQSQ,
          RNUM, DENOM, WP
CHARACTER  DATYP*20, LOCATN*25, YEAR*25

```

```

WRITE(6,*) 'ENTER TYPE OF SAMPLE DATA IN APOSTROPHES (MAX. 20
.CHARACTERS): '
READ*, DATYP
WRITE(6,*) 'ENTER LOCATION IN APOSTROPHES (MAX. 25 CHARACTERS): '
READ*, LOCATN
WRITE(6,*) 'ENTER WATER YEAR OR EQUIVALENT IN APOSTROPHES --
.EX: WATER YEAR 1986 (MAX. 25 CHARACTERS): '
READ*, YEAR
WRITE(6,*) 'ENTER MEAN ANNUAL DISCHARGE (CFS): '
READ*, QP
N = 1
10 WRITE(6,*) 'ENTER SAMPLE DATA FOR ONE DATE (MG/L): '
READ*, SAMPLE(N)
WRITE(6,*) 'ENTER CORRESPONDING MEAN DAILY FLOW (CFS): '
READ*, DAYFLO(N)
WRITE(6,*) 'MORE SAMPLE DATA? YES = 1 NO = 2 '
READ*, I
IF(I.EQ.1) THEN
  N = N + 1
  GOTO 10
ENDIF

DO 20 J = 1, N
  W(J) = DAYFLO(J) * SAMPLE(J) * 893
20 CONTINUE

WSUM = 0.0
DO 30 J = 1, N
  WSUM = WSUM + W(J)
30 CONTINUE
WC = WSUM / N

QSUM = 0.0
DO 40 J = 1, N
  QSUM = QSUM + DAYFLO(J)
40 CONTINUE
QC = QSUM / N

QCIWCI = 0.0
DO 50 J = 1, N

```

```

      QCIWCI = QCIWCI + (DAYFLO(J) * W(J))
50 CONTINUE

      QCIQCI = 0.0
      DO 60 J = 1,N
        QCIQCI = QCIQCI + (DAYFLO(J)**2)
60 CONTINUE

      SQW = (1./FLOAT((N-1))) * (QCIWCI - (N * QC * WC))
      SQSQ = (1./FLOAT((N-1))) * (QCIQCI - (N * (QC**2)))
      RNUM = 1. + (SQW / (N * QC * WC))
      DENOM = 1. + (SQSQ / (N * (QC**2)))
      WP = (QP * WC * RNUM) / (QC * DENOM)

C      To print out results:
      WRITE(6,70)
70  FORMAT(25X, 'ANNUAL AVERAGES OF ')
      WRITE(6,72) DATYP
72  FORMAT(24X, 'MASS LOADING OF ', A)
      WRITE(6,74) LOCATN
74  FORMAT(25X, A)
      WRITE(6,76) YEAR
76  FORMAT(27X, A, '/')
      WRITE(6,82)
82  FORMAT(14X, 'MEAN', 16X, 'MEAN', 7X, 'MEAN', 6X, 'MEAN')
      WRITE(6,84)
84  FORMAT(13X, 'ANNUAL', 4X, 'SAMPLE', 4X, 'SAMPLE', 5X, 'SAMPLE',
.    4X, 'ANNUAL')
      WRITE(6,86)
86  FORMAT(14X, 'FLOW', 6X, 'DATA', 6X, 'FLOW', 5X, 'LOADING', 4X,
.    'LOADING')
      WRITE(6,88)
88  FORMAT(14X, '(CFS)', 4X, '(MG/L)', 4X, '(CFS)', 5X, '(KG/YR)',
.    4X, '(KG/YR)',/)
      WRITE(6,92) QP, SAMPLE(1), DAYFLO(1), W(1), WP
92  FORMAT(14X, I4, 6X, I4, 6X, I4, 4X, G9.3, 3X, G9.3)
      DO 100 J = 2,N
        WRITE(6,95) SAMPLE(J), DAYFLO(J), W(J)
95  FORMAT(24X, I4, 6X, I4, 4X, G9.3)
100 CONTINUE
      END

```



```

C      PROGRAM SSLOAD (Adapted from HILOADS)

C      This program calculates suspended sediment loading from
C      watershed tributaries using the SCS method for estimating
C      storm runoff. The user must create a separate file to enter
C      all data.

      REAL TBSUMQ, SEDLOAD

      DIMENSION CN(20,20), AREA(25,4), ASOIL(25), BSOIL(25), CSOIL(25),
      .DSOIL(25), CNLU(25,4), PREC(25,3), XSTOR(25,3), STOR(25,4),
      .QLU(25,4,3), SUMQ(25,4,3), CONC(25,4), SLOAD(25,4,3), TLOAD(25,4),
      .BLOAD(25), BSUMQ(25), TSUMQ(25,4), TLAND(25), YIELD(25)

C      OPEN FILES

      OPEN(5, FILE='INPUT', ACCESS='SEQUENTIAL')
      OPEN(6, FILE='OUTPUT')

C      READ NUMBER OF SUBBASINS, NSB, AND NUMBER OF PRECIPITATION
C      EVENTS, NPREC

      READ(5,*) NSB, NPREC

C      READ MATRIX OF CN(I,J), STORM EVENT CATEGORIES

      WRITE(6,10)
10      FORMAT(/,10X,'MATRIX OF CN(I,J), I=LAND USE, J=SOIL TYPE',/,
      .5X,'LAND USE I',10X,'SOILS 1-4',/)
      DO 15 I=1,4
      READ(5,*)(CN(I,J), J=1,4)
      WRITE(6,20) I, (CN(I,J), J=1,4)
20      FORMAT(5X,I5,10X,4F5.0)
15      CONTINUE

C      INPUT LAND USE AREAS FOR RANGELAND, FOREST, CROPLAND, URBAN
C      IN SQ KM

      WRITE(6,25)
25      FORMAT(///,20X,'LAND USE (KM2)',/,3X,'SUBBASIN',3X,'RANGELAND',
      .3X,'FOREST',3X,'CROPLAND',4X,'URBAN',4X,'TOTAL',/)
      DO 30 IW=1, NSB
      TLAND(IW)=0.0
      READ(5,*)(AREA(IW,I), I=1,4)
      DO 35 I=1,4
      TLAND(IW)=TLAND(IW)+AREA(IW,I)
35      CONTINUE
      WRITE(6,40) IW, (AREA(IW,I), I=1,4), TLAND(IW)
40      FORMAT(2X,I5,4X,5F10.1)
30      CONTINUE

```

```

C      INPUT FRACTION OF EACH HYDROLOGIC SOIL TYPE IN SUBBASIN

      WRITE(6,45)
45     FORMAT(///,10X,'FRACTION OF EACH HYDROLOGIC SOIL TYPE',//,
      .3X,'SUBBASIN',6X,'ASOIL',5X,'BSOIL',5X,'CSOIL',5X,'DSOIL',/)
      DO 50 IW=1,NSB
      READ(5,*)ASOIL(IW),BSOIL(IW),CSOIL(IW),DSOIL(IW)
      WRITE(6,55)IW,ASOIL(IW),BSOIL(IW),CSOIL(IW),DSOIL(IW)
55     FORMAT(2X,I5,4X,4F10.2)
50     CONTINUE

C      COMPUTE CN FOR EACH LAND USE CATEGORY

      WRITE(6,60)
60     FORMAT(///,22X,'CURVE NUMBERS',//,3X,'SUBBASIN',3X,'RANGELAND'
      .,3X,'FOREST',3X,'CROPLAND',4X,'URBAN',/)

      DO 65 IW=1,NSB
      DO 70 I=1,4
      CNLU(IW,I)=ASOIL(IW)*CN(I,1)+BSOIL(IW)*CN(I,2)+
      .CSOIL(IW)*CN(I,3)+DSOIL(IW)*CN(I,4)
70     CONTINUE
      WRITE(6,75)IW,(CNLU(IW,I),I=1,4)
75     FORMAT(2X,I5,5X,4F10.2)
65     CONTINUE

C      INPUT STORM DATA

      WRITE(6,80)
80     FORMAT(///,30X,'STORM DATA',//,3X,'SUBBASIN',5X,'PRECIPITATION(IN)
      .',10X,'NUMBER OF EVENTS PER YEAR',/)
      DO 85 IW=1,NSB
      READ(5,*)(PREC(IW,K),K=1,NPREC),(XSTOR(IW,K),K=1,NPREC)
      WRITE(6,90)IW,(PREC(IW,K),K=1,NPREC),(XSTOR(IW,K),K=1,NPREC)
90     FORMAT(5X,I2,4X,3F8.2,7X,3F8.2)
85     CONTINUE

C      COMPUTE STORM RUNOFF WITH SCS EQUATION

      WRITE(6,95)
95     FORMAT(///,22X,'STORM EVENT RUNOFF(IN)',//,3X,'SUBBASIN',3X,
      . 'PRECIP(IN)',2X,'RANGELAND',3X,'FOREST',3X,'CROPLAND',
      .3X,'URBAN',/)
      DO 100 IW=1,NSB
      DO 105 I=1,4
      STOR(IW,I)=1000./CNLU(IW,I)-10.
      DO 110 K=1,NPREC
      TOP=(PREC(IW,K)-.2*STOR(IW,I))**2
      BOT=(PREC(IW,K)+.8*STOR(IW,I))
      QLU(IW,I,K)=TOP/BOT
110     CONTINUE
105     CONTINUE
      DO 115 K=1,NPREC

```



```

WRITE(6,120)IW,PREC(IW,K),(QLU(IW,I,K),I=1,4)
120 FORMAT(2X,I5,3X,F10.2,3X,4F10.2)
115 CONTINUE
100 CONTINUE

C      COMPUTE FLOWS FOR EACH SUBBASIN CATEGORY

WRITE(6,125)
125 FORMAT(///,18X,'FLOWS FROM LAND USE CATEGORIES (CU.M/YR)'/,
.1X,'SUBBASIN',2X,'PREC(IN)',2X,'RANGELAND',3X,'FOREST',4X,
.'CROPLAND',5X,'URBAN',4X,'SUBBASIN TOTAL',/)
DO 130 IW=1,NSB
BSUMQ(IW)=0.0
DO 135 I=1,4
TSUMQ(IW,I)=0.0

DO 140 K=1,NPREC
SUMQ(IW,I,K)=QLU(IW,I,K)*XSTOR(IW,K)*AREA(IW,I)*2.54E4
TSUMQ(IW,I)=TSUMQ(IW,I)+SUMQ(IW,I,K)
140 CONTINUE
BSUMQ(IW)=BSUMQ(IW)+TSUMQ(IW,I)
135 CONTINUE
DO 145 K=1,NPREC
WRITE(6,150)IW,PREC(IW,K),(SUMQ(IW,I,K),I=1,4),BSUMQ(IW)
150 FORMAT(1X,I5,1X,F10.2,2X,E10.3,3(1X,E10.3),3X,E12.5)
145 CONTINUE
130 CONTINUE

C      CALCULATE SUM OF FLOWS FROM ALL SUBBASINS

TBSUMQ=0.0
DO 155 IW=1,NSB
TBSUMQ=TBSUMQ+BSUMQ(IW)
155 CONTINUE
WRITE(6,160)NSB,TBSUMQ
160 FORMAT(/,1X,'TOTAL OVERLAND FLOW FROM ',I2,' SUBBASINS =',E12.5,
.' (CU.M/YR)')

C      INPUT RUNOFF SUSPENDED SEDIMENT (MG/L) FOR EACH LAND USE CATEGORY

WRITE(6,165)
165 FORMAT(///,10X,'SUSPENDED SEDIMENT IN RUNOFF (MG/L)',/,
.2X,'SUBBASIN',3X,'RANGELAND',3X,'FOREST',3X,'CROPLAND',3X,
.'URBAN',/)
DO 170 IW=1,NSB
READ(5,*)(CONC(IW,I),I=1,4)
WRITE(6,175)IW,(CONC(IW,I),I=1,4)
175 FORMAT(2X,I5,3X,4F10.3)
170 CONTINUE

```

C COMPUTE MASS LOADS (G/YR)

```

WRITE(6,180)
180 FORMAT(///,24X,'SEDIMENT LOADING (G/YR)',//,2X,'SUBBASIN',2X,
  'RANGELAND',5X,'FOREST',5X,'CROPLAND',7X,'URBAN',8X,'TOTAL',/)
DO 185 IW=1,NSB
  BLOAD(IW)=0.0
  DO 190 I=1,4
    TLOAD(IW,I)=0.0
    DO 195 K=1,NPREC
      SLOAD(IW,I,K)=SUMQ(IW,I,K)*CONC(IW,I)
      TLOAD(IW,I)=TLOAD(IW,I)+SLOAD(IW,I,K)
195 CONTINUE
    BLOAD(IW)=BLOAD(IW)+TLOAD(IW,I)
190 CONTINUE
  WRITE(6,200)IW,(TLOAD(IW,I),I=1,4),BLOAD(IW)
200 FORMAT(2X,I5,4(3X,E10.3),3X,E10.3)
185 CONTINUE

```

C CALCULATE SUM OF SEDIMENT LOADING FROM ALL SUBBASINS

```

SSLOAD=0.0
DO 205 IW=1,NSB
  SSLOAD=SSLOAD+BLOAD(IW)
205 CONTINUE
  WRITE(6,210)NSB,SSLOAD
210 FORMAT(/,1X,'TOTAL SEDIMENT LOADING FROM ',I2,' SUBBASINS =',
  E10.3,' (G/YR)')

```

C CALCULATE SEDIMENT YIELD (KG/KM2/YR)

```

WRITE(6,215)
215 FORMAT(///,20X,'SEDIMENT YIELD (KG/KM2/YR)',//,24X,'SUBBASIN',
  .4X,'YIELD',/)
DO 220 IW=1,NSB
  YIELD(IW)=(BLOAD(IW)/1000.0)/TLAND(IW)
  WRITE(6,225)IW,YIELD(IW)
225 FORMAT(27X,I2,5X,E8.3)
220 CONTINUE

```

END

TABLE 1

MEAN OF 20-1.75-1-LONG 2-2000 TYPE

TABLE 1	TABLE 1-1
1	20
2	20
3	20
4	20

APPENDIX C

TABLE 1-1 (CONT)

TABLE 1-1	TABLE 1-1	TABLE 1-1	TABLE 1-1	TABLE 1-1	TABLE 1-1
1	20	20	20	20	20
2	20	20	20	20	20
3	20	20	20	20	20
4	20	20	20	20	20
5	20	20	20	20	20
6	20	20	20	20	20
7	20	20	20	20	20
8	20	20	20	20	20
9	20	20	20	20	20
10	20	20	20	20	20
11	20	20	20	20	20
12	20	20	20	20	20
13	20	20	20	20	20
14	20	20	20	20	20
15	20	20	20	20	20
16	20	20	20	20	20
17	20	20	20	20	20
18	20	20	20	20	20
19	20	20	20	20	20
20	20	20	20	20	20

TABLE 1-1 (CONT)

TABLE 1-1	TABLE 1-1	TABLE 1-1	TABLE 1-1	TABLE 1-1
1	20	20	20	20
2	20	20	20	20
3	20	20	20	20
4	20	20	20	20
5	20	20	20	20
6	20	20	20	20
7	20	20	20	20
8	20	20	20	20
9	20	20	20	20
10	20	20	20	20
11	20	20	20	20

OUTPUT

MATRIX OF CN(I,J), I=LAND USE, J=SOIL TYPE

LAND USE I	SOILS 1-4			
1	49.	69.	69.	74.
2	36.	60.	62.	69.
3	65.	65.	74.	80.
4	61.	64.	73.	79.

LAND USE (KM2)

SUBBASIN	RANGELAND	FOREST	CROPLAND	URBAN	TOTAL
1	62.1	86.0	274.0	5.9	428.0
2	262.4	83.0	363.0	23.4	731.8
3	236.0	243.0	236.0	.0	715.0
4	201.8	116.0	389.0	20.2	727.0
5	94.7	196.0	196.0	5.3	492.0
6	112.7	269.0	268.0	5.3	655.0
7	109.0	164.0	274.0	.0	547.0
8	88.8	121.0	339.0	10.2	559.0
9	14.0	27.0	233.0	.0	274.0
10	36.9	51.0	367.0	4.1	459.0
11	.0	128.8	129.0	11.2	269.0
12	.0	247.9	168.0	4.1	420.0
13	32.0	103.0	187.0	.0	322.0
14	4.0	21.0	60.0	.0	85.0
15	1.9	4.0	160.0	7.1	173.0
16	27.0	68.0	41.0	.0	136.0

FRACTION OF EACH HYDROLOGIC SOIL TYPE

SUBBASIN	ASOIL	BSOIL	CSOIL	DSOIL
1	.00	.20	.00	.80
2	.00	.15	.10	.75
3	.00	.15	.00	.85
4	.00	.13	.00	.87
5	.00	.33	.00	.67
6	.00	.06	.00	.94
7	.00	.21	.00	.79
8	.00	.11	.00	.89
9	.00	.38	.00	.62
10	.00	.08	.00	.92
11	.00	.42	.00	.58

12	.00	.15	.00	.85
13	.00	.47	.00	.53
14	.00	.20	.00	.80
15	.00	.12	.00	.88
16	.00	.95	.00	.05

CURVE NUMBERS

SUBBASIN	RANGELAND	FOREST	CROPLAND	URBAN
1	73.00	67.20	77.00	76.00
2	72.75	66.95	77.15	76.15
3	73.25	67.65	77.75	76.75
4	73.35	67.83	78.05	77.05
5	72.35	66.03	75.05	74.05
6	73.70	68.46	79.10	78.10
7	72.95	67.11	76.85	75.85
8	73.45	68.01	78.35	77.35
9	72.10	65.58	74.30	73.30
10	73.60	68.28	78.80	77.80
11	71.90	65.22	73.70	72.70
12	73.25	67.65	77.75	76.75
13	71.65	64.77	72.95	71.95
14	73.00	67.20	77.00	76.00
15	73.40	67.92	78.20	77.20
16	69.25	60.45	65.75	64.75

STORM DATA

SUBBASIN	PRECIPITATION(IN)			NUMBER OF EVENTS PER YEAR		
1	1.50	2.50	4.00	8.00	.00	.00
2	1.50	2.50	4.00	8.00	.00	.00
3	1.50	2.50	4.00	8.00	.00	.00
4	1.50	2.50	4.00	8.00	.00	.00
5	1.50	2.50	4.00	11.00	4.00	.00
6	1.50	2.50	4.00	11.00	4.00	.00
7	1.50	2.50	4.00	11.00	4.00	.00
8	1.50	2.50	4.00	11.00	4.00	.00
9	1.50	2.50	4.00	11.00	4.00	.00
10	1.50	2.50	4.00	11.00	4.00	.00
11	1.50	2.50	4.00	11.00	4.00	.00
12	1.50	2.50	4.00	11.00	4.00	.00
13	1.50	2.50	4.00	11.00	4.00	.00
14	1.50	2.50	4.00	11.00	4.00	.00
15	1.50	2.50	4.00	4.00	2.00	1.00
16	1.50	2.50	4.00	4.00	2.00	1.00

STORM EVENT RUNOFF(IN)

SUBBASIN	PRECIP(IN)	RANGELAND	FOREST	CROPLAND	URBAN
1	1.50	.13	.05	.21	.19
1	2.50	.57	.36	.74	.69
1	4.00	1.53	1.16	1.81	1.74
2	1.50	.13	.05	.21	.19
2	2.50	.56	.35	.75	.70
2	4.00	1.51	1.14	1.82	1.75
3	1.50	.13	.06	.23	.20
3	2.50	.58	.38	.78	.73
3	4.00	1.54	1.18	1.87	1.79
4	1.50	.14	.06	.23	.21
4	2.50	.58	.38	.79	.74
4	4.00	1.55	1.19	1.89	1.82
5	1.50	.12	.04	.17	.15
5	2.50	.54	.33	.65	.61
5	4.00	1.48	1.09	1.67	1.60
6	1.50	.14	.06	.26	.24
6	2.50	.60	.40	.84	.79
6	4.00	1.58	1.23	1.97	1.89
7	1.50	.13	.05	.21	.18
7	2.50	.57	.36	.73	.69
7	4.00	1.52	1.15	1.80	1.73
8	1.50	.14	.06	.24	.22
8	2.50	.59	.39	.81	.76
8	4.00	1.56	1.21	1.91	1.84
9	1.50	.11	.04	.15	.13
9	2.50	.53	.31	.62	.58
9	4.00	1.47	1.06	1.62	1.55
10	1.50	.14	.06	.25	.23
10	2.50	.59	.40	.83	.78
10	4.00	1.57	1.22	1.95	1.87
11	1.50	.11	.03	.14	.12
11	2.50	.52	.30	.60	.56
11	4.00	1.45	1.04	1.58	1.51
12	1.50	.13	.06	.23	.20
12	2.50	.58	.38	.78	.73
12	4.00	1.54	1.18	1.87	1.79
13	1.50	.11	.03	.13	.11
13	2.50	.52	.29	.57	.53
13	4.00	1.44	1.02	1.52	1.46
14	1.50	.13	.05	.21	.19
14	2.50	.57	.36	.74	.69
14	4.00	1.53	1.16	1.81	1.74
15	1.50	.14	.06	.24	.21
15	2.50	.58	.39	.80	.75
15	4.00	1.55	1.20	1.90	1.83
16	1.50	.07	.00	.04	.03
16	2.50	.43	.18	.32	.29
16	4.00	1.28	.78	1.07	1.01

FLOWS FROM LAND USE CATEGORIES (CU.M/YR)

SUBBASIN	PREC(IN)	RANGELAND	FOREST	CROPLAND	URBAN	SUBBASIN TOTAL
1	1.50	.164E+07	.887E+06	.117E+08	.225E+06	.14409E+08
1	2.50	.000E+00	.000E+00	.000E+00	.000E+00	.14409E+08
1	4.00	.000E+00	.000E+00	.000E+00	.000E+00	.14409E+08
2	1.50	.669E+07	.814E+06	.157E+08	.906E+06	.24109E+08
2	2.50	.000E+00	.000E+00	.000E+00	.000E+00	.24109E+08
2	4.00	.000E+00	.000E+00	.000E+00	.000E+00	.24109E+08
3	1.50	.642E+07	.274E+07	.109E+08	.000E+00	.20054E+08
3	2.50	.000E+00	.000E+00	.000E+00	.000E+00	.20054E+08
3	4.00	.000E+00	.000E+00	.000E+00	.000E+00	.20054E+08
4	1.50	.557E+07	.135E+07	.185E+08	.864E+06	.26312E+08
4	2.50	.000E+00	.000E+00	.000E+00	.000E+00	.26312E+08
4	4.00	.000E+00	.000E+00	.000E+00	.000E+00	.26312E+08
5	1.50	.314E+07	.216E+07	.918E+07	.220E+06	.39763E+08
5	2.50	.522E+07	.651E+07	.130E+08	.329E+06	.39763E+08
5	4.00	.000E+00	.000E+00	.000E+00	.000E+00	.39763E+08
6	1.50	.447E+07	.485E+07	.196E+08	.349E+06	.70430E+08
6	2.50	.682E+07	.110E+08	.229E+08	.427E+06	.70430E+08
6	4.00	.000E+00	.000E+00	.000E+00	.000E+00	.70430E+08
7	1.50	.392E+07	.228E+07	.158E+08	.000E+00	.54652E+08
7	2.50	.626E+07	.599E+07	.204E+08	.000E+00	.54652E+08
7	4.00	.000E+00	.000E+00	.000E+00	.000E+00	.54652E+08
8	1.50	.341E+07	.201E+07	.229E+08	.620E+06	.67517E+08
8	2.50	.528E+07	.477E+07	.277E+08	.784E+06	.67517E+08
8	4.00	.000E+00	.000E+00	.000E+00	.000E+00	.67517E+08
9	1.50	.449E+06	.268E+06	.997E+07	.000E+00	.26996E+08
9	2.50	.757E+06	.861E+06	.147E+08	.000E+00	.26996E+08
9	4.00	.000E+00	.000E+00	.000E+00	.000E+00	.26996E+08
10	1.50	.145E+07	.890E+06	.260E+08	.262E+06	.64025E+08
10	2.50	.222E+07	.206E+07	.309E+08	.324E+06	.64025E+08
10	4.00	.000E+00	.000E+00	.000E+00	.000E+00	.64025E+08
11	1.50	.000E+00	.117E+07	.512E+07	.390E+06	.19096E+08
11	2.50	.000E+00	.397E+07	.781E+07	.632E+06	.19096E+08
11	4.00	.000E+00	.000E+00	.000E+00	.000E+00	.19096E+08
12	1.50	.000E+00	.384E+07	.107E+08	.233E+06	.37770E+08
12	2.50	.000E+00	.949E+07	.132E+08	.304E+06	.37770E+08
12	4.00	.000E+00	.000E+00	.000E+00	.000E+00	.37770E+08
13	1.50	.962E+06	.835E+06	.673E+07	.000E+00	.23994E+08
13	2.50	.168E+07	.305E+07	.107E+08	.000E+00	.23994E+08
13	4.00	.000E+00	.000E+00	.000E+00	.000E+00	.23994E+08
14	1.50	.145E+06	.298E+06	.351E+07	.000E+00	.94712E+07
14	2.50	.231E+06	.774E+06	.451E+07	.000E+00	.94712E+07
14	4.00	.000E+00	.000E+00	.000E+00	.000E+00	.94712E+07
15	1.50	.264E+05	.237E+05	.387E+07	.154E+06	.19220E+08
15	2.50	.563E+05	.783E+05	.648E+07	.270E+06	.19220E+08
15	4.00	.750E+05	.122E+06	.773E+07	.329E+06	.19220E+08
16	1.50	.203E+06	.376E+05	.154E+06	.000E+00	.56325E+07
16	2.50	.589E+06	.634E+06	.664E+06	.000E+00	.56325E+07
16	4.00	.879E+06	.135E+07	.112E+07	.000E+00	.56325E+07

TOTAL OVERLAND FLOW FROM 16 SUBBASINS = .52345E+09 (CU.M/YR)

SUSPENDED SEDIMENT IN RUNOFF (MG/L)

SUBBASIN	RANGELAND	FOREST	CROPLAND	URBAN
1	66.000	66.000	66.000	66.000
2	61.000	61.000	61.000	61.000
3	95.000	95.000	95.000	95.000
4	82.000	82.000	82.000	82.000
5	52.000	52.000	52.000	52.000
6	60.000	60.000	60.000	60.000
7	60.000	60.000	60.000	60.000
8	60.000	60.000	60.000	60.000
9	60.000	60.000	60.000	60.000
10	60.000	60.000	60.000	60.000
11	60.000	60.000	60.000	60.000
12	62.000	62.000	62.000	62.000
13	60.000	60.000	60.000	60.000
14	60.000	60.000	60.000	60.000
15	60.000	60.000	60.000	60.000
16	60.000	60.000	60.000	60.000

SEDIMENT LOADING (G/YR)

SUBBASIN	RANGELAND	FOREST	CROPLAND	URBAN	TOTAL
1	.108E+09	.586E+08	.770E+09	.148E+08	.951E+09
2	.408E+09	.496E+08	.958E+09	.553E+08	.147E+10
3	.610E+09	.260E+09	.103E+10	.000E+00	.191E+10
4	.456E+09	.111E+09	.152E+10	.709E+08	.216E+10
5	.435E+09	.451E+09	.115E+10	.285E+08	.207E+10
6	.678E+09	.952E+09	.255E+10	.466E+08	.423E+10
7	.611E+09	.497E+09	.217E+10	.000E+00	.328E+10
8	.522E+09	.407E+09	.304E+10	.843E+08	.405E+10
9	.724E+08	.678E+08	.148E+10	.000E+00	.162E+10
10	.220E+09	.177E+09	.341E+10	.351E+08	.384E+10
11	.000E+00	.309E+09	.776E+09	.613E+08	.115E+10
12	.000E+00	.826E+09	.148E+10	.333E+08	.234E+10
13	.158E+09	.233E+09	.105E+10	.000E+00	.144E+10
14	.225E+08	.643E+08	.481E+09	.000E+00	.568E+09
15	.946E+07	.134E+08	.109E+10	.453E+08	.115E+10
16	.100E+09	.122E+09	.116E+09	.000E+00	.338E+09

TOTAL SEDIMENT LOADING FROM 16 SUBBASINS = .326E+11 (G/YR)

BIBLIOGRAPHY

A. H. Dale Corp. 1967. 1966-1967 Texas Almanac and State Industrial Guide. Publ. by the Dallas Morning News, distributed by Texas Monthly Press, Austin, Texas.

SEDIMENT YIELD (KG/KM²/YR)

SUBBASIN	YIELD
1	.222E+04
2	.201E+04
3	.266E+04
4	.297E+04
5	.420E+04
6	.645E+04
7	.599E+04
8	.725E+04
9	.591E+04
10	.837E+04
11	.426E+04
12	.558E+04
13	.447E+04
14	.669E+04
15	.667E+04
16	.248E+04

Armstrong, W. E. 1964. Personal communication (Professor of Civil Engineering, The University of Texas at Austin, Austin, Texas).

Armstrong, W. E., K. B. Cleveland, V. M. Gordon, L. E. Kneid, and M. Johns. 1967. Final Report: Investigation of the Impact of Nutrient Discharges on the Water Quality and Flots in the Colorado River Below the City of Austin. Center for Research in Water Resources, The University of Texas at Austin, Austin, Texas, in press.

Baker, V. E. and W. M. Fontaine-Drellman. 1977. Adjustment to Quaternary climatic change by the Colorado River in central Texas. Journal of Geology 85: 498-513.

Baker, V. E. and W. M. Fontaine-Drellman. 1978. Fluvial sedimentation conditioned by Quaternary climatic change in central Texas. Journal of Sedimentary Petrology 48(3): 433-451.

BIBLIOGRAPHY

- A. H. Belo Corp. 1987. 1988-1989 Texas Almanac and State Industrial Guide. Publ. by the Dallas Morning News, distributed by Texas Monthly Press, Austin, Texas.
- Agricultural Stabilization and Conservation Service. Aerial photographs taken January 16 and 18, 1951, October 22, 1964, and October 15, 1966. Black and white prints, 1:12,276 scale (1" = 1023').
- American Society For Testing and Materials. 1980. Standard Practice for Determining Suspended Sediment Concentration in Water Samples. Designation: D 3977-80, pp. 1-9.
- American Society For Testing and Materials. 1984. Standard Guide for Sampling Fluvial Sediment in Motion. Designation: D4411-84, pp. 814-837.
- Armstrong, N. E. 1989. Personal communication (Professor of Civil Engineering, The University of Texas at Austin, Austin, Texas).
- Armstrong, N. E., K. D. Cleveland, V. N. Gordon, L. E. Koenig, and N. Johns. 1987. Final Report: Investigation of the Impacts of Nutrient Discharges on the Water Quality and Biota in the Colorado River Below the City of Austin. Center for Research in Water Resources, The University of Texas at Austin, Austin, Texas, in press.
- Baker, V. R. and M. M. Penteado-Orellana. 1977. Adjustment to Quaternary climatic change by the Colorado River in central Texas. *Journal of Geology* 85: 395-422.
- Baker, V. R. and M. M. Penteado-Orellana. 1978. Fluvial sedimentation conditioned by Quaternary climatic change in central Texas. *Journal of Sedimentary Petrology* 48(2): 433-451.

- Blatt, H., G. Middleton, and R. Murray. 1972. Origin of Sedimentary Rocks. Prentice-Hall, Inc., Englewood Cliffs, New Jersey, 634 pp.
- Brune, G. and G. L. Duffin. 1983. Occurrence, Availability, and Quality of Ground Water in Travis County, Texas. Texas Department of Water Resources Report 276, 219 pp.
- Bureau of Economic Geology. 1974. Geologic Atlas of Texas, Austin Sheet. The University of Texas at Austin.
- Bureau of Economic Geology. 1988. Computerized company listing of active producers of non-petroleum mineral resources. The University of Texas at Austin.
- Chow, V. T., D. R. Maidment, and L. W. Mays. 1988. Applied Hydrology. McGraw-Hill, New York, 572 pp.
- City of Austin Electric Utility. 1988. Departmental data sheet entitled "Longhorn Dam and Town Lake".
- Culkin, G. W. 1986. Assessment of Toxicant Impacts in an Urban Receiving System. Unpub. M.S. thesis in Engineering, The University of Texas at Austin, 243 pp.
- Das, B. M. 1985. Principles of Geotechnical Engineering. PWS Publishers, Boston, 571 pp.
- Dowell, C. L. and R. G. Petty. 1971. Engineering Data on Dams and Reservoirs in Texas, Part III. Texas Water Development Board Report 126.
- Einstein, H. A., A. G. Anderson, and J. W. Johnson. 1940. A distinction between bed-load and suspended-load in natural streams. Transactions, American Geophysical Union, Reports and Papers, Hydrology 21: 628-633.
- Follett, C. R. 1970. Groundwater Resources of Bastrop County, Texas. Prepared by the U. S. Geological Survey in cooperation with the Texas Water Development Board, Texas Water Development Board Report 109 (Third Printing, 1981), 138 pp.

- Furbish, D. J. 1988. River-bend curvature and migration: How are they related? *Geology* 16: 752-755.
- Galloway, W. E. and D. K. Hobday. 1983. Terrigenous Clastic Depositional Systems - Applications to Petroleum, Coal, and Uranium Exploration. Springer-Verlag, New York.
- Garner, L. E. and K. P. Young. 1976. Environmental Geology of the Austin Area: An Aid to Urban Planning. Report of Investigations No. 86, Bureau of Economic Geology, The University of Texas At Austin, 39 pp.
- Graf, W. L. 1975. The impact of suburbanization on fluvial geomorphology. *Water Resources Research* 11(5): 690-692.
- Hubbell, D. W. 1987. Bed Load Sampling and Analysis. In: Sediment Transport in Gravel-Bed Rivers, C. R. Thorne, J. C. Bathurst, and R. D. Hey, eds., John Wiley and Sons, New York, pp. 89-105.
- Jackson, W. L. and R. L. Beschta. 1984. Influences of increased sand delivery on the morphology of sand and gravel channels. *Water Resources Bulletin* 20(4): 527-533.
- Koenig, L. E. 1987. Food, Flood, or Flow? A Study of Nutrients, Flow Regime and Submerged Aquatic Macrophytes in the Colorado River, Texas. Unpub. M.S. thesis in Engineering, The University of Texas at Austin, 118 pp.
- Komar, Paul D. 1988. Sediment Transport by Floods. In: Flood Geomorphology, V. R. Baker, R. C. Kochel, and P. C. Patton, eds., John Wiley and Sons, New York, pp. 97-111.
- Leopold, L. B., M. G. Wolman, and J. P. Miller. 1964. Fluvial Processes in Geomorphology. W. H. Freeman and Company, San Francisco, 522 pp.
- Lower Colorado River Authority. Aerial photographs taken January 11, 1987. Color infrared film, approx. 1:12,000 scale (1" = 1000').

MacRae, R. 1988. Personal communication via telephone on September 2, 1988. Wetland Resources Coordinator, Texas Parks and Wildlife.

Mathis, R. W. 1944. Heavy minerals of Colorado River terraces of Texas. *Journal of Sedimentary Petrology* 14(2): 86-93.

McGowen, J. H. and L. E. Garner. 1970. Physiographic features and stratification types of coarse-grained point bars: Modern and ancient examples. *Sedimentology* 14: 77-111.

Miertschin, J. D. and N. E. Armstrong. 1986. Evaluation of the Effects of Point and Nonpoint Source Phosphorus Loads Upon Water Quality in the Highland Lakes. CRWR Technical Report 215, Center for Research in Water Resources, The University of Texas at Austin.

Mills, W. B., D. B. Porcella, M. J. Unga, S. A. Gherini, K. V. Summers, Lingfung Mok, G. L. Rupp, G. L. Bowie, and D. A. Haith. 1985. Water quality assessment: A screening procedure for toxic and conventional pollutants in surface and ground water. Prepared in cooperation with the U. S. Environmental Protection Agency, EPA/600/6-85/002a.

Morton, R. A. and J. H. McGowen. 1980. Modern Depositional Environments of the Texas Coast. Guidebook 20, Bureau of Economic Geology, The University of Texas at Austin, 167 pp.

Petts, G. E. 1984. Impounded Rivers - Perspectives for Ecological Management. John Wiley and Sons, New York, 326 pp.

Putnam, W. C. and A. B. Bassett. 1971. Geology. Oxford University Press, New York, 586 pp.

Reinech, H. E., and I. B. Singh. 1980. Depositional Sedimentary Environments, With Reference to Terrigenous Clastics. Second Ed., Springer-Verlag, New York, 549 pp.

Schumm, S. A. 1977. The Fluvial System. John Wiley and Sons, New York, 333 pp.

- Schwab, G. O., R. K. Frevert, T. W. Edminster, and K. K. Barnes. 1981. Soil and Water Conservation Engineering. Third Ed., John Wiley and Sons, New York.
- Sears, R. B. 1978. Selective Modification of Sand Size Alluvium, Colorado River, Texas. Unpub. M.A. thesis in Geology, The University of Texas at Austin, 138 pp.
- Sharp, J. M. and R. G. Larkin, eds. 1988. Hydrogeology of Hornsby Bend, Travis County, Texas. Preliminary report by the Hydrogeology field methods class, Department of Geological Sciences, The University of Texas at Austin, 30 pp.
- Sheldon, R. A. 1979. Roadside Geology of Texas. Mountain Press Publishing Co., Missoula, Montana, 180 pp.
- Simons, D. B. 1979. Effects of Stream Regulation on Channel Morphology. In: The Ecology of Regulated Streams, J. V. Ward and J. A. Stanford, eds., Plenum Press, New York, pp. 95-111.
- Simons, Li, and Associates. 1982. Engineering Analysis of Fluvial Systems. Simons, Li, and Associates, Fort Collins, Colorado.
- Sneed, E. D., and R. L. Folk. 1958. Pebbles in the lower Colorado River, Texas - A study in particle morphogenesis. *Journal of Geology* 66: 114-150.
- Soil Conservation Service. 1971. National Engineering Handbook, Section 3: Sedimentation. U. S. Department of Agriculture, U. S. Government Printing Office, Washington, D. C.
- Soil Conservation Service. 1972. National Engineering Handbook, Section 4: Hydrology. U. S. Department of Agriculture, U. S. Government Printing Office, Washington, D. C.
- Soil Conservation Service. 1974. Soil Survey of Travis County, Texas. U. S. Department of Agriculture.

- Soil Conservation Service. 1979. Soil Survey of Bastrop County, Texas. U. S. Department of Agriculture.
- Sutton, S. M. 1980. Urban Fluvial Geometamorphosis. Unpub. M.A. thesis in Geology, The University of Texas at Austin.
- Taylor, C. H. 1977. Seasonal variations in the impact of suburban development on runoff response: Peterborough, Ontario. Water Resources Research 13(2): 464-468.
- Taylor, T. U. 1910. The Austin Dam. University of Texas Bulletin No. 164, Scientific Series No. 16, The University of Texas at Austin.
- Taylor, T. U. 1930. Silting of Reservoirs. University of Texas Bulletin No. 3025, The University of Texas at Austin.
- Texas Water Commission. 1984. Water For Texas, Technical Appendix, Volume 2. Texas Department of Water Resources (Texas Water Commission) Publication GP-4-1.
- Texas Water Commission. 1988a. Sand and Gravel Washing. Permanent Rule 31, Texas Administrative Code Chapter 321, Subchapter D.
- Texas Water Commission. 1988b. Information obtained from the August 3, 1988 microfilm listing on current permits, Water Quality Division.
- Thomann, R. V. and J. A. Mueller. 1987. Principles of Surface Water Quality Modeling and Control. Harper and Row, New York, 644 pp.
- Tinkler, K. J. 1971. Active valley meanders in south-central Texas and their wider implications. Geological Society of America Bulletin 82: 1783-1800.
- Tovar, F. H. and B. N. Maldonado. 1981. Drainage Areas of Texas Streams, Colorado River Basin. Prepared under cooperative agreement between the U. S. Geological Survey and the Texas Department of

- Water Resources (TWC), Texas Department of Water Resources LP-145, 36 pp.
- Urbanec, D. A. 1963. Stream terraces and related deposits in the Austin area, Texas. Unpub. M.A. thesis in Geology, The University of Texas at Austin, 93 pp.
- U. S. Army Corps of Engineers, Fort Worth District. 1973. Wastewater Management Plan, Colorado River and Tributaries, Texas. Prepared by the Governor's Planning Committee: Turner, Collie, and Braden, Inc., consulting engineers, Vol. I, VII.
- U. S. Army Corps of Engineers. 1976. Flood Plain Information: Colorado River - Onion Creek to Montopolis Bridge, Austin, Texas. Prepared for the city of Austin, Texas.
- U. S. Department of the Interior. Aerial photographs taken June 1, 1984. Color infrared film, approx. 1:12,000 scale (1" = 1000').
- U. S. Geological Survey. Quadrangle maps: Austin East (7.5') 1966, 1973; Austin West (7.5') 1966, 1973; Bastrop (7.5') 1982; Lake Bastrop (7.5') 1982; Montopolis (7.5') 1966, 1973; Utley (7.5') 1982; Webberville (7.5') 1973, 1987.
- U. S. Geological Survey. Water Resources Data, published annually by water year (Oct.-Sept.), U. S. Geological Survey Water-Data Reports.
- van Eysinga, F. W. B. 1978. Geologic Time Table. Elsevier Scientific Publishing Company, The Netherlands.
- Weber, G. E. 1968. Geology of the Fluvial Deposits of the Colorado River Valley, Central Texas. Unpub. M.A. thesis in Geology, The University of Texas at Austin, 119 pp.
- Weeks, A. W. 1941. Late Cenozoic Deposits of the Texas Coastal Plain Between the Brazos River and the Rio Grande. Unpub. M.A. thesis in Geology, The University of Texas at Austin, 267 pp.

Wischmeier, W. H. 1976. Use and misuse of the
Universal Soil Loss Equation. Journal of Soil and
Water Conservation 31(1): 5-9.

W. H. Wischmeier, an August 24, 1907, the daughter of
Dr. William Harrison Wischmeier and Joseph Elmer Wischmeier.
After graduating from J. L. Pearce High School,
Meriden, Texas, in 1925, she entered Stephen F.
Austin State University at San Marcos, Texas. She was
graduated from the college, receiving the degree of Bachelor
of Science from Stephen F. Austin State University,
Department of Zoology, in December, 1928. During the
following years, she was employed as a geologist with
Department of Geology, a subsidiary of Texas, in
Houston, Texas. In June, 1932, she entered the
University of Illinois, University Park campus, and
transferred to The University of Texas at Austin in
August, 1932. In September, 1937, she entered the
graduate school of The University of Texas at Austin.

Present Address: 12 South Service Pl.
The Woodlands, Texas

This document was typed by Karen Bartlett.

The vita has been removed from the digitized version of this document.